2003

Investigation of oxides of nitrogen emissions from biodiesel-fueled engines

Mustafa Ertunc Tat
Iowa State University

Investigation of oxides of nitrogen emissions from biodiesel-fueled engines

by

Mustafa Ertunc Tat

A dissertation submitted to the graduate faculty

in partial fulfillment of the requirements for the degree of

DOCTOR OF PHILOSOPHY

Major: Mechanical Engineering

Program of Study Committee:
Jon H. Van Gerpen, Major Professor
Howard N. Shapiro
Ron M. Nelson
Brent H. Shanks
Steven J. Hoff

Iowa State University

Ames, Iowa

2003

Graduate College

Iowa State University

This is the certify that the doctoral dissertation of

Mustafa Ertunc Tat

has met the dissertation requirements of Iowa State University

Signature was redacted for privacy.

Major Professor

Signature was redacted for privacy.

For the Major Program

TABLE OF CONTENTS

LIST OF FIGURES

LIST OF TABLES

ABSTRACT

Biodiesel is an environmentally friendly alternative diesel fuel consisting of the alkyl monoesters of fatty acids. It is obtained from triglycerides through the transesterfication process. The objective of this research was to determine the reason for the higher levels of NOx emissions that have been observed from biodiesel fueled engines. A concept map was developed to show the interrelationships between the fuel and engine variables that affect NOx production. It was determined that a change in combustion timing caused by changes in fuel properties between diesel fuel and biodiesel might be the source of the NOx increase. Tests were conducted to determine the effect of blending biodiesel with diesel fuel on these properties, and to determine the effect of biodiesel fuel properties such as the lower heating value, density, speed of sound, bulk modulus, cetane number, and volatility on the NOx emissions from a diesel engine fueled with biodiesel.

It was found that biodiesel is more dense and less compressible than No. 1 and No. 2 diesel fuels and that the chain length and saturation increase the density, speed of sound, and isentropic bulk modulus. It was also found that the higher oxides of nitrogen emission could be explained by a start of combustion advance. Half of the start of combustion advance originated from a start of injection advance of which about half is due to the automatic timing advance of the pump as it injects more fuel to compensate for the lower heating value of biodiesel and half is due to the bulk modulus, viscosity, and density of the fuel, which show significant differences from pump to pump. The other half of the start of combustion timing advance was due to the higher cetane number of the biodiesel. The higher cetane number in the soybean biodiesel advances the start of combustion and therefore contributes to the increase of the NOx. However, the cetane number of the yellow grease biodiesel was so high

that it suppressed the premixed portion of the combustion and lowered the brake specific oxides of nitrogen emission relative to soybean oil biodiesel.

1. INTRODUCTION

Biodiesel is an environmentally friendly alternative diesel fuel consisting of the alkyl monoesters of fatty acids. It is obtained from triglycerides through the transesterfication process. Triglycerides are the constituents of vegetable oils and fats and are one of the dominant means of energy storage in nature. Biodiesel can be derived from food grade vegetable oils, nonfood grade vegetable oils, animal fats, and waste restaurant greases. *Transesterfication* is a chemical reaction where the triglyceride is reacted with alcohol in the presence of a catalyst, as shown in Figure 1.1. The symbols R_1, R_2, and R_3 represent straight chain fatty acid radicals. In this reaction, the fatty acid radicals of the triglyceride molecule split away from the glycerin backbone, and the fatty acid radicals make new ester connections with the alcohol molecules, resulting in free glycerin and fatty acid esters. These fatty acid esters are known as *biodiesel.*

Biodiesel use in diesel engines reduces diesel engine exhaust emissions with the exception of nitrogen oxides (NOx). The objective of this project is to determine the reasons for the higher nitrogen oxide emissions of diesel engines fueled by biodiesel.

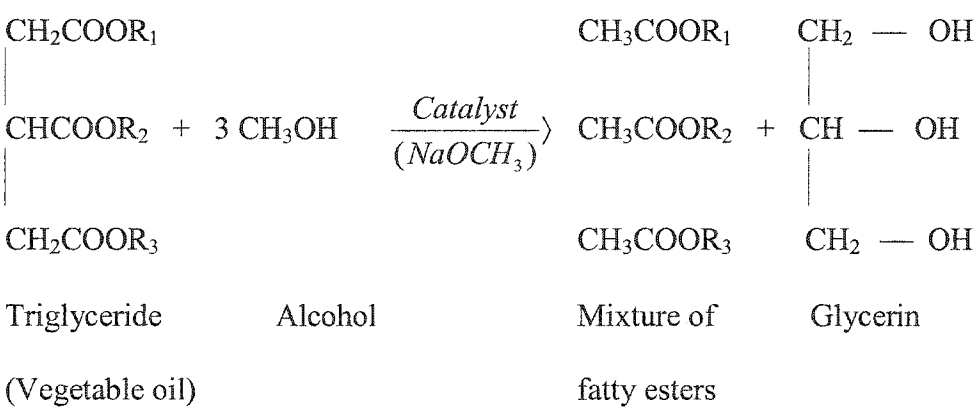

Figure 1.1. Transesterfication reaction between triglyceride and alcohol.

Biodiesel is an alternative fuel that may help to reduce the world's dependence on fossil fuels and which also has very significant environmental benefits. The reasons for these environmental benefits are that it is an oxygenate, sulfur free, and a biodegradable fuel. The presence of oxygen in the fuel leads to more complete combustion in the diesel engine. It has been reported by researchers that biodiesel has lower exhaust emissions compared with petroleum-based diesel fuel; 20% less carbon monoxide (CO) emission, 30% less hydrocarbon (HC) emission, 50% less soot emission, and 40% less particulate matter emission [1, 2, 3]. Also, since biodiesel is a sulfur-free fuel, it has 99% less sulfur oxide (SOx) emission than diesel fuel and SOx is known to be one cause of acid rain. However, biodiesel has about 10% to 15% higher NOx emissions.

Biodiesel has a low toxicity level and more than 90% of biodiesel will be biodegraded in four weeks in the case of an accidental spill [4]. In addition, biodiesel is derived from renewable resources, such as vegetable oil, and it can also be produced from waste restaurant greases and animal fats, which are difficult to dispose of. This is a major and unique advantage in terms of waste management.

Biodiesel-fueled vehicles are called non-dedicated flexible fuel vehicles because biodiesel use does not require any significant modifications to the engine, so that the engine does not have to be dedicated for biodiesel use only. It is completely soluble in commercial petroleum-based diesel fuel, so biodiesel can be used as a blend and one fuel tank can be used for storage of both fuels. This makes the vehicle flexible. This is a unique advantage compared with most other alternative fuels, because this will give users the opportunity to use the alternative fuel where and when it is available without paying any extra money for engine modifications.

Biodiesel was standardized by the ASTM in 1999 as provisional standard PS121-99 and became a full standard, ASTM D6751, in 2002 [5, 6, 7]. In Europe, the biodiesel standard is DIN V 51506 in 1994. Biodiesel is widely available in Europe and it is becoming more available in the United States. Many large engine and car manufacturers have included biodiesel fuel in their warranties [8]. Depending on the trade-off between cost and its environmental benefits, biodiesel is most commonly used in blends with No. 1 or No. 2 diesel fuels.

The advantageous features of biodiesel result from the fact that biodiesel has different physical and chemical properties than petroleum-based diesel fuel. Eleven percent of biodiesel is oxygen by weight and this results in more complete combustion. Also, it has a higher cetane number that makes the combustion smoother and the engine less noisy. However, biodiesel has higher values of viscosity, density, speed of sound, and bulk modulus that may cause injection system and combustion anomalies [9, 10, 11]. For example, the fuel density, viscosity, and compressibility have very significant effects on the diesel fuel injection system. The fuel quantity, injection timing, and injection spray pattern in the combustion chamber are directly effected by these parameters. Biodiesel's lower heating value is about 12% less than petroleum-based diesel fuel and this causes a power loss that must be compensated for by increasing the injected fuel amount. When injecting this greater quantity of fuel, some fuel injection systems start the injection earlier and hold the injection needle open longer, changing the fuel injection timing and the start of combustion timing.

The faster propagation of pressure waves caused by biodiesel's higher speed of sound and the more rapid pressure rise that results from biodiesel's greater bulk modulus may shift the injection timing settings from their optimized factory settings, leading to earlier

combustion. This can result in higher combustion temperatures and pressures causing higher nitrogen oxide (NOx) emission in the exhaust of a biodiesel-fueled diesel engine. Another reason for the combustion timing change may be the higher cetane number of biodiesel. If the cetane number is higher, this means that the ignition delay time, which is the time between the start of injection and the start of ignition, gets shorter. The start of combustion will come earlier, which tends to increase NOx, but shorter ignition delay also tends to decrease premixed combustion, which usually decreases NOx. Which effect is dominant depends on the specific situation.

Therefore, more research is required about the physical and chemical properties of biodiesel fuel and their effects on the diesel fuel injection system and diesel combustion. This project has the following specific goals.

1. Measurement of the density, speed of sound, and isentropic bulk modulus of biodiesel and its constituents at the temperatures and pressures that are representative of the diesel injection process.

2. Determination of the effect of blending biodiesel with diesel fuel on the density, speed of sound, and isentropic bulk modulus.

3. Determination of the effect of biodiesel fuel properties such as the lower heating value, density, speed of sound, bulk modulus, and cetane number on the higher NOx emissions from a diesel engine fueled with biodiesel.

Measurements of the physical properties of biodiesel at higher temperatures and pressures can supply essential information to determine fuel injection system and combustion behavior. The fuel injection system is the main determinant of diesel engine combustion. This information, combined with studies designed to isolate the effect of specific fuel

properties on the injection system, should give enough information to explain the higher NOx emission observed in diesel engine exhaust when fueled by biodiesel.

2. LITERATURE REVIEW AND BACKGROUND

In this chapter, background information about biodiesel, fuel properties, the speed of sound in hydrocarbons and petroleum oils, and biodiesel emissions is provided. The first section presents information about the chemical structure of biodiesel and the transesterfication process. The next section presents speed of sound and bulk modulus data for hydrocarbons and petroleum oils. In the last section, oxides of nitrogen emission for biodiesel are discussed.

2.1. Chemical Structure of Biodiesel and Transesterfication

Biodiesel is usually derived from vegetable oils and animal fats by a chemical process known as *transesterfication*. In order to explain biodiesel's chemical structure, it is useful to start the explanation with the chemical structure of the oils and the transesterfication process. As shown in Figure 2.1, vegetable oils and fats are composed of glycerin esters with long chain hydrocarbons as the functional ester groups. These long hydrocarbon chains are represented by R_1, R_2, and R_3 in the figure.

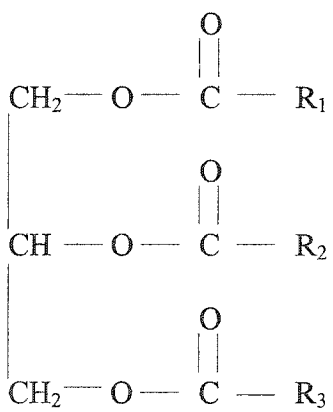

Figure 2.1 The chemical structure of vegetable oil

When detached from the glycerin (the 3 carbon chain on the left side of the molecule), these long chain hydrocarbons have acid functionality and are known as fatty acids. Up to three fatty acids can be attached to the glycerin molecule, and it is named according to the number of fatty acids that are linked to it. For example, if one fatty acid is attached to the glycerin molecule it is called a monoglyceride, if two fatty acids are attached to a glycerin molecule it is called a diglyceride, and there are three it is called a triglyceride. Vegetable oils and animal fats are composed of triglycerides, as was shown in Figure 2.1 [12 - 16].

There are many different kinds of fatty acids that differ in carbon chain length and in the number of carbon-carbon double bonds. The percentage of the different fatty acids in fats or oils varies depending on the source. Table 2.1 shows the fatty acid composition of some common vegetable oils [17]. Fatty acids compose 90% of the total mass of a triglyceride molecule. Thus, the fatty acids have the greatest impact on the physical properties of an oil. For example, when the chain length increases, the viscosity increases, and when the number of double bounds increases, the viscosity decreases [17]. As a result, any alternative fuel derived from oils should be analyzed to determine its fatty acid composition in order to characterize its physical properties.

Even though the physical and chemical properties of vegetable oils are close enough to diesel fuel to run diesel engines for short periods without any modifications, using vegetable oils in direct injection diesel engines results in severe engine deposits, dilution of the lubricating oil with unburned fuel, injector choking, piston ring sticking, and high exhaust emissions [18 - 22]. Most of these problems are a consequence of the high viscosity of the vegetable oils.

Table 2.1 Fatty acid composition in some vegetable oils (%, by weight) [17]

Fatty acid	Structure	Formula	Cotton seed	Rape seed	Safflower	Soybean	Sunflower	Peanut
Myristic	14:0	$C_{14}H_{28}O_2$	0.00	0.00	0.00	0.00	0.00	0.00
Palmitic	16:0	$C_{16}H_{32}O_2$	28.33	3.49	8.60	11.76	6.08	11.38
Stearic	18:0	$C_{18}H_{36}O_2$	0.89	0.85	1.93	3.15	3.26	2.39
Oleic	18:1	$C_{18}H_{34}O_2$	13.27	64.40	11.58	23.26	16.93	48.28
Linoleic	18:2	$C_{18}H_{30}O_2$	57.51	22.3	77.89	55.52	73.72	31.95
Linolenic	18:3	$C_{18}H_{28}O_2$	0.00	8.23	0.00	6.31	0.00	0.93
Arachidic	20:0	$C_{20}H_{40}O_2$	0.00	0.00	0.00	0.00	0.00	1.32
Behenic	22:0	$C_{22}H_{44}O_2$	0.00	0.00	0.00	0.00	0.00	2.52
Lignoceric	24:0	$C_{24}H_{48}O_2$	0.00	0.00	0.00	0.00	0.00	1.23

High viscosity causes poor atomization of the fuel in the combustion chamber [21] and affects the peak injection pressure, the injection duration, the injection pressure-time history, the spray cone angle, and the quality of atomization [23, 24]. These changes can lead to poor injection cut-off and nozzle dribble, resulting in injector choking, deposits, and high emissions [22]. Also, it is known that when the viscosity of the fuel increases, the cone angle decreases, and the diameter of the fuel droplets and their penetration increase. Thus, the liquid core of the fuel spray can touch the cylinder wall and the piston surface, causing heavy carbon deposits on the walls, piston ring sticking and breaking, and dilution of the lubricating oil [22].

Moreover, high viscosity can cause early injection due to high line pressure, which moves the combustion of the fuel closer to top dead center, increasing the maximum pressure and temperature in the combustion chamber [23, 25].

Transesterfication is a way to lower the viscosity of the vegetable oil by breaking up the triglyceride molecule and separating the fatty acid molecules from the glycerin molecule. This makes the properties of the vegetable oils and animal fats closer to diesel fuel, solving the problems due to the high viscosity of vegetable oils. Transesterfication is a reaction between an ester and an alcohol that results in a different ester [26, 27]. The transesterfication process was shown in Figure 1.1, and for convenience is duplicated here as in Figure 2.2. In this process, a triglyceride, which is itself an ester, is reacted with an excess of the stoichiometric amount of alcohol and a catalyst (KOH, NaOH, or $NaOCH_3$), and the triglyceride molecule splits into glycerin and a mixture of fatty esters.

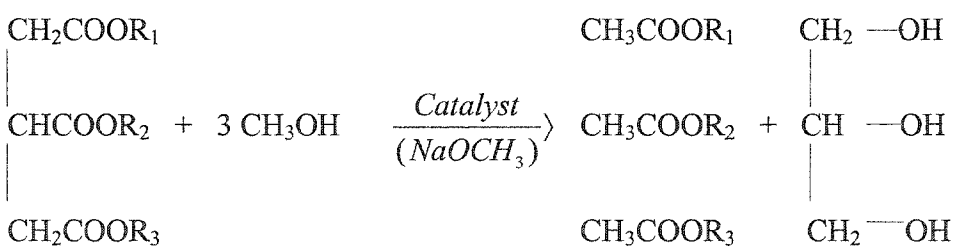

Figure 2.2 Chemical reaction of triglyceride with alcohol.

Esters are named according to the alcohol that is used, such as methanol, ethanol, or butanol, and the source of the triglyceride. If methanol or ethanol is reacted with soybean oil, it is called methyl ester of soybean oil or ethyl ester of soybean oil, or sometimes methyl or ethyl *soyate*. *Biodiesel* is a general term that covers esters from all kinds of fats and oils.

2.2. Speed of Sound for Petroleum-Based Diesel Fuel and Petroleum Oils

Speed of sound and bulk modulus data are very important in terms of fuel injection system design. The data is also scarce. In the fuel injection system, the speed of sound and the bulk modulus of the fuel have an impact on the fuel injection timing. The pressure wave propagation from the fuel injection pump to the injectors, especially in pump-line-nozzle injection systems, takes a couple of degrees of crank angle and the fuel can also show spring-like behavior related to its bulk modulus. For example, the John Deere 4276T engine has injection lines that are 0.76 m long. If the fuel is at 40 °C, the speeds of sound for No. 2 diesel fuel and soy methyl ester are 1302 m/s and 1345 m/s, respectively [11]. Simple calculations show that the speed of sound and the isentropic bulk modulus together can advance the fuel injection timing about 1° crank angle. In this section, a literature survey is presented of the literature relating to the speed of sound and isentropic bulk modulus of petroleum-based diesel fuel and petroleum oils.

Wright [28] reviewed the published data for the secant and tangent isothermal bulk modulus of petroleum oils and pure hydrocarbons. He first discussed the definitions of the isothermal and isentropic secant and tangent bulk modulus. He defined the bulk modulus as a measure of a liquid's resistance to volume reduction under pressure and the reciprocal of compressibility with units of pressure. The isothermal and isentropic bulk modulus were explained as the bulk modulus under constant temperature and constant entropy, respectively.

Isothermal and isentropic tangent bulk modulus are the thermodynamically true bulk modulus, that is the true rate of change of pressure with volume change at the pressure of interest as given by Equations 2.1 and 2.2.

$$K_T = -V\left(\frac{\partial P}{\partial V}\right)_T \tag{2.1}$$

$$K_S = -V\left(\frac{\partial P}{\partial V}\right)_S \tag{2.2}$$

Varde [29] measured the isothermal compressibility of Number 2 diesel fuel as a function of temperature at 7 °C, 24 °C, and 40 °C, and at pressures up to 150 MPa. A basic plunger-cylinder compression set up was designed to measure the P-V-T relationship. A piezoelectric transducer was used to measure the fuel pressure and a temperature compensated displacement sensor was used for piston location. The fuel sample was compressed by a fast-acting hydraulic ram with a speed of 600 MPa/s. In the publication it was reported that the isothermal bulk modulus K_T, was calculated using Equation (2.3) by recording the pressure rise and volume change.

$$K_T = \left(\frac{\partial p}{(\partial v / v)}\right)_T \tag{2.3}$$

Varde [29] also found that lowering the compression rate from 600 MPa/s to 50 MPa/s lowered the measured value of the isothermal bulk modulus.

It was concluded by Varde [29] that the isothermal bulk modulus increased almost linearly with pressure. However, at lower pressures the slope was higher than that at higher pressures. It was found that the compression rate had an effect on the bulk modulus they

measured. However, this effect was found to be much less than the pressure and temperature effect and therefore was not considered significant.

Wang et al. [30] published acoustic velocity data for petroleum oils including 3 light oils, 2 refined petroleum hydrocarbons, 5 heavy oils, and 1 live or gas-saturated oil, at temperature and pressure ranges from a minimum of 21 °C to a maximum of 117 °C and from 0 psi to 44.2 MPa, using the ultrasonic pulse transition method. It was reported that temperature and pressure have a strong effect on the speed of sound in all oils. Also, it was said that the acoustic velocity in live oils was reduced substantially by dissolved gases. Several liquid state theories and models were studied for the relationship between the speed of sound in the samples and PVT measurements. Some correlations were developed by Wang et al. [30] for acoustic velocities in dead oils with temperature, pressure, API gravities, and molecular weights. The API gravity scale was developed by the American Petroleum Institute and is an alternative method to prevent specific gravity data, as shown in Equation 2.4.

$$API\ gravity = \frac{141.5}{specific\ gravity\ of\ the\ sample\ at\ 60\ °F\ (15.5\,°C)} - 131.5 \qquad (2.4)$$

Wang et al. [30] developed an empirical equation that allows calculation of the sound velocity in oils if the API gravity is known at atmospheric pressure. Experimental results showed that, in light oils, the speed of sound increased about linearly with increasing pressure and decreased approximately linearly with increasing temperature. In heavy oils it also increased linearly with increasing pressure but decreased nonlinearly with increasing temperature. It was found that this nonlinearity was dependent on the API gravity; the nonlinearity increased with increasing API gravity.

Wang et al. [30] also measured the speed of sound in live oil at two temperatures, 23 °C and 72 °C, while dropping the pressure from 44.2 MPa (6400 psi) to about 12.8 MPa (1860 psi). They could not get any measurements lower than this pressure because the signal disappeared from the oscilloscope screen. They reported that the velocity of sound linearly decreased as the pressure dropped until the pressure reached the bubbling pressure level of the live oil, then it flattened for a while. Reducing pressure more made the signal disappear. After the measurement was done on this sample they reduced the pressure to zero and waited for 18 hours before a new measurement to let the dissolved gas out and make the same sample equivalent to a dead oil, or degassed oil, and repeated the same measurement. They concluded that dissolved gases in the fuel sample reduced the speed of sound of the oils by about 15% to 17%, explaining that the much more compressible gases increase the compressibility but do not greatly affect the density, thus the speed of sound decreases in the fuel sample. They made plots of the API gravity versus the speed of sound at temperatures of 23 °C and 80 °C, finding that there was an approximately linear relationship for the velocity decrease with increasing API gravity.

They also reported that they were able to represent oil density as a linear function of pressure and temperature that could be correlated by an equation of the form shown in Equation 2.5.

$$\rho = \rho_o(1 - AT + Bp + DpT) \tag{2.5}$$

where ρ_o is the density at atmospheric pressure and A, B, and D are correlation constants that are not given in the paper.

Moreover, correlations for velocity, pressure, temperature, specific gravity, and molecular-weight were discussed in Wang et al.'s paper. Assuming the speed of sound has a linear relationship with pressure and temperature, Equation 2.6 was used and correlation constants calculated with correlation factors better than 0.98 except for one sample that was around 0.96. When the relationship was considered to be second degree and Equation 2.7 used, the error was between 2.5% and 4.5%.

$$v = b_0 + b_1 T + b_2 p + b_3 pT \tag{2.6}$$

$$v = a_{00} + a_{01} T + a_{02} T^2 + (a_{10} + a_{11} T + a_{12} T^2) p + (a_{20} + a_{21} T + a_{22} T^2) * p^2 \tag{2.7}$$

Equation 2.8 was proposed by Wang et al. for correlation of the sound velocity as a function of temperature and molecular weight,

$$v = v_0 + k_1 (T - T_0) + k_2 [(1/M) - (1/M_0)] \tag{2.8}$$

where v is the speed of sound, T is temperature, M is molecular weight, the k's are correlation constants, and T_0 and M_0 are the property values at a reference point. For light oils this correlation was within 2% which was considered extremely good, but for heavy oils the error was 7% for one sample and 5% percent for another. Wang et al. [30] were not able to find the correlation constants of Wang and Nur's equation (Equation 2.8) for high molecular weight oils at low temperatures.

It was discussed by Wang et al. [30] that in order to be able to calculate the speed of sound from PVT relationships, it was required to have the relative volume data to be accurate to the fifth digit. However, accurate speed of sound data could be used to determine the PVT relationships with better accuracy using a equation like Equation 2.9.

$$v_{s2} = v_{s1} u^2 / [u^2 + \gamma (p_2 - p_1) v_{s1}] \tag{2.9}$$

where u is the speed of sound, v_{s1} is the specific volume at p_1, v_{s2} is the specific volume at p_2 and γ is the ratio of specific heats.

Accurate physical property data, specifically the density, speed of sound, and isentropic bulk modulus, can aid the design of fuel injection systems. Diesel engines rely heavily on the fuel injection system for power, emissions, and control. Therefore, these properties were expected to have significant effects on the diesel engine NOx and other emissions. These particular physical properties of biodiesel are significantly different from the corresponding values for petroleum-based No. 1 and No. 2 diesel fuels. This could explain the advanced injection timing and higher NOx emission observations made by some researchers [11, 31]. Biodiesel has other fuel properties that are different from petroleum-based diesel fuels such as the cetane number and volatility. Cetane number and volatility of the fuel are also very important combustion parameters that should be investigated for biodiesel with higher NOx emissions.

2.3. NO and NOx Formation Theories

In this section, the chemical kinetics of NO and NO_2 are presented. The oxides of nitrogen formation pathways such as thermal NO, prompt NO, nitrous oxide, fuel NO, and the NNH mechanism, and nitrogen dioxide formation will be discussed.

2.3.1. Thermal, or Zeldovich, NO

It was Ya. B. Zeldovich that introduced the NO formation reactions for the first time in 1946. These reactions describe the NO formation in the post flame region and are also called the thermal NO mechanism given in Reactions 2.1 and 2.2 [32, 33].

$$O + N2 \leftrightarrow NO + N \qquad (2.1)$$

$$N + O2 \leftrightarrow NO + O \qquad (2.2)$$

In 1956, Fenimore and Jones proposed a third equation in addition to those of Zeldovich suggesting that Reaction 2.3 might be more important than Reaction 2.2 for fuel rich reactions. The three equations are now known as the Extended Zeldovich mechanism [32].

$$N + OH \leftrightarrow NO + H \qquad (2.3)$$

The first reaction is the rate limiting reaction in NO formation because it has the highest activation energy, about 320 kJ/mol. Temperature is very important for the Zeldovich mechanism because of the high activation energy requirement of the first reaction and the need for dissociation of O_2. The extended Zeldovich mechanism describes the formation of NO in the post-flame gases of fuel-lean and slightly fuel-rich mixtures ($\phi < 1.2$).

2.3.2. Prompt, or Fenimore, NO

In 1970, Fenimore first described the phenomenon of "prompt NO". It is called prompt because it is initiated by rapid production of NO in a flame front where there is fuel rich mixture [34].

$$CH + N2 \leftrightarrow HCN + N \qquad (2.4)$$

$$C2 + N2 \leftrightarrow 2CN \qquad (2.5)$$

Fenimore suggested that the N-atom produced from Reaction 2.4 could form NO through Reaction 2.3. Also hydrogen cyanide (HCN) could react with oxygen and produce another atomic nitrogen. The cyanogen (CN) produced in Reaction 2.5 would react with diatomic oxygen or with oxygen atom to form nitric oxide.

Fenimore measured NO concentrations downstream of the primary reaction zone of premixed hydrocarbon and non-hydrocarbon flames. When he plotted the NO concentration against time, the nitric oxide showed linear behavior in the post flame region, but when the

measurement was extrapolated to time zero the NO concentration was non-zero. Fenimore concluded that NO was present in the reactants and the NO had formed early in the flame at a rate faster than described by Zeldovich mechanism. He also observed that the prompt NO was seen only in hydrocarbon flames, it was very weakly dependent on temperature, and increased as the equivalence ratio increased.

2.3.3. The Nitrous Oxide (N_2O) Route

First proposed by Malte and Prade (1974) [35], there is another pathway by which atomic oxygen and molecular nitrogen can produce NO via the intermediate formation of N_2O through a "recombination reaction"

$$O + N_2 + M \leftrightarrow N_2O + M \qquad (2.6)$$

where M is called a collision partner and represents all the molecules present. The N_2O then reacts with atomic oxygen and atomic hydrogen to produce NO.

$$O + N_2O \leftrightarrow NO + NO \qquad (2.7)$$

$$H + N_2O \leftrightarrow NO + NH \qquad (2.8)$$

NO formation via the nitrous oxide pathway is more complicated than thermal NO but not as complicated as prompt NO.

2.3.4. The Fuel NO

Some fuels, such as coals and heavy oils, may have molecules that contain from 0.7% to 2.5% bound nitrogen organic molecules. NH_3 derivatives may be contained, where the H atoms are replaced by organic radicals with N atoms. The amount of fuel NO is dependent on the amount of nitrogen in the fuel and the rate of NO formation is strongly affected by the rate of fuel air mixing [32, 36].

2.3.5. The NNH Mechanism

Some combustion processes include reactions between diazanul (NNH) and atomic oxygen, and based on the concentration of NNH this mechanism can contribute significantly to NO production.

$$O + NNH \leftrightarrow NO + NH \quad (2.9)$$

It was suggested by Bozzelli and Dean [37] that sufficiently high concentrations of NNH can occur when Reaction 2.10 is equilibrated.

$$NNH \leftrightarrow N_2 + H \quad (2.10)$$

During combustion, hydrogen builds up and equilibrium is achieved at the flame front. Then, the NNH concentration increases and undergoes reaction with oxygen atom to form NO following Reaction 2.9.

2.3.6. Nitrogen Dioxide (NO_2) Formation

In combustion flue gas, the concentration of NO_2 is generally not more than 5% of the NOx concentration [32].

$$2\,NO + O_2 \leftrightarrow 2\,NO_2 \quad (2.11)$$

$$NO + HO_2 \leftrightarrow NO_2 + OH \quad (2.12)$$

It has been claimed that Reaction 2.11 is too slow to be significant at typical NO concentrations in industrial applications [38, 39]. Reaction 2.12 is the faster path for NO_2 formation. Reaction 2.12 is important when HO_2 concentration is high between 600 -1000K. At higher temperatures, HO_2 dissociates to atomic H, O_2, and OH and leads to destruction of NO_2 by the following reactions.

$$O + NO_2 \leftrightarrow NO + O_2 \quad (2.13)$$

$$H + NO_2 \leftrightarrow NO_2 + OH \quad (2.14)$$

$$OH + NO_2 \leftrightarrow NO + HO2 \quad (2.15)$$

Thermal NO is the dominant mechanism in diesel combustion. Engine and fuel parameters will be studied in this research, in terms of their effect on temperature as this is the main determinant of thermal NO

2.4. Biodiesel Engine Emission Tests

In this section biodiesel emissions will be discussed. Researchers have published data for biodiesel emissions obtained with different engines and vehicles, and with different test procedures. In this section a brief overview will be presented about the biodiesel emissions obtained with steady state engine test cycles, transient engine test cycles, and chassis dynamometer vehicle test cycles.

2.4.1. Steady State Engine Test Results

Monyem et al. [40] investigated the effect of injection timing on biodiesel emissions. They used a John Deere 4276T lightly turbocharged diesel engine fueled with oxidized and nonoxidized neat biodiesel, No. 2 diesel fuel and 20% biodiesel blends of these two biodiesels with No. 2 diesel fuel. They measured exhaust emissions and engine performance while changing the injection timing at light and full load engine conditions, and at a single engine speed of 1400 rpm. They varied the fuel injection timing as 3° advanced, standard, and 3° retarded. They reported that the engine performance and the thermal efficiency were about the same with biodiesel and diesel fuels. However, they observed that NOx emissions increased from 0.5% to 18% for the two neat biodiesel fuels and for the biodiesel blends at all injection timings, relative to the base diesel fuel. Similar to full load, the light load

biodiesel NOx emission increased at standard and 3° advanced injection timing, but was reduced at the 3° retarded injection timing. They found a linear relationship between NOx emission and injection timing. The retard (delay) of injection timing lowered the NOx emission for all the biodiesel fuel samples. They pointed out that there was a NOx emission reduction of 35% to 43% for all biodiesel fuel samples at 3° retarded injection timing relative to the 3° advanced injection timing for the same fuel at the same load and speed condition. The most significant finding was that when biodiesel and diesel fuel were compared at the same start of combustion timing, the biodiesel had less NOx emission than diesel fuel.

Monyem et al. [40] also reported that the actual injection timing was advanced about 2.3° for the neat biodiesel fuels compared to diesel fuel at the same fuel injection pump setting. The timing advance was attributed to the physical property differences between biodiesel and diesel fuel.

Feldman and Peterson [41] optimized a diesel engine for methyl ester of rapeseed oil by varying the fuel injection timing and fuel injection pressure. They found that rapeseed oil ester had a shorter ignition delay, a more gradual pressure rise, smoother combustion, and a lower maximum pressure than diesel fuel. They noted that advancing the injection timing increased the power output and lowered the smoke level and increasing the fuel injection pressure decreased the fuel quantity per injection and thus was not considered satisfactory for the diesel engine due to increased internal pump leakage. They concluded that the diesel engine can be tuned for biodiesel fuel using fuel injection timing, and they also pointed out that biodiesel use lowered the exhaust temperature below the value for diesel fuel, which they considered as a potential reason for the reduction in NOx emission observed in their tests.

Senatore et al. [42] analyzed the performance and emissions of a turbocharged DI diesel engine fueled with biodiesel and diesel fuel. They paid particular attention to a comparative analysis of the combustion process. They noticed that the concentrations of nitrogen oxides increased about 20%, and that the heat release occurred 3-5 degrees of crank angle earlier with biodiesel fuel than with diesel fuel at all conditions. They found that both instantaneous injection pressure and injection needle lift showed greater advance with biodiesel. They proposed two reasons for this, the first was the higher density of biodiesel, and the second was the different quantity of injected fuel mass per cycle.

2.4.2. Transient Engine Test Results

McCormick et al. [43] examined the effect of biodiesel source material and chemical structure on the regulated emissions from a heavy-duty diesel engine. They specifically focused on the impact of biodiesel's fatty acid chain length and the number of double bonds on the emissions of oxides of nitrogen (NOx) and particulates (PM). Seven biodiesel fuels produced from different feedstocks and 14 different pure fatty acid esters, which are the constituents of biodiesel fuels, were tested. A heavy-duty truck engine was tested and the U.S. E.P.A. heavy-duty Federal Test Procedure was used.

McCormick et al. found that the molecular structure of biodiesel can have a significant effect on diesel engine emissions. They pointed out that density, cetane number, and iodine number are highly correlated with each other and increasing density and decreasing cetane number increased NOx emission. They found that increasing the number of double bounds can be correlated with increased NOx emission. The NOx increase could not be explained by the normal NOx/PM tradeoff and so was not thought to be associated with thermal NO formation. They observed that NOx emission increased with decreasing

chain length for fully saturated fatty acid esters. They reported no significant difference in NOx and PM emission of methyl and ethyl esters of identical fatty acid distribution biodiesel fuels.

McCormick et al. [44] investigated fuel additive and blending approaches to find a solution to the problem of higher NOx emission of diesel engines when fueled with neat biodiesel or a 20% blend with petroleum diesel fuel. Testing was completed with a 1991 DDC Series 60 truck engine using the U.S. heavy-duty Federal Transient Test Procedure (FTP) defined by the EPA. The blending approach was conducted with the following test fuels.

- 10% aromatic diesel fuel
- Zero aromatic Fisher-Tropsch (FT) diesel
- Biodiesel produced from soybean oil
- Biodiesel produced from yellow grease
- Certification fuel with aromatic content of 31.9%

The additive approach was conducted with the following additives:

- Di-tert-butyl peroxide (DTBP)
- 2-ethyl-hexyl nitrate (EHN)
- Ferrocene

Their results are presented in Table 2.2. They found that the 10% aromatic fuel showed 12% lower PM and 6% lower NOx than the EPA emissions certification fuel. The zero aromatic Fisher-Tropsch diesel fuel showed the lowest emission with 33% lower PM and 16% lower NOx. They also tested a B20 blend of biodiesel from soybean oil. Blending lowered the aromatic content of the base certification fuel from 31.9 to 7.5%, decreasing the NOx by 6.5%. They found that if all other factors are equal, when the base fuel with 25.8% aromatic was blended with 20% biodiesel fuel (B20), it would give NOx emissions that were neutral to B20 made with regular certification diesel fuel. They also suggested that blending

up to 55% biodiesel with zero aromatic Fisher-Tropsch (FT) diesel may produce NOx equal to a B20 blend with certification diesel fuel. Cetane improvers di-tert-butyl peroxide and 2-ethyl-hexyl nitrate were found to be effective for NOx reduction with B20. Ferrocene had no effect on the NOx emission.

Table 2.2 Effect of various strategies for NOx reduction from blends of 20% soydiesel in certification diesel, NOx=g/bhp-h [44].

Additive	NOx	% Reduction*	Significance (p-value)
Certification Diesel	4.85	---	---
B20 (soy + cert)	4.93	---	---
46% FT diesel	4.85	1.62	Predicted
10% Aromatic base	4.61	6.49	<0.001
1% DTBP	4.75	3.65	0.030
0.5% EHN	4.83	2.03	<0.001
500 ppm Ferrocene	4.82	2.24**	0.018

* Relative to B20 (soy + cert)
** Also caused an increase in PM

Sharp et al. [45] investigated the effect of biodiesel fuels on transient emissions from three modern diesel engines, as shown in Table 2.3. 100% neat biodiesel (B100), 100% neat diesel fuel, and a 20% blend of biodiesel in diesel fuel were used in the study. A summary of their emissions results is given in Table 2.4. They found lower emissions of HC, CO, and particulate with B100 and B20 biodiesel fuels. Particulate emissions were about 25 to 50% lower and NOx was increased about 13% with B100 and 4% with B20 fuel, depending on the engine. They pointed out that the NOx emissions of the B5.9 engine were not significantly affected by biodiesel fuel. Although there was an increase in NOx emissions, it was not as high as for the other two engines. It was discussed that the oxygen content in biodiesel may be responsible with the NOx increase. However, the B5.9 engine's smaller NOx emission

increase could not be explained by the oxygen content of biodiesel. The B5.9 engine had a pump-line-nozzle fuel injection system that operates at much lower fuel injection pressures than the electronic unit injector systems used on the other two engines but it isn't clear why this would affect the NOx levels.

They concluded that the difference in the fuel injection system would create differences in the injection characteristics, such as atomization and penetration rate, and this could have a role in NOx emission of biodiesel. They also mentioned that neat biodiesel generally causes about 8% power loss while B20 causes about 2% loss. The transient cycle fuel consumption was about 13% worse with neat biodiesel (mass basis).

Table 2.3. Test Engines [45]

Engine		Rated Power, kW	Application
1997		276	Highway Truck
1997	DDC	205	Urban Transit Bus
1995		119	Full-Size Pickup Truck

Table 2.4. Exhaust Emissions (g/hp-hr) Data for Three DI Diesel Engines [45].

Test Engine	Test Fuel	HC	CO	Total PM	NOx	Relative increase in NOx to 2-D
Cummins N-14	B100	0.01	0.41	0.076	5.17	13% more NOx
Cummins N-14	B20	0.19	0.64	0.102	4.76	4% more NOx
Cummins N-14	2-D	0.23	0.75	0.106	4.57	
DDC Series 50	B100	0.01	0.92	0.052	5.01	11% more NOx
DDC Series 50	B20	0.06	1.38	0.088	4.66	3.5% more NOx
DDC Series 50	2-D	0.06	1.49	0.102	4.50	
Cummins B5.9	B100	0.08	1.27	0.081	4.90	4.25% more NOx
Cummins B5.9	B20	0.21	1.61	0.109	4.79	1.9% more NOx
Cummins B5.9	2-D	0.31	2.05	0.128	4.70	

2.4.3. Chassis Dynamometer Tests

Peterson et al. [46] investigated the effect of biodiesel feedstock on the regulated emissions for chassis dynamometer tests of a pickup truck. They tested a total of 13 fuel samples including Philips D2 low sulfur diesel, six different biodiesel fuels from coconut oil, used hydrogenated soy oil, rapeseed oil, mustard oil, safflower oil, and soy oil, and their 20% blends with Phillips D2 diesel fuel. The fuels had iodine numbers that ranged from 8 to 133. They pointed out that even though most studies showed NOx increases and particulate matter reductions with biodiesel fuel, their research with a PTO dynamometer showed decreases in the oxides of nitrogen and increases in particulate matter with biodiesel even though the same engine was tested. A 1994 Dodge 2500 pickup truck with a Cummins 5.9L turbocharged and inter-cooled direct injection diesel engine was used. They found that lower iodine numbers, which means fewer double bonds and a more saturated feedstock, could be correlated with lower NOx. They recorded that when the iodine number increased from 8 to 129.5, the NOx increased 29.3%. They were able to use a linear relationship to correlate iodine number and NOx emission with an R^2 of 0.091. They also concluded that increasing iodine number did not affect the other regulated emissions of HC, CO, CO_2 and PM for either hot start or cold start tests.

Peterson et al. [46] also found that small increases in the amount of total glycerin lowered the heat of combustion and viscosity. Total glycerin includes the glycerin attached to the unreacted mono- and diglycerides and the free glycerin molecules due to insufficient separation during biodiesel production. They also observed that an increase in the number of double bonds increased the viscosity, density, and heat of combustion of the sample. They added that transesterification was more difficult with the lower chain length feedstock.

Peterson and Reece [47] performed research on the emission characteristics of ethyl and methyl esters of rapeseed oil (RME and REE) compared with low sulfur diesel fuel in a chassis dynamometer test of a 1994 pickup truck with a Cummins 5.9 L turbocharged, intercooled direct injected diesel engine. They found that neat methyl and ethyl esters of rapeseed oil reduced HC, CO, and NOx emissions 52.4, 47.6, and 10.1%, respectively. However, CO_2 and particulate emissions increased 0.9 and 9.9%. Neat REE produced about 8.7% less HC, 4.3% less CO, and 4% less NOx than neat RME.

Peterson and Reece [48] measured the emissions of rapeseed oil biodiesel with and without a catalytic converter. Two pickup trucks with Cummins 5.9 L turbocharged and intercooled direct injected diesel engines were used, and tests were conducted at the Los Angeles Metropolitan Transit Authority Emission Testing Facility in two different years of 1994 and 1995. In 1994, the catalytic converter was not available. However, the 1995 tests were conducted with and without a converter. They found that CO_2 and PM emissions increased and HC and CO emissions decreased as the REE was increased in the fuel blend. It was also found that NOx decreased as the percentage of REE increased in the fuel blend with the catalytic converter installed. However, NOx increased for 20 and 50% REE and declined with 100% REE without the catalytic converter.

NOx emissions were reduced about 12% compared with diesel fuel for both the 1994 and 1995 tests. PM emissions were increased 17% and 43% compared to diesel fuel emissions in 1994 and 1995 tests. It was also concluded that 100% REE produced HC emissions that were only 47% that of diesel in 1994 and 38% in 1995 and CO emissions that were 47% that of diesel and 65% that of diesel in 1994 and 1995. 20% REE CO emission was 65% that of diesel in 1994 and 82% of diesel in 1995.

Peterson and Reece [48] observed that 100% RME produced 10.5% more HC, 3.7% more NOx, and 5.8% more PM than 100% REE. They also noted that the 1995 data were 37% lower in HC, 5.5% lower in CO_2, and 48% lower in PM compared to the 1994 data. Carbon monoxide was 18.1% less for diesel and 14.1% higher for 100% REE in 1995 relative to 1994. The catalytic converter was effective for HC and PM emissions only. The catalytic converter lowered the HC emission about 9% and reduced the PM emission by 43.4%. However, the converter had almost no effect on the other compounds. They found that, at cold start, all biodiesel emissions increased; the HC, CO, NOx, CO_2, and PM were higher by 95.7%, 94.7%, 35.5%, 14.7%, and 57.9% than diesel fuel, respectively.

At this point it can be concluded that the NOx emission of biodiesel is higher than regular diesel fuel for steady state and transient engine dynamometer (FTP) tests. However, the NOx emission of biodiesel is lower than regular diesel fuel for chassis dynamometer tests. The biggest difference in chassis dynamometer tests is that the average load is much less than for the FTP transient and the steady state engine tests. It has been observed and will be shown later in this dissertation that biodiesel doesn't give higher NOx emission at light load conditions. Different reasons for this can be considered such as the start of injection and combustion could be delayed and this could be lowering the combustion temperature and the NOx emission or at light loads and (lower temperatures) the combustion kinetics of biodiesel would be different.

3. EXPERIMENTAL METHODS AND APPARATUS

In this chapter, the equipment that was used, the modifications that were made to the equipment, and the procedures that were followed for this study are discussed. The chapter is divided into three sections. In the first section, the speed of sound and density measurements are described. In the second section, the diesel engine and the emission measurement equipment are introduced. In the last section, information about the data acquisition system and the engine test schedules are given.

3.1. Density and Speed of Sound Measurements

In this research, the speed of sound and density were measured in the thirty fuel samples listed in Table 3.1, at atmospheric pressure to 32.5 MPa, and at temperatures of 20, 40, 60, 80, and 100 °C. In addition to the thirty fuel samples, the speed of sound and density were measured for biodiesel from soybean oil and its blends with No. 2 and No. 1 diesel fuel at 20 °C and 40 °C and from atmospheric pressure to 32.5 MPa to see the effect of blend level on the density and speed of sound. The blends tested are listed in Table 3.2. The isentropic bulk modulus for the fuels and fuel blends was also calculated at each pressure and temperature level using Equation 3.1 [49, 50].

$$\beta = c^2 \times \rho \tag{3.1}$$

where β is the isentropic bulk modulus in Pascal, c is the speed of sound in the sample in m/s, and ρ is the density in kg/m^3.

As shown in Table 3.1, the thirty fuel samples included sixteen fatty acid alkyl esters or simple mixtures of esters, ten biodiesel fuels produced from vegetable oils or animal fats, three pure hydrocarbons, and a sample of emissions certification grade No. 2 diesel fuel. Additional information about the physical and chemical properties of the samples are given in Appendix A in Tables A1-A4.

Table 3.1 Fuel samples.

Alkyl Monoesters of Fatty Acids			
1	Methyl Butyrate	9	2:1 Methyl Linseed Methyl Stearate
2	Methyl Laurate	10	Ethyl Butyrate
3	Methyl Palmitate	11	Ethyl Caprylate
4	Methyl Stearate	12	Ethyl Stearate
5	Methyl Oleate	13	Ethyl Linoleate
6	Methyl Linoleate	14	Ethyl Linseed
7	Methyl Linolenate	15	Isopropyl Palmitate
8	2:1 Methyl Stearate Methyl Linseed	16	Isopropyl Stearate
Alkyl Esters of Vegetable Oils and Animal Fats			
17	Methyl Oxidized Soy	22	Methyl Yellow Grease
18	Methyl Hydrogenated Soy	23	Methyl Tallow
19	Methyl Lard	24	Ethyl Oxidized Soy
20	Methyl Canola	25	Ethyl Hydrogenated Soy
21	Methyl Soy Gold	26	Ethyl Soy Ester
Hydrocarbons and Diesel Fuel			
27	n-Octadecane	29	n-Dodecane
28	n-Hexadecane	30	Certified D2 Diesel Fuel

Table 3.2 Biodiesel and its blends with No. 2 and No. 1 diesel fuels

No. 2 Diesel Fuel Blends		***No. 1 Diesel Fuel Blends***	
1	**100% Biodiesel**	1	**100% Biodiesel**
2	75% Biodiesel w/ No.2 Diesel Fuel	6	75% Biodiesel w/ No.1 Diesel Fuel
3	50% Biodiesel w/ No.2 Diesel Fuel	7	50% Biodiesel w/ No.1 Diesel Fuel
4	20% Biodieselw/ No.2 Diesel Fuel	8	20% Biodieselw/ No.1 Diesel Fuel
5	No.2 Diesel Fuel	9	No.1 Diesel Fuel

In order to measure the speed of sound in the fuel samples, the pulse echo technique was used [50-56]. A pressure vessel with a piston and cylinder assembly for raising the pressure was fabricated and an ultrasonic transducer was located at the bottom of the vessel as shown in Figure 3.1. A Panametrics Model 5072 PR general purpose ultrasonic pulser/receiver and a Panametrics 10 MHz video scan immersion transducer (Waltham, MA) were used. Signals were captured with a Hewlett Packard Model 54601A 100 MHz, 4 channel digital oscilloscope (Colorado Springs, CO). System pressure was measured using a Sensotec Model 2 Z/1108-04Z9 pressure transducer (Columbus, OH). To obtain elevated temperatures the entire pressure vessel was submerged in a temperature-controlled mineral oil bath.

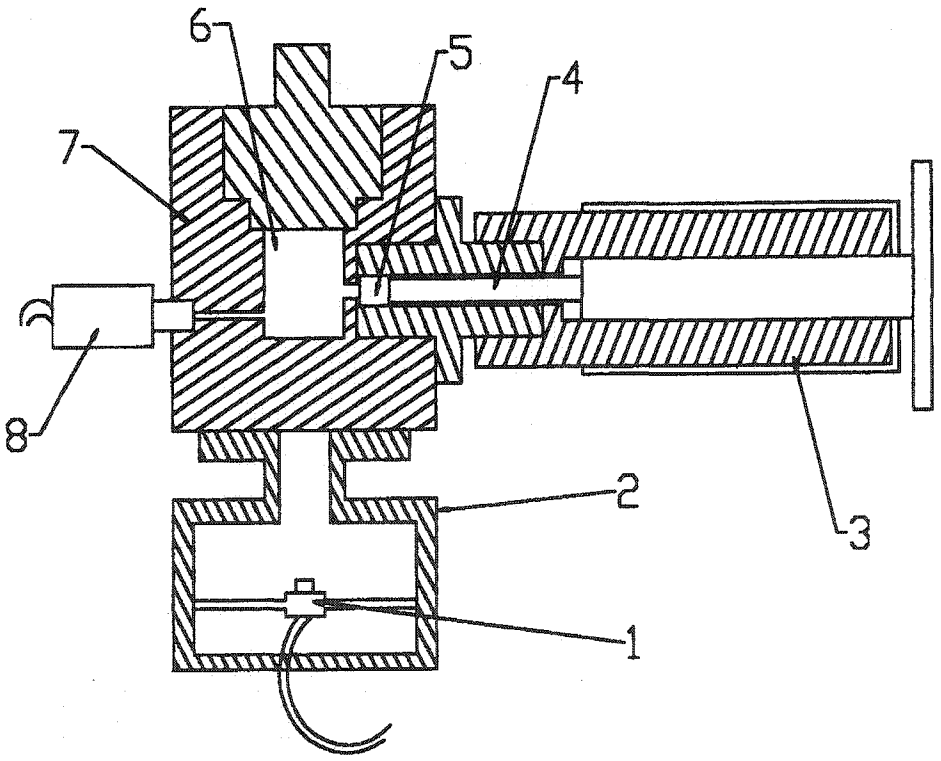

Figure 3.1 Cross Section of the Pressure Vessel. [1 = 5MHz ultrasonic transducer, 2 = cooled chamber for transducer, 3 = pressure screw, 4 = plunger, 5 = piston, 6 = sample chamber, 7 = pressure vessel, 8 = pressure transducer.]

The speed of sound was determined by measuring the time difference between the ultrasound echo reflected back to the transducer from the interface where the signal passed from the pressure vessel into the sample fluid, called the first echo, and from the reflection when the signal left the sample and reentered the vessel wall, called the second echo. A diagram showing the echoes is given in Figure 3.2. The distance traveled by the sound wave during this time period, which is two times the sample thickness, was divided by the elapsed time to give the speed of sound in the fluid.

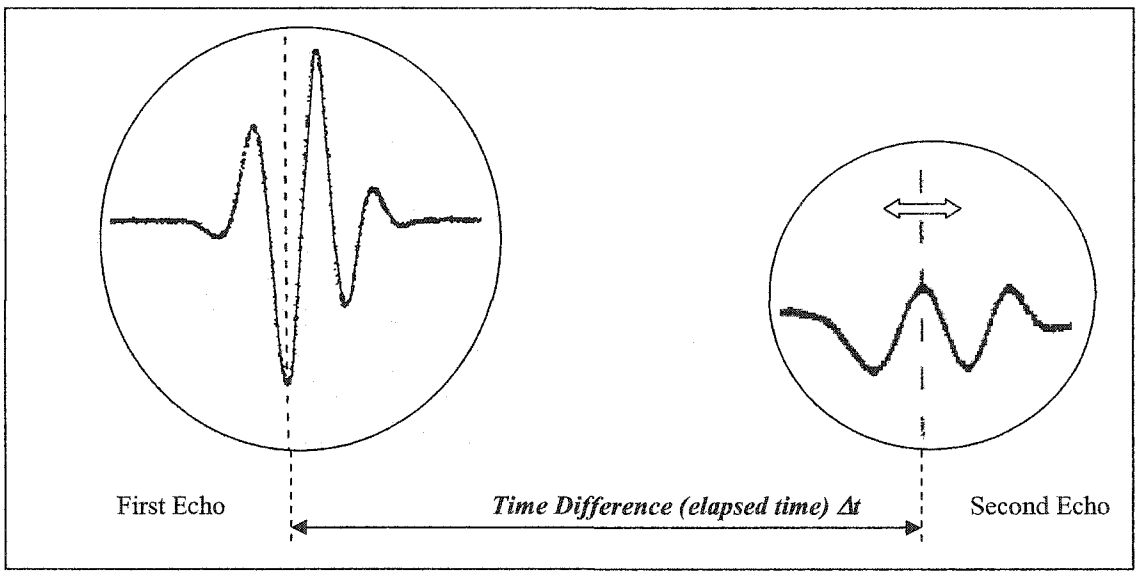

Figure 3.2 Ultrasonic Signals

The first echo was a stationary echo with a fixed time delay from the zero trigger event. It was identified using calculations based on the speed of sound in water and stainless steel. The second echo was found from observation and was the only echo that moved with pressure fluctuations in the cell. After finding the second echo, the elapsed time was recorded starting with the atmospheric pressure level. Then, the pressure level in the cell was raised to 34.5 MPa and lowered to atmospheric pressure in 6.9 MPa steps.

Density measurements were conducted in two steps. The first step was to measure densities at atmospheric pressure and the second step was to measure densities at elevated pressures. For the first step, densities were measured at atmospheric pressure and at temperatures from 20 °C to 100 °C in 20 °C temperature increments using a modified specific gravity balance (Troemner Company, Philadelphia, PA). A copper cylinder to hold the sample and a small constant temperature bath were adapted to the balance. The temperature in the cylinder was monitored with a thermocouple. A detailed explanation of this measurement was given in reference 12. At each temperature level, 4 consecutive measurements were taken and then the entire temperature sequence was repeated a second time. Therefore, at atmospheric pressure, 8 measurements were obtained. The balance was calibrated with distilled water to 1.0000 at 15.5 °C before each set of measurements.

For the second step, density measurements were taken simultaneously with the speed of sound measurements by using a vernier to show the piston location in the cylinder to calculate the relative fuel volume under pressure. As the sample pressure was raised using the piston and cylinder, the piston position was used to calculate the volume change. Since the sample mass was constant, the volume change was used to determine the density change. This density change was added to the density measured during the first step to get the density at the elevated pressure. A correction was calculated for the expansion of the vessel at high pressure and high temperature, although this was small for all of the data presented here.

Figure 3.3 shows the complete experimental setup. The adjustment screw for raising the sample pressure is visible extending from the right side of the stainless steel pressure vessel. The metal housing on top of the pressure vessel contains the ultrasonic transducer and provides the cooling the transducer needs to stay below 50°C. Figure 3.4 shows an end

view of this housing looking into the transducer. The adjustable supports for the transducer are visible in this view. They allow the transducer to be aligned for maximum signal strength.

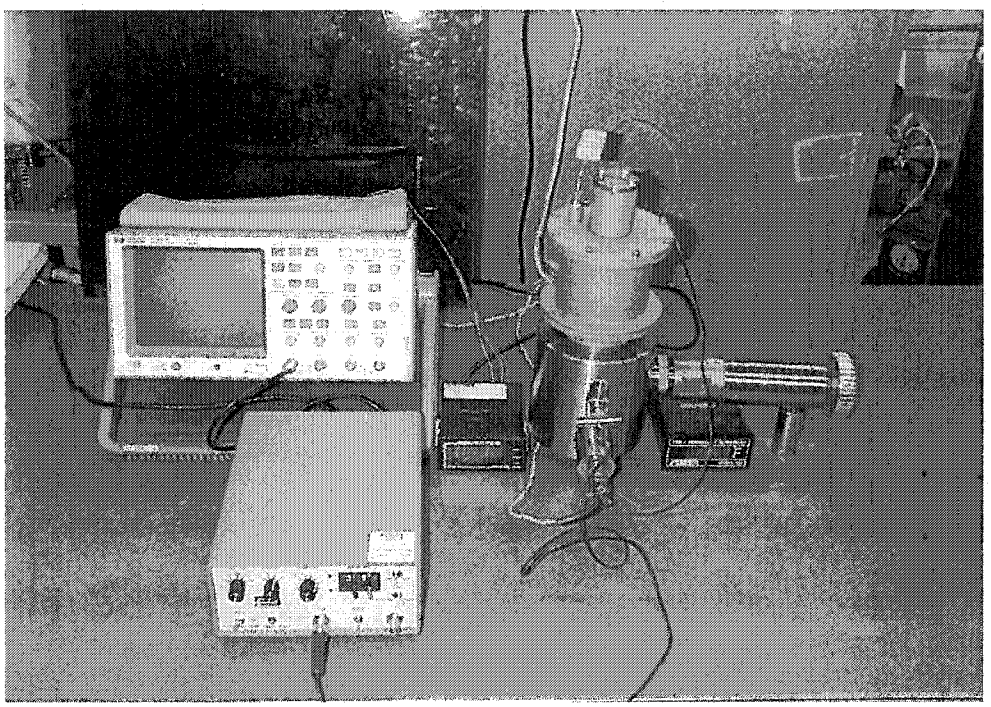

Figure 3.3. Experimental apparatus for ultrasound measurements.

The two primary concerns with the use of the pressure vessel technique for density measurement were ensuring that air bubbles were eliminated from inside the vessel and that no fluid leaked from the vessel during the test. If air bubbles were present, their presence was expected to cause variations in the measurements as the pressure vessel was filled, emptied, and refilled again. Thus, the pressure vessel was filled with the sample fluid two times and each time two sets of data were collected as the pressure was varied. Half of the measurements were collected while increasing the pressure and half while decreasing the pressure. This was to identify leakage from the chamber or any other hysteresis effects. Thus, a total of four data points were collected for each pressure and temperature level.

Subsequent analysis showed no statistically significant difference between the measurements associated with different filling operations or with measurements taken while increasing or decreasing the pressure. Therefore, all 4 measurements were averaged and included in the confidence limit calculations. All measurements were taken from 20 °C to 100 °C except for methyl palmitate, methyl stearate, the 2:1 mixture of methyl stearate and methyl linseed, methyl hydrogenated soy, ethyl hydrogenated soy, ethyl stearate, and n-octadecane, which were solid at 20 °C. The lowest temperature at which measurements were taken for these esters was 40 °C.

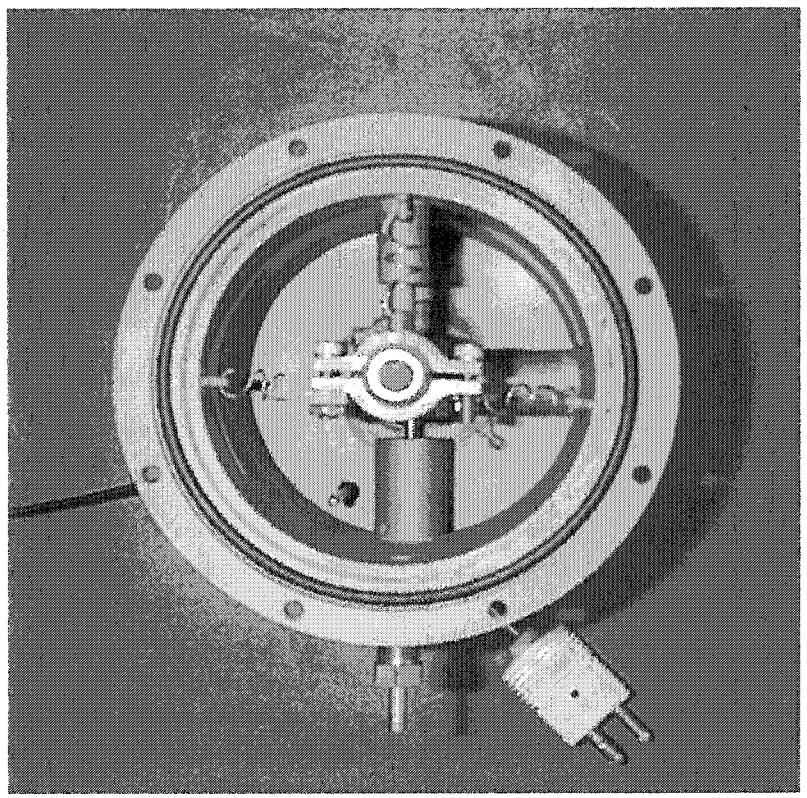

Figure 3.4 End view of ultrasonic transducer showing alignment screws.

3.2 Validation of the Measurement Technique

The literature contains an extensive amount of very accurate data for the speed of sound in distilled water. These data were used as a reference to validate the speed of sound measurement technique [57-63]. In this study, comparisons were also made with dodecane because it is much more compressible than distilled water and is more representative of the behavior expected of the biodiesel samples. This means that the speed of sound and density show greater variability and sensitivity to temperature and pressure changes.

Reagent water was purchased from Aldrich and was freshly boiled and cooled before the density and speed of sound measurements, in order to lower the dissolved air amount in the distilled water to reach the standard point. Dodecane was purchased from Aldrich with a purity of 99+%.

The density measurements at atmospheric pressure were compared with literature values and representative comparisons are provided in Table 3.3. The speed of sound and density measurements at higher temperatures and pressures, using the pressure vessel, were compared with the reference values and the maximum deviations are listed in Table 3.4. In the tables, the percentage error was calculated using Equation 3.2.

$$Percentage\ Error = \left(\frac{Measurement\ Result - Literature\ Value}{Literature\ Value} \right) * 100 \qquad (3.2)$$

The density, speed of sound, and isentropic bulk modulus data comparisons for water and dodecane are summarized in Table 3.4 with the maximum errors at the temperature and pressure levels. Although the results were in very good agreement for water, the deviations with dodecane were larger. This is due to the greater property changes with hydrocarbons and perhaps to the lower reliability of the published data for this compound.

Table 3.3 Atmospheric pressure density measurement comparisons for some of the samples with their maximum differences.

Samples	**Measured Value (g/cm^3)**	Literature Value	% error	Temperature	Reference
Water	0.9730	0.9716-0.9718	0.14-0.12	80°C	20,21
Dodecane	0.7482	0.7487-0.7491	-0.06-0.12	20°C	22,23
Methyl Laurate	0.8094	0.8073	0.26	100°C	23
Methyl Palmitate	0.8075	0.8065	0.12	100°C	23
Methyl Stearate	0.8213	0.8210	0.04	80°C	23
Methyl Butyrate	0.8970	0.8980	-0.11	20°C	23
Ethyl Butyrate	0.8156	0.8147	0.11	80°C	23
Ethyl Caprylate	0.8658	0.8672	-0.16	20°C	23

Table 3.4 Maximum Errors in Water and Dodecane measurement comparisons at higher temperatures and pressures.

Properties	Water		Dodecane	
Density	-0.19%	60 °C, 34.4 MPa	0.24%	60 °C, 34.4 MPa
Speed of Sound	0.19%	80 °C, 34.4 MPa	0.68%	100 °C, 1 Atm
Isentropic Bulk Modulus	0.19%	80 °C, 34.4 MPa	1.41%	100 °C, 1 Atm

3.3 Diesel Engine Setup and Emission Measurement Equipment

A four stroke, four cylinder, turbocharged, direct injected John Deere 4045 T diesel engine was used for this research. The engine had a bowl-in-piston combustion system and a distributor-type fuel pump, manufactured by STADYNE with model # D8 DB 44 29-5415. The engine had fuel injectors with four 0.305 mm diameter holes with an opening pressure of 250 bar. The basic specifications of the engine are given in Table 3.5. A 112 kW General Electric model TLC2544 direct current dynamometer was used to load and motor the engine.

Table 3.5 John Deere 4045T diesel engine specifications

Bore	106.5 mm
Stroke	127.0 mm
Connecting Rod Length	203.0 mm
Compression Ratio	17.0:1
Maximum Power	66.5 kW at 2200 rpm
Peak Torque	374 N-m at 1200 rpm

Engine temperatures were measured at nine different points during the engine runs, and these points are given in Table 3.6. The engine's turbocharger boost pressure and lubricating oil pressure were monitored with Bourdon pressure gages. Engine intake air flow rate was measured using a Meriam laminar flow element and the engine fuel flow rate was measured using a digital scale and a stopwatch.

Table 3.6 Engine temperature measurement points

1. Engine Oil Temperature	4. Building. Cooling Water Outlet Temperature
2. Engine Cooling Water Outlet Temperature	6. Intake Air Temp
3. Engine Cooling Water Inlet Temperature	7. Intake Manifold Temp.
4. Building. Cooling Water Inlet Temperature	8. Exhaust Temp.

The engine exhaust emissions of the diesel engine were measured using the following emission instruments:

- Rosemount Analytical, Inc., model 755R paramagnetic O_2 measurement system
- Rosemount Analytical, Inc., model 880A non-dispersive infrared CO analyzer
- Rosemount Analytical, Inc., model 880A non-dispersive infrared CO_2 analyzer
- J.U.M. Engineering, model VE7, flame ionization detector (FID), HC analyzer
- Beckman Industrial Corp., model 955 chemiluminescent NO/NOx analyzer
- Robert Bosch GMBH, model ETD02050 smoke meter

Calibrations of the analyzers were done and these calibration curves are given in Appendix B. Using these calibration curves, the measurement errors were lowered to less than two percent as is recommended in the exhaust emission bench manual. The schematic of the exhaust emission measurement setup is illustrated in Figure 3.5.

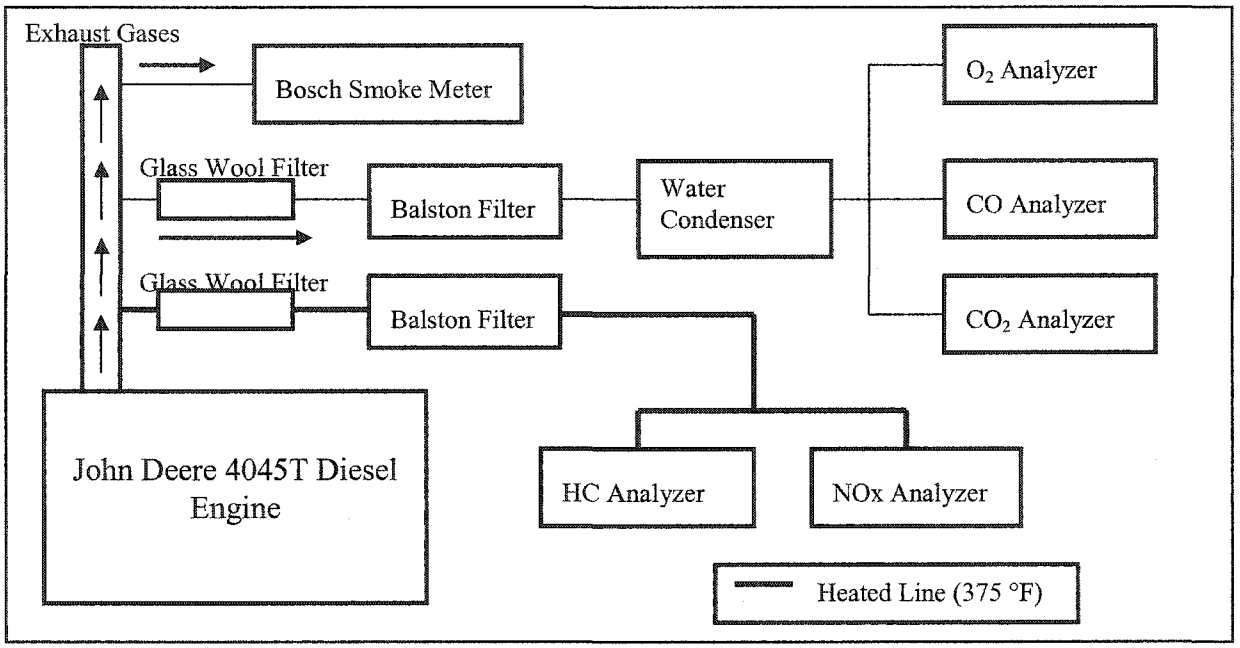

Figure 3.5 The schematic diagram of the exhaust emission setup

3.4 Data Acquisition System and Test Schedule

The fourth cylinder of the John Deere 4045T diesel engine was instrumented with a cylinder pressure transducer, a fuel injection line pressure transducer, and a needle lift sensor, which was installed on the fourth cylinder injector. The cylinder pressure and the fuel injection line pressure of the engine were measured with Kistler Model 6121B and 6230M1 quartz crystal pressure transducers, respectively. Detailed information about the transducers and their calibration curves are given in Appendix C. The signals from the transducers were amplified by two PCB Piezotronics Model 462A amplifiers. The needle lift sensor was

donated by the John Deere Product Engineering Center, and it was a Bentley-Nevada type sensor coupled with a Bentley-Nevada Proximitor 3300 Ram amplifier. These three sensors were connected to a National Instruments model AT-M10-16E-10 data acquisition PC board, and controlled using the Labview program. The Labview program started data collection with two sets of needle lift sensor data, then two sets of fuel injection line pressure data, ten sets of cylinder pressure data collection, two more sets of fuel injection line pressure, and finally two more sets of needle lift data. A set of data includes 3600 data points which were collected every 0.2° of 720° of crank angle, which makes four strokes of the cylinder. All of these data were averaged and stored. Engine timing and the data collection were monitored with BEI Electronics, Inc. Incremental Optical Encoder (Model H-25). The encoder produced two types of signals, a triggering signal called the Z pulse that was sent when the fourth cylinder was at top dead center and a timing signal, which was called the A pulse, that was sent every 0.2° of crank angle. The triggering signal, the Z pulse, triggered the National Instruments board and the board started to collect data with the timing signal at every 1/5 of a degree during two engine revolutions, or for one engine cycle. The NOx and the FID analyzers were also connected to a National Instruments model AT-M10-16E-10, data acquisition PC board, accompanied with a Labview program. This Labview program collected data every second for five minutes during engine runs.

3.5 The concept map and test schedule

NOx production of diesel engines is very complex, because it is influenced by many factors and many of these factors interact at different levels. A concept map was developed to organize the information about the factors and their interrelationships and to sort out the

knowns and the unknowns of biodiesel fuel effects on the NOx emissions of diesel engines. Then, engine test plans were developed to solve the unknown parts of the concept map.

The concept map shown in Figure 3.6 shows the interrelationships between NOx emissions and the diesel engine combustion parameters, such as combustion timing and premixed combustion. Nitrogen oxide emission mainly is a function of high temperature in the combustion chamber [64, 65, 66]. As shown in Figure 3.6, there are two main combustion characteristics that will determine the temperature in the cylinder and thus the NOx emission. These are the combustion timing and combustion rate.

Combustion timing relates to the start of combustion relative to the piston position in the cylinder. Early combustion timing causes combustion to occur closer to TDC and perhaps during the compression process, increasing the pressure, temperature, and NOx emission [64, 67, 68]. Combustion timing in a diesel engine is mainly affected by the injection timing, or the start of injection, and the ignition delay, which is the time between the start of injection and the start of combustion [64-68]. The ignition delay time is mostly affected by the fuel's cetane number. The cetane number of biodiesel is higher than diesel fuel. A higher cetane number shortens the ignition delay time and advances the combustion timing. Early injection timing and higher cetane number advance the combustion timing which tends to increase the NOx emission [64-68]. Biodiesel has a lower energy content than diesel fuel and when a greater volume of fuel is injected to correct for this, some fuel injection pumps will advance the start of injection timing, causing an additional increase in NOx emission. Biodiesel also has different physical properties such as higher density, speed of sound, and bulk modulus, which can also lead to an earlier start of injection [9-11].

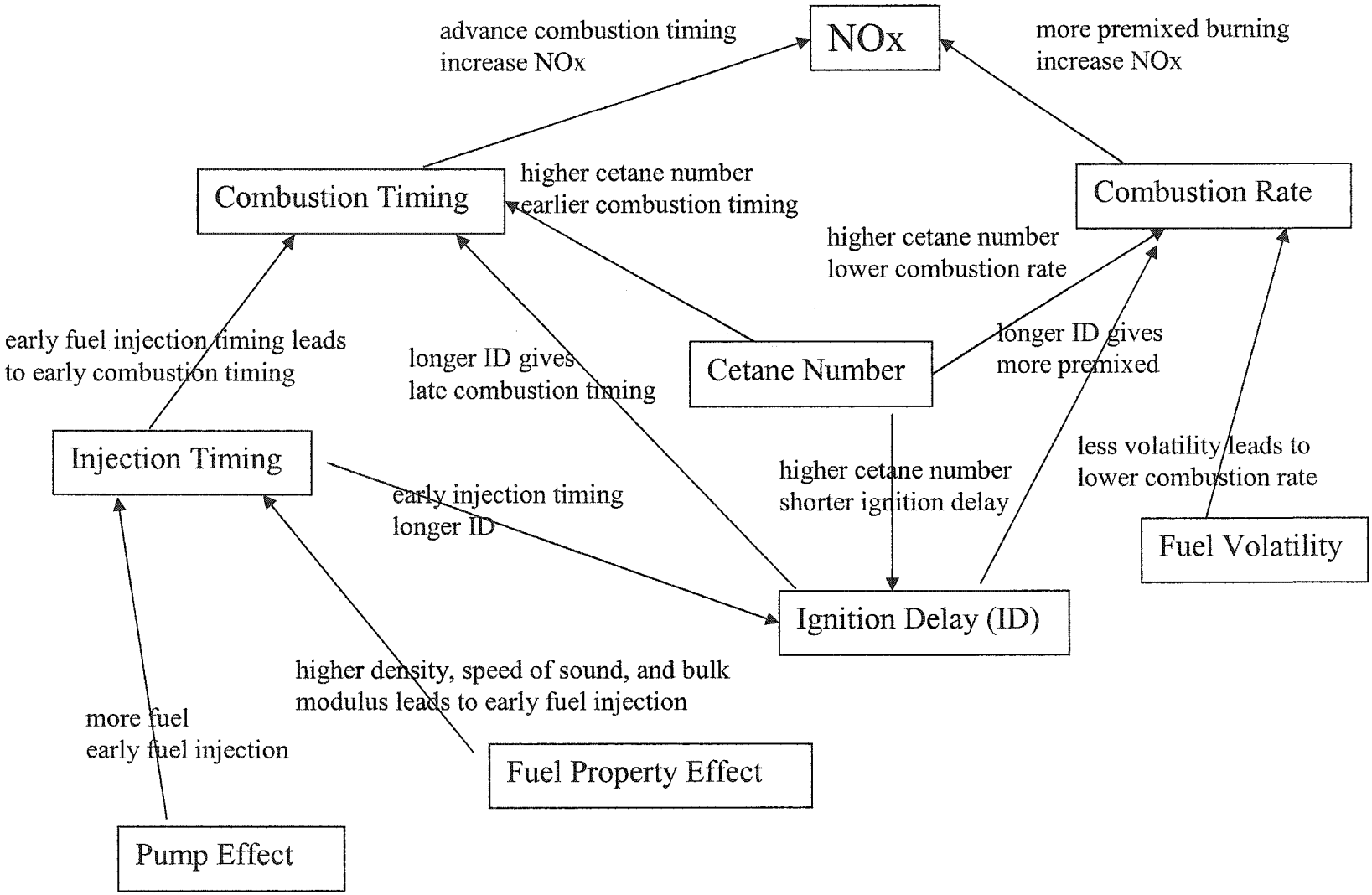

Figure 3.6 Concept map of NOx emission and combustion characteristics.

Combustion rate, as indicated by the heat release rate, also has an effect on NOx production. More premixed combustion means a high initial rate of combustion which increases NOx emission [64]. Premixed combustion corresponds to the fuel that is mixed with air and prepared to burn during the ignition delay period. When this fuel auto ignites it usually burns very quickly. Cetane number and fuel volatility are the two most important fuel properties that determine the combustion rate. High cetane number and low volatility lowers the combustion rate [69, 70]. Biodiesel's high cetane number is expected to shorten the ignition delay period and thus lower the amount of fuel that is involved with the premixed combustion portion of the biodiesel combustion, lowering NOx emission.

The objective of this study was to determine the reasons for the NOx emission increase due to biodiesel fuel use in diesel engines. In support of this goal, the physical properties of biodiesel fuel and its constituents were measured, including the density and speed of sound of a total of thirty fuel samples, several pure hydrocarbons, biodiesel fuels derived from different oils and fats, and their constituent pure fatty acid esters. Measurements have been conducted from 20 °C to 100 °C and from atmospheric pressure to 34.5 psi. These are the conditions that diesel fuel may encounter in the fuel injection system. Also, the isentropic bulk modulus of the samples was calculated at each pressure and temperature level. Data were fitted and two variable regression equations were obtained. The data were analyzed with respect to molecule length, saturation level, alcohol effect, and compared with diesel fuel. Also, the properties of 20, 50, and 75 % blends of biodiesel with No. 2 and No. 1 diesel fuel were measured at 20 and 40 °C, in order to see blending effects.

The engine tests laid out in Table 3.7 were developed to provide an improved understanding of the biodiesel fuel property effects on the diesel engine combustion and NOx production as guided by the concept map. A four-stage test process was planned and applied.

Table 3.7 Test proposal

Step Number	*Purpose*	*Variables*	*Held constant*	*Monitored*
1	Determination of overall differences in the diesel and biodiesel fuels	Fuels	Pump timing	Emissions, Injection and Combustion timings, Combustion rates
2	Determination of fuel injection pump and fuel physical property (density, speed of sound, and bulk modulus) effect on fuel injection timing and NOx production	Load, Fuel	Engine speed	Injection timing Fuel delivery
3	Determination of cetane number effect on fuel combustion	Fuel, cetane number	Volatility and Start of combustion	Combustion rate and NOx emission
4	Determination of fuel volatility effect on fuel combustion	Fuel, volatility	Cetane number and Start of combustion	Combustion rate and NOx emission

In the first step, biodiesel produced from soybean oil and yellow grease was compared with regular diesel fuel. This was to determine the overall effects of the different factors included in the concept map. The differences in the injection timing and combustion timing, emissions, and combustion were compared with no changes in the pump timing. For the second step, the research investigated the effect of the pump timing advance and the fuel property effects on the fuel injection timing. This effect is shown in the lower left hand corner of the concept map. The engine was run at different load conditions, and the injection timing and the fuel delivery were recorded in grams per injection for both the biodiesel fuel and diesel fuel. This test provides information about the fuel property effect and the injection

pump load advance on the injection timing advancement seen in the diesel engines fueled with biodiesel fuel.

In the third and fourth steps, the cetane number and fuel volatility effects of biodiesel on the combustion rate were investigated. The engine was run with No. 2 diesel fuel with the same cetane number as the soybean-based biodiesel. The fuel injection timing was set at five different conditions. Although they had the same cetane number, these fuels had different volatilities. In order to do this, the cetane number of the diesel fuel was increased using a cetane improver additive, but the volatility of the diesel fuel was still higher than for the biodiesel fuel. This test was intended to answer the question about the effect of volatility effect on the combustion rate and NOx emission.

In the fourth step, with the same start of combustion timing and by using fuels that have same volatility but different cetane numbers, such as soybean oil-based biodiesel and animal fat-based biodiesel, the cetane number effect on biodiesel combustion rate was investigated.

After these tests, information was obtained about the effect of other physical properties, specifically the higher density, viscosity, speed of sound, and isentropic bulk modulus of biodiesel on the injection timing advance. This provided enough information so that the biodiesel property effect on higher NOx emission of the diesel engine fueled with biodiesel fuel could be explained. Based on the four-step engine test explained above, three categories of engine tests were planned. Each run was repeated three times for accuracy.

4. DATA COLLECTION AND ANALYSIS

In this section, the exhaust emission data analysis, calculations, and corrections are described. The heat release analysis, cylinder pressure smoothing techniques, start of combustion calculations are also explained in detail. In addition to these, the fuel injection line pressure, needle lift, and ignition delay period definitions, and calculations are presented.

4.1 Exhaust Emission Analysis

4.1.1. Brake Specific Exhaust Emission Analysis

Exhaust emissions are generally presented on a brake specific basis. In order to calculate the brake specific emissions from the measured exhaust gas concentration, usually based on volume percentage or parts per million, a balanced chemical equation for diesel fuel combustion was used. The equation is given below and complete combustion was assumed.

$$C_xH_yO_z + (A/F)\,(0.21\,O_2 + 0.79\,N_2) \rightarrow B\,(y_{CO2,dry}\,CO_2 + y_{O2,dry}\,O_2 + y_{N2,dry}\,N_2) + C\,H_2O \quad (4.1)$$

where x = number of carbon molecule in an average fuel molecule

y = number of hydrogen molecule in an average fuel molecule

z = number of oxygen molecule in an average fuel molecule

$y_{i,dry}$ = mole fraction of chemical species on a dry bases

A/F = molar air/fuel ratio

B = number of moles of dry products per mole of fuel

C = number of moles of water per mole of fuel

After balancing the number of atoms in Equation 4.1, the constants B and C can be calculated as:

$$B = (A/F) + z/2 - y/4 \quad (4.2)$$

$$C = y/2 \quad (4.3)$$

The brake specific emissions can be calculated using the equations given below.

$BSCO_2$ = [kmol CO_2/kmol dpg] * [kmol dpg/kmol fuel] * [kmol fuel/kg fuel] * [kg fuel/hr] * [kg CO_2/kmol CO_2] * [1/Pb] (4.4)

$=[y_{CO2}] * [B] * [1/MW_{fuel}] *[m_{fuel}/1] * [MW_{CO2}/1] * [1/Pb]$

=kg/kW hr

BSCO = [kmol CO/kmol dpg] * [kmol dpg/kmol fuel] * [kmol fuel/kg fuel] * [kg fuel/hr] *[kg CO/kmol CO] * [1/Pb] (4.5)

BSNO = [kmol NO/kmol wpg] * [kmol wpg/kmol fuel] * [kmol fuel/kg fuel] * [kg fuel/hr] *[kg NO/kmol NO] * [1/Pb] (4.5)

BSNOx = [kmol NOx/kmol wpg] * [kmol wpg/kmol fuel] * [kmol fuel/kg fuel] * [kg fuel/hr] *[kg NOx/kmol Nox..] * [1/Pb] (4.5)

BSHC = [kmol HC/kmol wpg] * [kmol wpg/kmol fuel] * [kmol fuel/kg fuel] * [kg fuel/hr] *[kg HC/kmol HC] * [1/Pb] (4.6)

where y_i = measured emission, %

dpg = dry product gas

wpg = wet product gas

MW = molecular weight

m_{fuel} = mass flow rate, kg/hr

Pb = brake power, kW

kmol = kilo mole

4.1.2 Humidity Correction Factor for Oxides of Nitrogen (NOx)

The humidity correction of the oxides of nitrogen emission was made based on the Society of Automotive Engineers [71] recommendation. The procedure is summarized here.

$$NO_{corrected} = NO_{wet} * 1/K \quad (4.7)$$

where $NO_{corrected}$ = corrected nitric oxide (NO) concentration, ppm

NO_{wet} = measured nitric oxide (NO) concentration on a wet basis, ppm

$$K = 1 + 7\,A\,(h - 10.714) + 1.8\,B\,(T - 29.444) \quad (4.8)$$

$A = 0.044\,(F/A) - 0.0038$

$B = -0.116\,(F/A) + 0.0053$

T = intake air temperature, °C

F/A = fuel-air ratio (dry basis)

The specific humidity of the engine intake air, h is calculated using Equation 4.9.

$$h = 621.10 * Pv / (Pb - Pv) \quad (4.9)$$

where h = specific humidity, g H_2O/kg dry air

Pb = observed barometric pressure, kPa

Pv = partial pressure of water vapor, kpa

Ferrel's equation [72] can be used to calculate the partial pressure of water vapor,

$$Pv = Pw - 1.8 * A * Pb (Td-Tw) \quad (4.10)$$

Where Pw = saturation pressure of water vapor at the wet bulb temperature, kPa

Td = dry bulb temperature, °C

Tw = wet bulb temperature, °C

A = experimentally derived constant = 3.67 * 10-4 (1 + 0.001152 Tw)

The saturation pressure of water at the wet bulb temperature can be calculated using a polynomial equation obtained the data from Keenan and Keye's steam table [73].

$$Pw = 0.6048346 + 4.59058*10^{-2} Tw + 1.2444*10^{-3} Tw^2 + 3.52248 * 10^{-5} Tw^3 + 9.3220610^{-8} Tw^4 + 4.18128*10^{-9} Tw^5 \quad (4.11)$$

where Pw = saturation pressure of water vapor, kPa

Tw = wet bulb temperature, °C

4.2 Heat Release Analysis and Start of Combustion

In this section, the heat release rate calculations and cylinder pressure smoothing technique are discussed. Also, examples of the heat release analysis with crank angle profiles and determination of the start of combustion are presented.

4.2.1 Calculation Procedure

To understand diesel engine combustion and to make comparisons between diesel fuel and biodiesel, heat release rate analysis was conducted. The basic heat release rate analysis was developed by Krieger and Borman [74]. Many other researchers have also investigated this technique and developed more complex heat release analysis procedures [75 - 77].

The basic heat release method used in this study included three assumptions. The first is that the charge air-fuel mixture inside the cylinder behaves as an ideal gas. The second is that the charge in the cylinder is a uniform single zone of constant composition from the intake valve closing to the exhaust valve opening. The last one is that the energy released due to fuel combustion can be considered as a heat addition to the cylinder. When the first law of thermodynamics was applied to this system, Equations 4.1 and 4.2 were obtained.

$$\frac{dU}{dt} = \dot{Q} - \dot{W} \tag{4.1}$$

$$mC_v \frac{dT}{dt} = \dot{Q} - P\frac{dv}{dt} \tag{4.2}$$

where: $\dot{Q}$ represents the sum of the heat transfer rate across the cylinder wall and the heat generation rate due to the combustion and $\dot{W}$ is the rate of work done by the system boundary.

The ideal gas assumption, Equation 4.3, can be applied at this point to Equation 4.2 and it becomes Equation 4.4. After rearranging it, Equation 4.5 is obtained and replacing the time term with crank angle, θ gives Equation 4.6.

$$PV = mRT \tag{4.3}$$

$$\frac{dT}{dt} = \frac{1}{mR}\left(P\frac{dV}{dt} + V\frac{dP}{dt}\right) \tag{4.4}$$

$$\dot{Q} = \left(\frac{C_v}{R} + 1\right)P\frac{dV}{dt} + \frac{C_v}{R}V\frac{dP}{dt} \tag{4.5}$$

$$\dot{Q} = \frac{\gamma}{\gamma - 1}P\frac{dV}{d\theta} + \frac{1}{\gamma - 1}V\frac{dP}{d\theta} \tag{4.6}$$

where γ is C_p/C_v, the specific heat ratio of the in-cylinder gas mixture. The generally assumed value for diesel fuel is between 1.3 and 1.35. In this study, the specific heat ratio of both diesel and biodiesel fuels was considered to be 1.3. The constant specific heat ratio is often used and even though it is not the most accurate analysis it works very well for prediction of the start of combustion.

4.2.2 Cylinder Pressure Data Smoothing Technique and Analysis

To conduct heat release analysis using Equation 4.6, we need to integrate two derivative terms, $(dV/d\theta)$ and $(dP/d\theta)$. The time derivative of volume can be easily calculated by differentiating the term analytically or numerically. However, the pressure often contains high amplitude oscillations. In the calculations, these oscillations have a significant impact on the time derivative. Van Gerpen [78] pointed that small oscillations in the pressure data lead to significant errors in the heat release analysis. Austin and Lyn [79] found that a one degree error in the pressure measurement results in a 50% error in the heat release rate. Therefore, for heat release analysis it is not only necessary to have very accurate pressure data, it is also necessary to have a very effective smoothing technique for the numerical differentiation. A four point finite difference equation was used for the pressure differentiation as shown in Equation 4.7. A numerical smoothing technique suggested by Hamming [80, 81] called "Digital Filtering" was found by Van Gerpen [81] to be effective. A four-point difference equation was successfully applied to first degree differentiation of the pressure data by Monyem [82]. The numerical differentiation and filtration techniques used in this study are summarized below in Equation 4.8 and 4.9.

$$(du/dx)_i = (-u_{i+2}+8\ u_{i+1} - 8\ u_{i-1} + u_{i-1}) / (12 \times \Delta\theta) \quad (4.7)$$

where i = data locations in crank angle

u_i = pressure at the crank angle of i

$\Delta\theta$ = crank angle interval between i and i+1

$$g_i = 1/2\ (f_{i+1} + f_{i+1}) \quad (4.8)$$

$$h_i = 1/3\ (g_{i-1} + g_i + g_{i+1}) \quad (4.9)$$

where f_i = the original data

g_i = intermediate value

h_i = the filtered data

4.2.3 Heat Release Analysis and Crank Angle Profiles

In this section, examples of single cycle pressure data, averaged cylinder pressure data, and smoothed, averaged cylinder pressure data are presented to show the nature of the cylinder pressure data and the effect of the smoothing technique. The smoothing effect on the heat release analysis is also presented here.

Figure 4.1 represents single cycle pressure data collected at full load using a 4045 T John Deere diesel engine fueled with soybean oil-based biodiesel. Cylinder pressure increases as the crank angle increases, as the piston moves towards top dead center until about 8° before top dead center. This point is considered to be the start of combustion, where cylinder pressure starts to increase sharply with lots of oscillation as a sign of combustion. In order to reduce the oscillation effects on the heat release analysis, it is common for heat release analysis to average ten to fifty consecutive cycles of data. In this study, ten consecutive sets of data were collected for each engine run test. Figure 4.2 is given as an example of a set of cylinder pressure data consisting of the average of 10 consecutive cycles.

The filtration given in Equations 4.8 and 4.9 can be applied to the average of 10 consecutive cycles to reduce the oscillations and improve the heat release analysis. As can be seen from Figure 4.3, averaging and smoothing greatly helps to reduce the oscillations.

The smoothing effect can be better understood when the heat release analysis of both unsmoothed cylinder pressure data and smoothed pressure data are compared, as shown in Figures 4.4 and 4.5, respectively. Figure 4.4 includes extremely noisy heat release based on unsmoothed pressure data. However, Figure 4.5 shows relatively much less noisy heat release after the data were processed with the cylinder pressure smoothing technique.

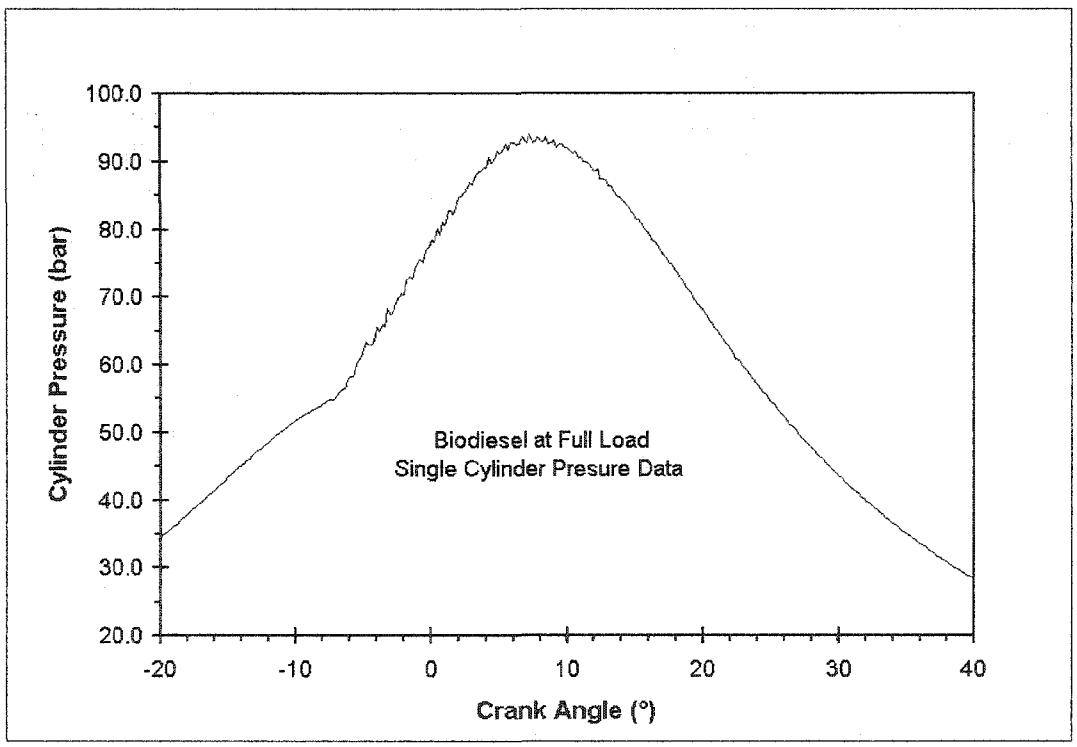

Figure 4.1. Single cylinder pressure data at TDC from 4045T John Deere engine fueled with biodiesel fuel from soybean oil.

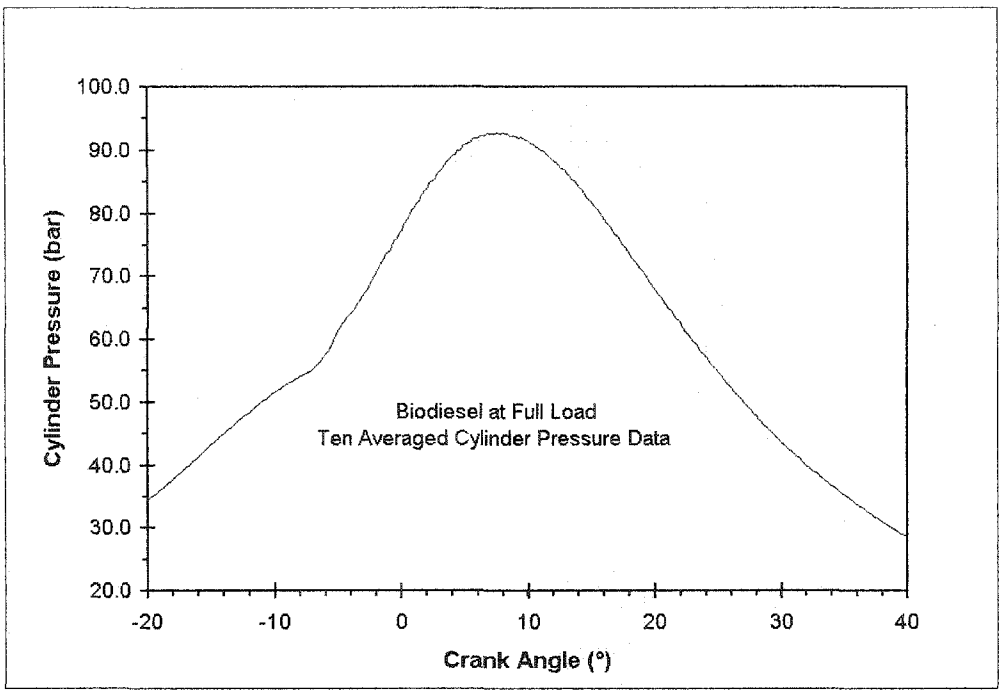

Figure 4.2. Ten averaged cylinder pressure data at TDC from 4045T John Deere engine fueled with biodiesel fuel from soybean oil.

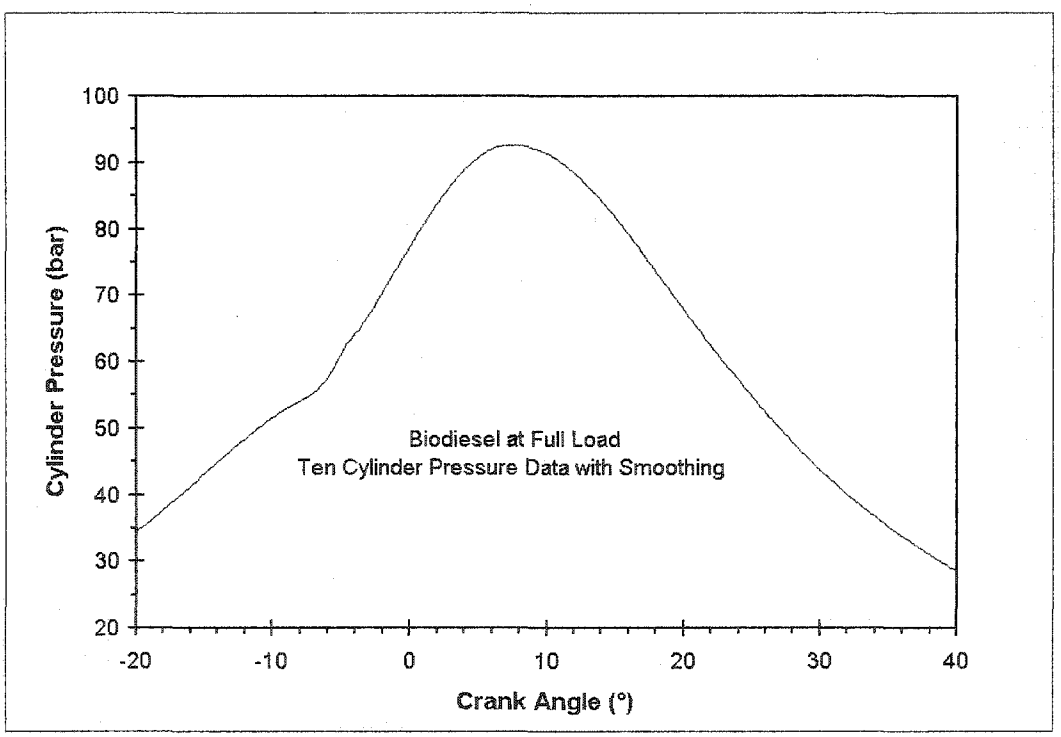

Figure 4.3. Smoothing result of ten averaged cylinder pressure data at TDC from 4045T John Deere engine fueled with biodiesel fuel from soybean oil.

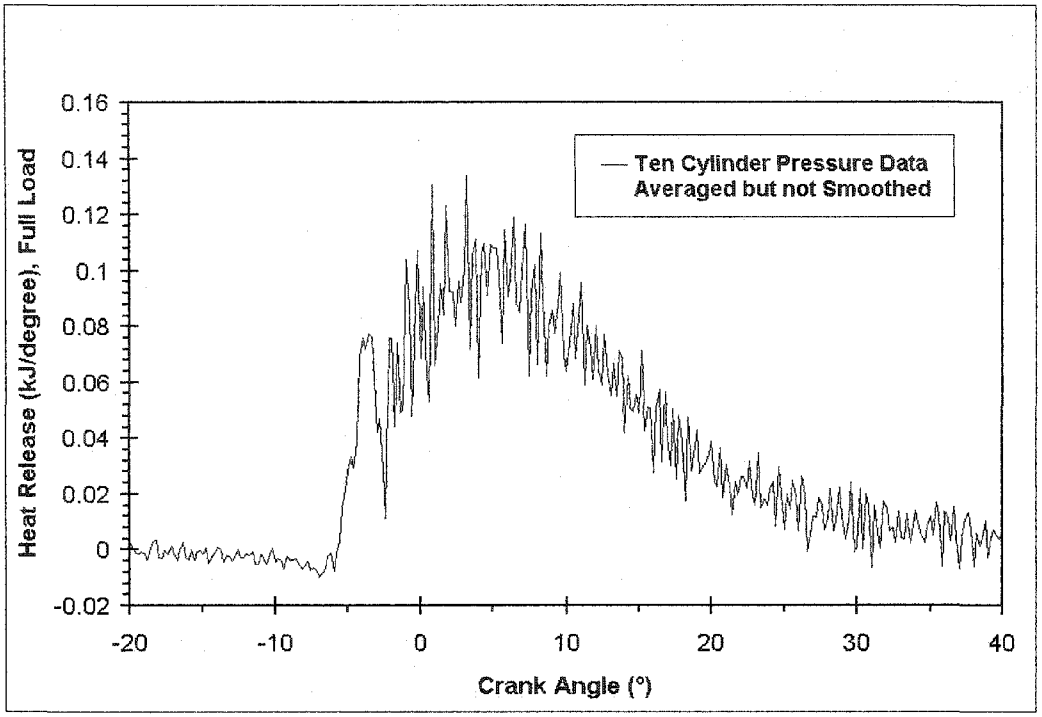

Figure 4.4. Heat release analysis from ten averaged cylinder pressure data without smoothing at TDC from 4045T John Deere engine fueled with biodiesel fuel from soybean oil.

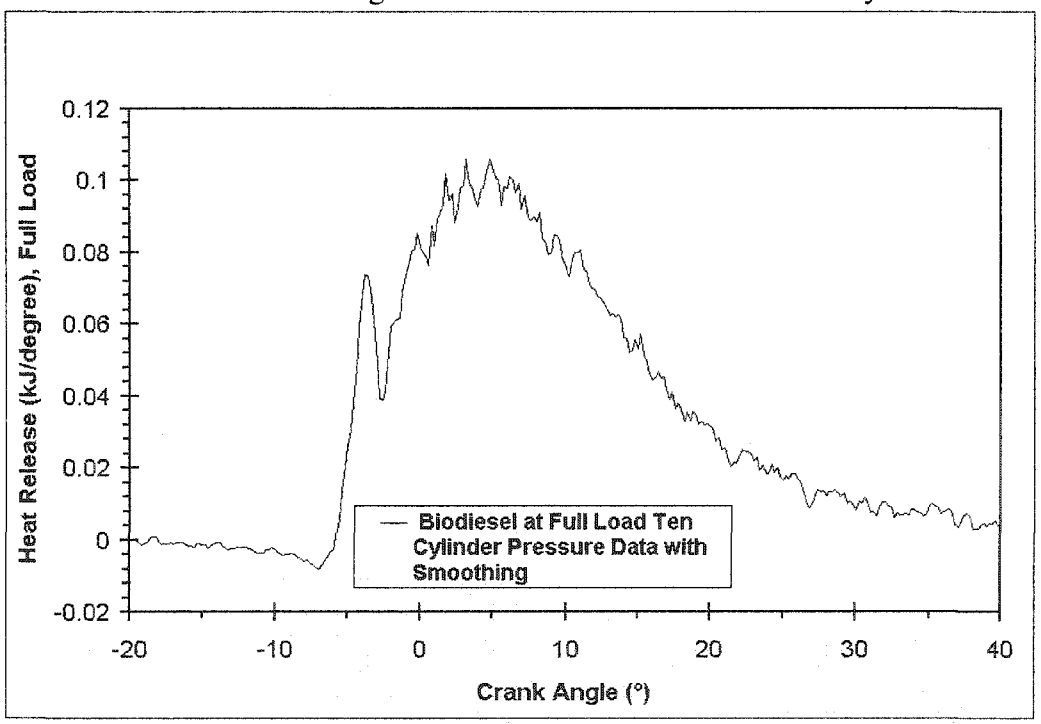

Figure 4.5. Heat release analysis from ten averaged cylinder pressure data with smoothing at TDC from 4045T John Deere engine fueled with biodiesel fuel from soybean oil.

4.3. Needle Lift Sensor Analysis and Fuel Injection Line Pressure

Examples of needle lift and fuel injection line pressure data are given in Figures 4.6 and 4.7, respectively. In Figure 4.6, needle lift data are presented in volts per degree for biodiesel from soybean oil and for No. 2 diesel fuel. Since these data are used only for determination of the start and end of injection, the actual needle movement corresponding to a certain voltage level is not needed. The start of injection is calculated as the crank angle corresponding to 10% of the maximum lift of the needle during the injection. The start of injection can also be estimated from the fuel injection line pressure. Depending on the engine type, the fuel injector nozzle opening pressure on the fuel injection line pressure data and the corresponding crank angle can be considered as the start of fuel injection point. The needle lift data gives the real needle opening, so it is more reliable and accurate.

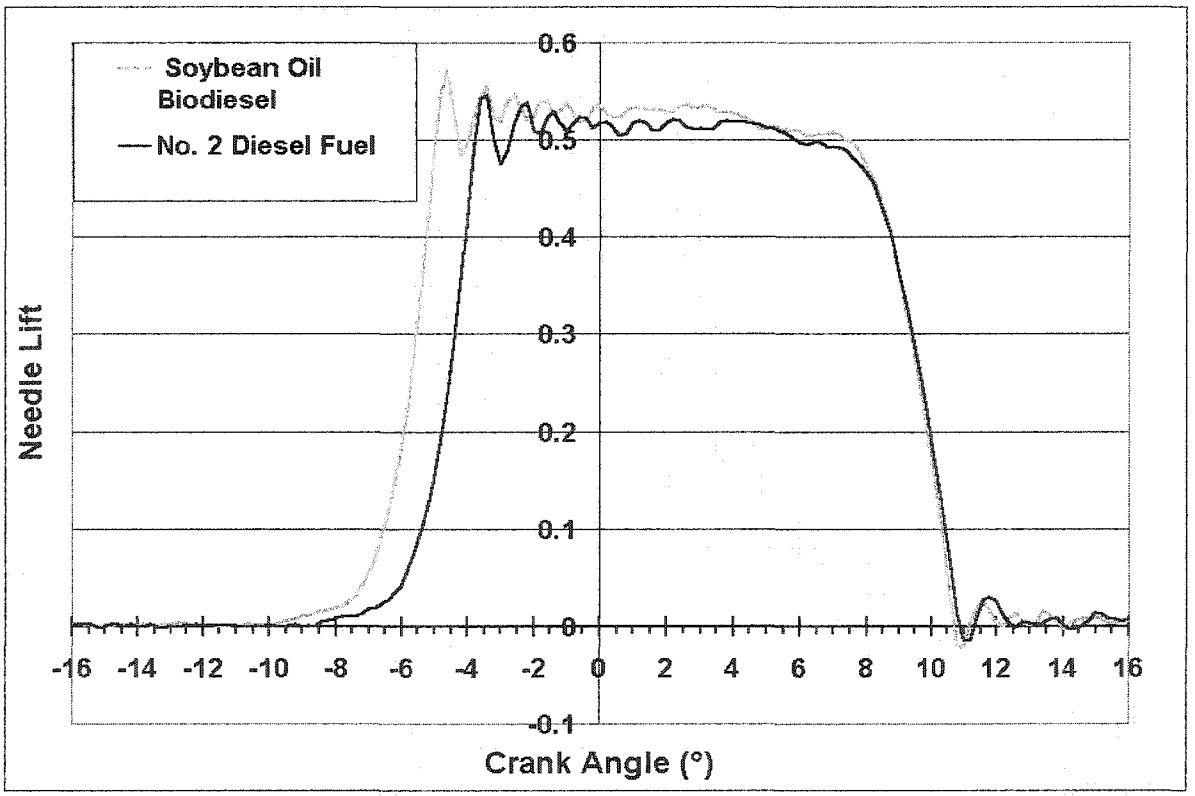

Figure 4.6 Example of needle lift versus crank angle data for biodiesel and diesel fuel.

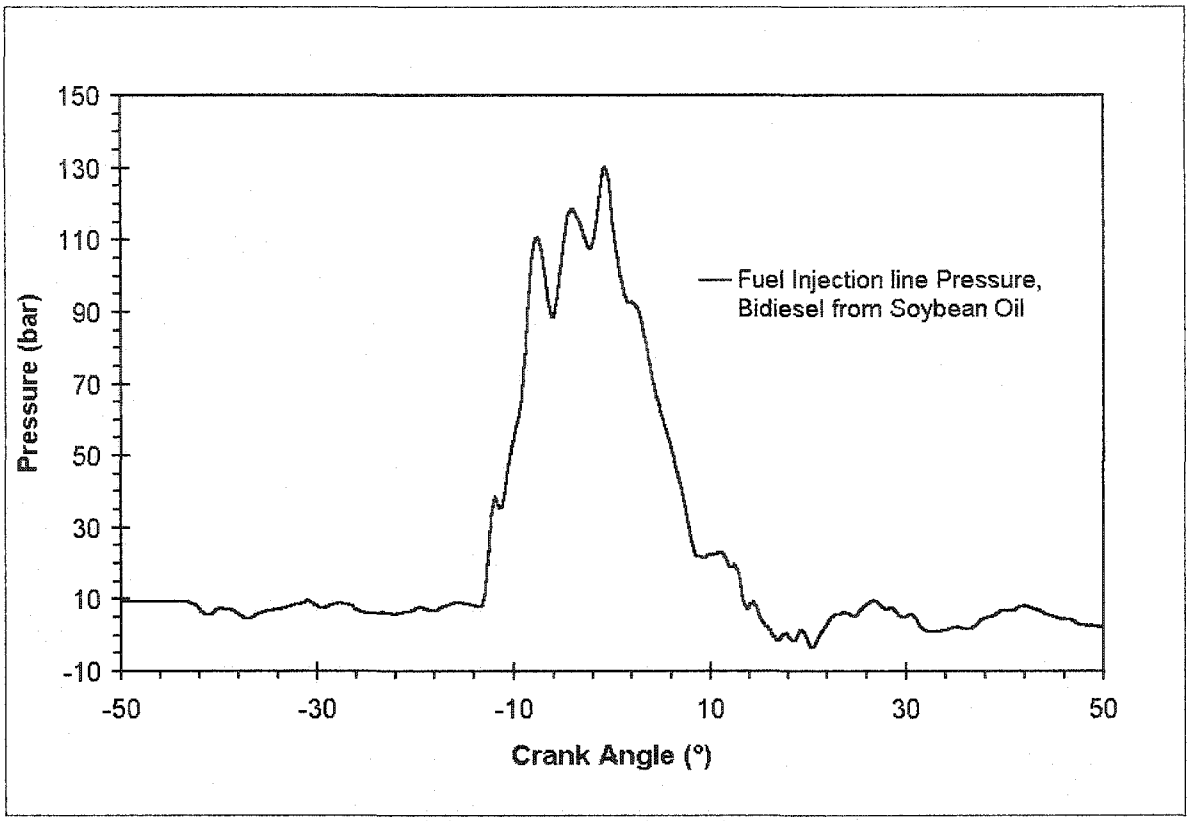

Figure 4.7 Example of fuel injection line pressure versus crank angle data for biodiesel.

5. RESULTS AND DISCUSSION

This chapter presents the results and discussions and is arranged into three sections. In the first section, the research chronology and the problems that occurred during the research are presented. In the second section, the density, speed of sound, and isentropic bulk modulus of biodiesel and its constituents are presented and correlation constants are given as functions of temperature and pressure. In the last section, the effects of biodiesel's physical and chemical properties on the fuel injection timing, combustion, and NOx production are discussed.

5.1. Research Chronology with the Pitfalls

To investigate the physical and chemical properties of biodiesel and their effects on the diesel fuel injection system, diesel combustion, and oxides of nitrogen emission, the objectives of this project were to measure the density, speed of sound, and isentropic bulk modulus of biodiesel and its constituents, to determine the effect of blending with diesel fuel on these properties, and to determine the effect of biodiesel fuel properties such as the lower heating value, volatility, and cetane number, on the injection timing, diesel combustion, and exhaust emissions.

Initially, the project started by measuring the density, speed of sound, and isentropic bulk modulus of methyl soyate, ethyl soyate, No. 1, and No. 2 diesel fuels at atmospheric pressure. As the project progressed, the same physical properties were measured for a total of thirty one samples of biodiesel from different feedstocks, including the pure ester constituents of biodiesel, at temperatures from 20°C to 100°C and at pressures from atmospheric to 32.5 MPa. During this research, the effect of the chain length of the molecules, saturation, feedstock, and the alcohol used in transesterification were investigated.

These pressure and temperature ranges should cover most of the commonly encountered start-of-injection conditions since most engines have nozzle-opening pressures below 32.5 MPa. The properties were also measured for distilled water and compared to published data to ensure that the technique and the test rig were capable of measuring the properties accurately. It was later noticed that since hydrocarbons are much more compressible and are more temperature and pressure sensitive than water, that distilled water was not an appropriate choice as a measurement standard. From that point on, dodecane was used for checking the accuracy of the test rig and error detection. The primary difficulties with these measurements were with pressure correction and with the atmospheric pressure density measurements.

After completing the physical property measurements for biodiesel and its pure constituents, a concept map was developed to explain the interrelationships between the physical and chemical properties of biodiesel and their effect on the start of combustion and combustion rate. These effects were investigated so that the higher biodiesel NOx emission could be understood. The concept map shows the interrelationships between biodiesel fuel properties, diesel combustion characteristics, and NOx emission was given as Figure 3.6 in Section 3.5. In that section, the concept map was discussed and it was concluded that a four step test matrix would provide the data needed to explain the key interrelationships in the concept map and would help explain the higher biodiesel NOx emission.

The first test of the matrix was called the Investigation of the Global Effects of Biodiesel Fuel Properties. This test was intended to compare soybean oil and yellow grease biodiesel with diesel fuel to determine the overall effect of the fuel properties on injection timing, combustion timing, and diesel combustion. In the second test, the lower heating

value of biodiesel and biodiesel's higher density, speed of sound, and isentropic bulk modulus were explored for their effect on the start of injection and emissions. The second test matrix was called the Investigation of the Effects of the Lower Heating Value and Higher Physical Properties of Biodiesel. The third and the fourth steps were also identified and were targeted to understand the effects of biodiesel's higher cetane number and lower volatility on the combustion rate and the higher NOx emission of biodiesel. This test matrix was called the Investigation of Biodiesel's Higher Cetane Number and Lower Volatility.

After the concept map and the test matrixes were completed, the engine research was initiated with step 2, the Investigation of Lower Heating Value and Higher Physical Properties Effects of Biodiesel. It was successfully completed. However, due to an unfortunate mistake, the engine's fuel injection pump was ruined before completing the full set of test matrices. The problem that caused the pump failure was not related to the fuels or to the tests that were underway. The fuel injection pump that was ruined in the test was the original pump that came with the engine. This pump is identified as pump #1 in the following sections. Since the pump could not be repaired, the rest of the tests could not be conducted with pump #1. A used fuel injection pump was donated by John Deere and this pump is called pump #2. All of the test matrices were completed with pump #2, including the test matrix that had been done with pump #1. During the analysis of these results, it was found that pump #2 had some problems with its light load timing advance system. It was observed that the fuel injection timing was gradually retarded by pump #2, as the engine load in decreased, until the light load advancement system is engaged. This is the expected behavior. After the system was engaged, the start of injection timing fluctuated significantly between each fuel and each repetition. The light load advancement system of pump #2 was

not able to consistently regulate the injection timing based on load. At 1800 and 2100 rpm, the light load advancement system had already been engaged at higher load conditions, and showed different behavior between fuels. From the tests conducted on the original pump, pump #1, the physical property effects were clearly evident on the fuel's start of injection timing, but with pump #2 this was not possible. To have a better understanding of the problem, the step 2 test matrix was extended to investigate the fuel property effects at the different speed levels of 1000, 1400, 1800, and 2100 rpm. The results showed some irregularities between the fuels. The irregularities in the results are believed to be related to the light load advancement mechanism of the pump and will be discussed later.

At this time, a new pump was purchased and called pump #3. The extension of the lower heating value and physical property effects test matrix was repeated at 1000, 1400, 1800, and 2100 rpm. The Investigation of Biodiesel's Higher Cetane Number and Lower Volatility, step 3, was also conducted with pump #3. Based on the tests with the previous pumps, some changes were made to the test conditions to improve the quality of the data. The cetane number of the diesel fuel in the test matrix was increased to be more closely match the ignition delay of soybean oil biodiesel. Diesel fuel without additive was also introduced into the test matrix. In addition to these changes, the effect of fuel viscosity on the fuel pump delivery was tested for pump #2 and pump #3. The engine was run at its full load, wide open throttle, condition and fuel temperatures were set to 25, 30, 40, 50, and 55 °C for soybean oil and No. 2 diesel fuel. It was found that as the viscosity was increased, the fuel delivery was also increased for both fuels. It was also found that at the same fuel delivery the start of injection of No. 2 diesel was about 0.3° advanced relative to the start of injection of biodiesel. It was judged that density also has an effect on the start of injection

timing, coupled with viscosity. When the research was originally started, it was thought that the speed of sound and bulk modulus had the most significant effect on the start of injection and higher NOx emission. In the process of running the test, it was learned that the cetane number, volatility, viscosity, and density effects also have a significant effect on timing and NOx. At this point it was determined that sufficient data had been obtained to address the original project objective and the research was concluded. As described above, multiple data sets are available for some tests and they will be included in the discussion.

5.2. Density, Speed of Sound, and Isentropic Bulk Modulus Measurements

5.2.1. High Pressure Measurements at Room Temperature

Figure 5.1 shows the measured density for methyl soyate, ethyl soyate, No. 1 diesel fuel and No. 2 diesel fuel. The points represent the average of 18 measurements. Error bars are not shown on this plot because they are so small that they obscure the data symbols. The 90% confidence limits for the measured densities were typically about ± 0.1% of the mean density values. The lines through the points are from linear regression and the coefficients are given in Table 5.1. The lines correlate the data well with the lowest R^2 value being 0.9978. The methyl esters were denser than the ethyl esters and both were more dense than the diesel fuels.

Speed of sound comparisons of the fuels are given in Figure 5.2. Published data for the speed of sound of n-paraffins indicates that longer chain paraffins have higher speeds of sound than shorter chain paraffins [49]. Therefore, biodiesel, with carbon chain lengths of 17-19 would be expected to have a higher speed of sound than No. 2 diesel fuel with chain lengths of 13-16 [83]. No. 1 diesel fuel contains even shorter chain lengths. As expected,

the methyl and ethyl esters have higher speeds of sound than No. 2 diesel fuel, which is higher than the No. 1 diesel fuel.

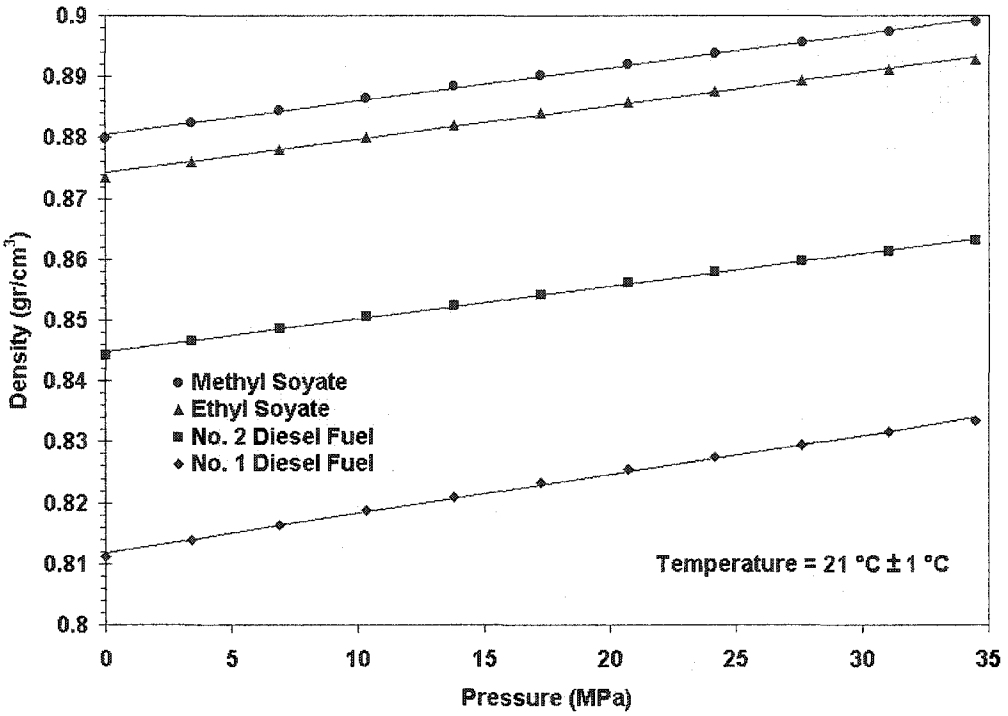

Figure 5.1. Density of methyl soyate, ethyl soyate, and No. 1 and No. 2 diesel fuels

Table 5.1. Correlation constants and equations [21 °C ± 1 °C].

Fuels	*Methyl Soyate*	*Ethyl Soyate*	*No. 2 Diesel*	*No. 1 Diesel*	*Distilled Water*
Density (g/cm^3) = A_1*[P (MPa)] + B_1					
A_1	5.4784E-04	5.5140E-04	5.4045E-04	6.4350E-04	4.8965E-04
B_1	0.88056	0.87423	0.84480	0.81182	0.99722
R^2	0.9978	0.9978	0.9985	0.9981	0.9995
Speed of Sound (m/s) = A_2*[P (MPa)] + B_2					
A_2	3.8555	3.8950	4.5129	4.7493	1.7034
B_2	1410	1403.1	1375.8	1327.8	1489.5
R^2	0.9988	0.9983	0.9979	0.9990	0.9997
Isentropic Bulk Modulus (MPa) = A_3*[P (MPa)] + B_3					
A_3	11.316	11.299	12.329	12.430	6.3324
B_3	1747.5	1717.8	1595.1	1423.1	2211.5
R^2	0.9996	0.9994	0.9993	0.9994	0.9998

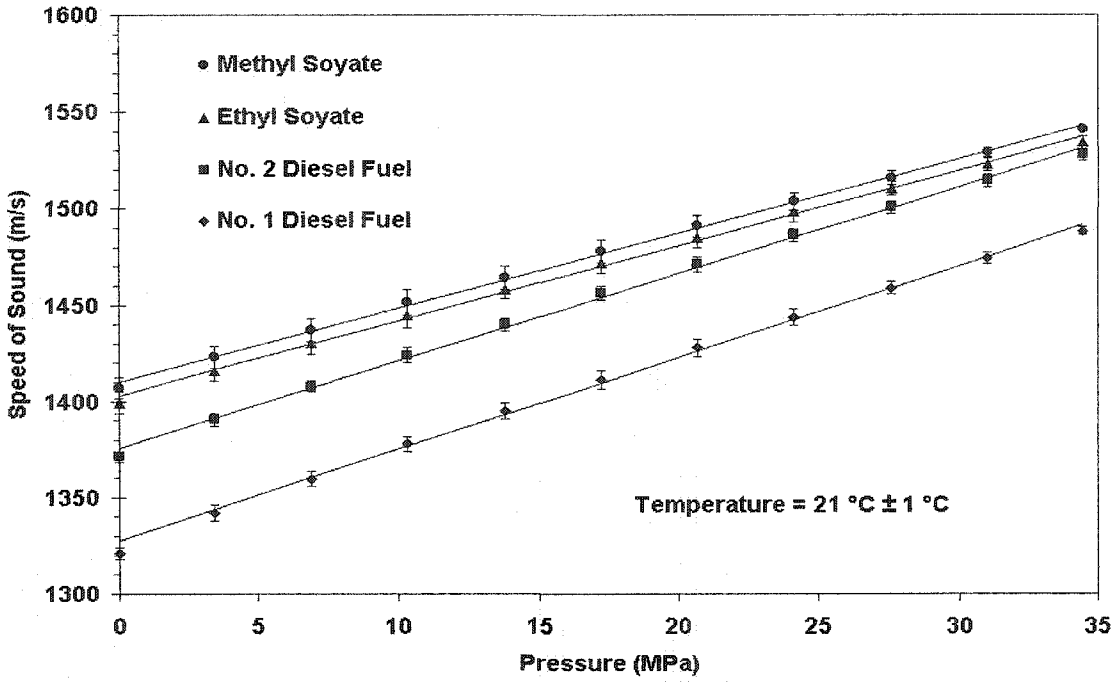

Figure 5.2. Speed of sound of methyl soyate, ethyl soyate, and No. 1 and No. 2 diesel fuels

The slopes of the lines for methyl and ethyl soyates are less steep than those for No. 1 and No. 2 diesel fuel, indicating less effect of pressure on the speed of sound. The error bars shown on the data points define the 90% confidence limits. The coefficients for the linear regression are provided in Table 5.1. Straight lines correlate the data with R^2 values greater than 0.9979.

The values of the isentropic bulk modulus calculated from the density and speed of sound data are shown in Figure 5.3. The methyl esters have a higher isentropic bulk modulus than the ethyl esters and are about as far above No. 2 diesel fuel as the No. 2 diesel fuel is above No. 1 diesel fuel.

The slopes of the lines appear to be approximately the same, but inspection of the linear regression coefficients in Table 5.1 indicates that the diesel fuels have larger slopes, which indicates a greater effect of pressure.

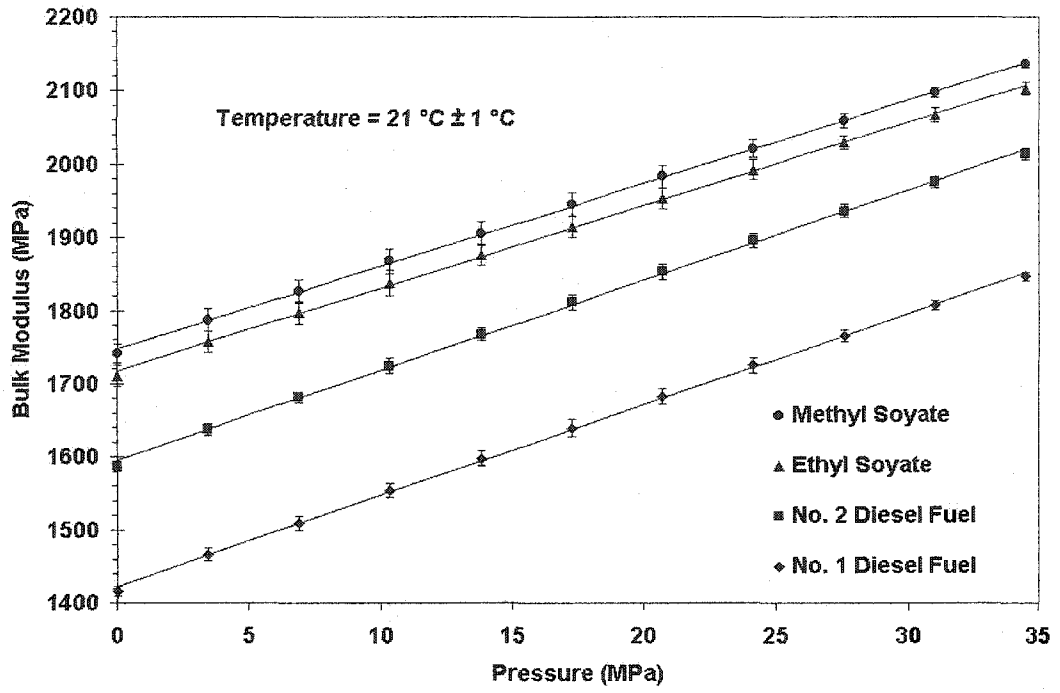

Figure 5.3. Isentropic bulk modulus for methyl soyate, ethyl soyate, and No. 1 and No. 2 diesel fuels

The isentropic bulk modulus of the methyl esters of soybean oil can be calculated at atmospheric pressure using density and speed of sound data published by Gouw and Vlugter [84, 85]. Their data indicates that the isentropic bulk modulus for methyl oleate is 1732 MPa and is 1784 MPa for methyl linoleate. These two species comprise about 80% of the methyl esters from soybean oil. These values are correspond well with the y-intercept value, 1747.5 MPa, given in Table 5.1 for the methyl esters.

Previous research has indicated that larger hydrocarbon molecules are less compressible than smaller molecules [86]. Less compressible fuels can cause early injection timing, and this can produce higher combustion pressures and temperatures, which in turn produces higher NOx emissions. The data presented here indicate that the isentropic bulk modulus and speed of sound for methyl and ethyl esters of fatty acids from soybean oil are

higher than for diesel fuel. These changes are at least part of the reason for the injection timing advance and are partially responsible for the increase in exhaust NOx observed by many researchers.

5.2.2 Measurements at High Temperature and Pressure

One of the objectives of this project was to measure the isentropic bulk modulus and speed of sound of biodiesel at temperatures from 20°C to 100°C and at pressures from atmospheric to 32.5 MPa. These ranges should cover most of the commonly encountered start-of-injection conditions since most engines have nozzle opening pressures below 32.5 MPa. In addition to measuring the properties of biodiesel made from soybean oil and other feedstocks, the properties of the pure ester constituents of biodiesel and some hydrocarbons were measured. A full list of the compounds tested is given in Table 5.2. The effect of chain length, saturation, feedstock, alcohol type, hydrogenation, and oxygenation were investigated.

The variations of density, speed of sound, and isentropic bulk modulus of the fuel samples were approximately linear with pressure and temperature. However, a polynomial that was second order in temperature and first order in pressure, as shown in Equation 5.1, provided the best fit to the data.

$$y = C_1 T^2 + C_2 TP + C_3 T + C_4 P + C_5 \qquad (5.1)$$

where y is the density, speed of sound, or the isentropic bulk modulus of the sample, T is the temperature in °C, P is the gage pressure in MPa and C_i, $i=1, 5$ are the correlation constants given in Tables 5.2, 5.3, and 5.4. The standard error for y is also shown in the tables. Higher order polynomials were tested, but the accuracy obtained with more coefficients did not justify the added complexity.

Table 5.2. Density of the Samples (g/cm^3).

Samples	$C_1\times10^7$	$C_2\times10^6$	$C_3\times10^4$	$C_4\times10^4$	$C_5\times10$	$Se_y\times10^4$
Methyl Esters of Fatty Acids						
Methyl Butyrate	-1.0711	6.4758	-11.068	6.3563	9.2018	8.0
Methyl Laurate	7.0375	3.5311	-8.3264	5.1716	8.8633	6.7
Methyl Palmitate	11.137	3.1087	-8.6821	4.8997	8.8374	6.4
Methyl Stearate	0.24181	2.8652	-7.0651	4.9171	8.7813	5.4
Methyl Oleate	-1.7442	2.8121	-6.7480	4.9471	8.9084	4.6
Methyl Linoleate	-2.4107	2.7030	-6.6629	5.0739	9.0533	4.7
Methyl Linolenate	0.91722	2.7982	-7.3107	4.8250	9.0582	4.3
2:1 M. Stearate M. Linseed	5.7612	3.1389	-7.7178	4.7513	8.9267	4.5
2:1 M. Linseed M. Stearate	5.5003	3.1407	-7.7590	4.6986	9.0297	5.3
Ethyl Esters of Fatty Acids						
Ethyl Butyrate	-2.3582	6.3538	-10.349	6.3947	9.0030	7.3
Ethyl Caprylate	-0.62125	4.0758	-8.3744	5.8994	8.8324	5.6
Ethyl Stearate	6.0752	3.6002	-7.7954	4.8898	8.7641	6.7
Ethyl Linoleate	0.49900	2.7530	-7.0449	5.1564	8.9772	6.8
Ethyl Linseed	-1.1161	2.5849	-6.9431	5.0375	9.0685	5.1
Isopropyl Esters of Fatty Acids						
Isopropyl Palmitate	-4.3583	3.1613	-6.2884	5.1645	8.6459	10.1
Isopropyl Stearate	-1.5717	3.0535	-6.7468	5.1279	8.6642	4.9
Methyl Ester Biodiesel Fuels						
Methyl Soy Ester	5.8985	2.9275	-7.7598	4.8517	8.9623	5.3
Methyl Canola	2.8659	2.8153	-7.5505	4.9403	8.9576	4.9
Methyl Tallow	6.8397	2.9019	-7.8136	5.0136	8.8721	4.7
Methyl Lard	-1.4499	2.6850	-6.9914	4.9947	8.8888	4.3
Methyl Yellow Grease	0.49788	2.9201	-7.0235	4.9010	8.8837	4.6
Methyl Oxidized Soy	2.0264	2.8895	-7.3502	4.8075	9.0026	4.0
Methyl Hydrogenated Soy	-1.7182	2.4881	-6.6732	5.0880	8.7854	5.8
Ethyl Ester Biodiesel Fuels						
Ethyl Soy Ester	-1.6990	2.9578	-6.9131	5.2530	8.8959	5.3
Ethyl Oxidized Soy	-1.9132	2.8622	-6.9397	4.9693	8.9555	4.5
Ethyl Hydrogenated Soy	-1.6629	2.9515	-6.6892	4.7997	8.7428	4.8
Hydrocarbons and Diesel Fuel						
n-Octadecane	2.2552	3.1164	-6.9982	4.8032	7.9525	4.5
n-Hexadecane	6.4165	2.7235	-7.5272	5.2803	7.9004	6.5
n-Dodecane	-3.4395	3.9310	-6.8834	5.3510	7.6278	5.6
Certified D-2	-2.6272	2.9186	-6.5999	5.3916	8.5422	6.2
$Density\ (g/cm^3)=C_1T^2(°C)^2+C_2TP(MPa)+C_3T+C_4P+C_5$						

Se_y: the standard error for the y estimate

Table 5.3. Speed of Sound of the samples (m/s).

Samples	$C_1\times10^3$	$C_2\times10^2$	C_3	C_4	$C_5\times10^{-3}$	Se_y
Methyl Esters of Fatty Acids						
Methyl Butyrate	7.1090	2.6780	-4.7542	4.0046	1.3037	5.8
Methyl Laurate	4.1639	1.6973	-3.9702	3.9322	1.4412	3.2
Methyl Palmitate	5.1325	1.5287	-4.0771	3.9214	1.4790	3.3
Methyl Stearate	4.0687	1.4657	-3.8059	3.8604	1.4806	2.8
Methyl Oleate	4.2764	1.4364	-3.8749	3.8429	1.4916	2.8
Methyl Linoleate	4.6079	1.4445	-3.8959	3.7565	1.4989	2.5
Methyl Linolenate	4.0790	1.4554	-3.8576	3.6984	1.5021	2.5
2:1 M. Stearate M. Linseed	6.1113	1.5489	-4.0767	3.7318	1.4946	3.4
2:1 M. Linseed M. Stearate	4.5796	1.5551	-3.9340	3.6368	1.4998	2.5
Ethyl Esters of Fatty Acids						
Ethyl Butyrate	4.2618	2.6945	-4.3512	4.1040	1.2858	4.0
Ethyl Caprylate	4.1106	1.8532	-4.0327	4.2110	1.3645	3.5
Ethyl Stearate	7.1445	1.4823	-4.1614	3.9704	1.4758	3.7
Ethyl Linoleate	3.8879	1.4545	-3.8099	3.7642	1.4888	2.6
Ethyl Linseed	3.7469	1.3822	-3.7770	3.7771	1.4939	2.8
Isopropyl Esters of Fatty Acids						
Isopropyl Palmitate	3.6438	1.5213	-3.7285	4.0840	1.4377	3.1
Isopropyl Stearate	4.9160	1.5096	-3.8565	4.0376	1.4541	4.3
Methyl Ester Biodiesel Fuels						
Methyl Soy Ester	3.7242	1.5141	-3.8329	3.7500	1.4945	2.9
Methyl Canola	3.8388	1.4662	-3.8009	3.7877	1.4934	2.5
Methyl Tallow	7.7473	1.5551	-4.3789	3.8101	1.5000	3.7
Methyl Lard	4.3140	1.4075	-3.8634	3.8487	1.4862	2.6
Methyl Yellow Grease	4.6346	1.4528	-3.8750	3.8458	1.4889	2.6
Methyl Oxidized Soy	4.1917	1.5081	-3.8504	3.7072	1.4961	2.8
Methyl Hydrogenated Soy	4.0553	0.95901	-3.8224	4.1518	1.4852	4.1
Ethyl Ester Biodiesel Fuels						
Ethyl Soy Ester	4.7384	1.5190	-3.8445	4.0151	1.4811	3.0
Ethyl Oxidized Soy	3.8501	1.4751	-3.7798	3.8172	1.4855	2.6
Ethyl Hydrogenated Soy	4.7127	1.5836	-3.9429	3.8237	1.4811	3.0
Hydrocarbons and Diesel Fuel						
n-Octadecane	5.5890	1.6046	-4.0992	4.2365	1.4655	3.8
n-Hexadecane	2.9168	1.5219	-3.6847	4.4486	1.4310	3.6
n-Dodecane	3.9613	2.1205	-4.0218	4.5267	1.3817	3.6
Certified D-2	4.7612	1.6718	-4.0413	4.2395	1.4580	3.2
Speed of Sound (m/s) $=C_1T^2(°C)^2+C_2TP(MPa)+C_3T+C_4P+C_5$						

Se_y: the standard error for the y estimate

Table 5.4. Isentropic Bulk Modulus (MPa).

Samples	$C_1\times10^{2}$	$C_2\times10^{3}$	$C_3\times10^{-1}$	$C_4\times10^{-1}$	$C_5\times10^{-3}$	Se_y
Methyl Esters of Fatty Acids						
Methyl Butyrate	3.1720	1.1600	-1.2074	1.2130	1.5382	9.9
Methyl Laurate	2.4982	1.4211	-1.1278	1.1999	1.8282	5.8
Methyl Palmitate	2.6737	-1.8906	-1.1644	1.2190	1.9109	6.2
Methyl Stearate	2.1157	0.41592	-1.0713	1.1880	1.9057	5.3
Methyl Oleate	2.3539	-0.67354	-1.1303	1.2123	1.9709	4.9
Methyl Linoleate	2.4433	0.53428	-1.1557	1.2119	2.0231	4.5
Methyl Linolenate	2.4167	1.0464	-1.1630	1.1928	2.0328	5.5
2:1 M. Stearate M. Linseed	2.7359	2.1624	-1.1670E	1.1839	1.9716	6.2
2:1 M. Linseed M. Stearate	2.5911	3.7365	-1.1792	1.1679	2.0185	4.9
Ethyl Esters of Fatty Acids						
Ethyl Butyrate	2.4760	1.2607	-1.0865	1.2073	1.4666	5.5
Ethyl Caprylate	2.3636	-1.6746	-1.0709	1.2283	1.6314	4.9
Ethyl Stearate	2.8333	0.24623	-1.1432	1.2113	1.8845	6.5
Ethyl Linoleate	2.2948	0.25081	-1.1245	1.2008	1.9786	4.9
Ethyl Linseed	2.3020	-1.2131	-1.1359	1.2158	2.0143	6.3
Isopropyl Esters of Fatty Acids						
Isopropyl Palmitate	1.9149	-2.0898	-0.99983	1.2219	1.7707	5.0
Isopropyl Stearate	2.2380	-1.2664	-1.0467	1.2175	1.8141	8.1
Methyl Ester Biodiesel Fuels						
Methyl Soy Ester	2.4172	1.3673	-1.1493	1.1936	1.9909	5.6
Methyl Canola	2.3572	0.19670	-1.1350	1.2048	1.9865	4.4
Methyl Tallow	3.3752	1.1433	-1.2644	1.1983	1.9826	8.0
Methyl Lard	2.3895	-1.7181	-1.1285	1.2073	1.9532	5.0
Methyl Yellow Grease	2.4528	0.11858E	-1.1296	1.2060	1.9582	4.7
Methyl Oxidized Soy	2.4307	2.1386	-1.1498	1.1850	2.0039	5.3
Methyl Hydrogenated Soy	2.2256	-13.593	-1.0906	1.2784	1.9237	8.0
Ethyl Ester Biodiesel Fuels						
Ethyl Soy Ester	2.4131	0.4.0191	-1.1150	1.2590	1.9404	5.4
Ethyl Oxidized Soy	2.2477	0.48846	-1.1126	1.2082	1.9656	4.5
Ethyl Hydrogenated Soy	2.2947	0.98222	-1.0975	1.1866	1.8995	5.0
Hydrocarbons and Diesel Fuel						
n-Octadecane	2.3332	-2.1502	-1.0272	1.1857	1.6875	5.8
n-Hexadecane	1.9595	-4.5985	-0.95101	1.2088	1.6091	4.8
n-Dodecane	1.9104	0.093166	-0.92151	1.1737	1.4414	4.1
Certified D-2	2.3791	-1.0217	-1.0944	1.2626	1.8043	4.8
Isentropic Bulk Modulus (MPa) $=C_1T^2(°C)^2+C_2TP(MPa)+C_3T+C_4P+C_5$						

Se_y: the standard error for the y estimate

The following discussion focuses on identifying common trends for the esters with different levels of saturation, chain length, or alcohol type. In the figures, the points represent the measured values and the lines represent predicted values from Equation 5.1.

Figure 5.4 shows the effect of temperature at atmospheric pressure on the isentropic bulk modulus for fuels with different levels of saturation. Methyl stearate, methyl oleate, methyl linoleate, and methyl linolenate are esters with an equal number of carbon atoms but an increasing number of carbon-carbon double bonds. The isentropic bulk modulus tends to increase as the degree of unsaturation increases (more double bonds). The methyl linolenate, because its purity was not high and it included substantial amounts of more saturated compounds (see Appendix A, Table A.1), showed very similar values with methyl linoleate. All of the compounds appear to have approximately the same property variation with temperature as indicated by similar slopes of the lines on these figures.

Figure 5.5 shows the variations in the isentropic bulk modulus as the pressure increases for the four levels of saturation. The temperature for these data was 40 °C. A complete comparison could not be made at 20 °C because methyl stearate is a solid at this temperature. Again, the slope of the isentropic bulk modulus as the pressure increases is about the same for the esters with different saturation levels. Figures 5.4 and 5.5 indicate that the increase in isentropic bulk modulus is fairly uniform as each double bond is added. The change in isentropic bulk modulus from stearate to oleate is about the same as from oleate to linoleate.

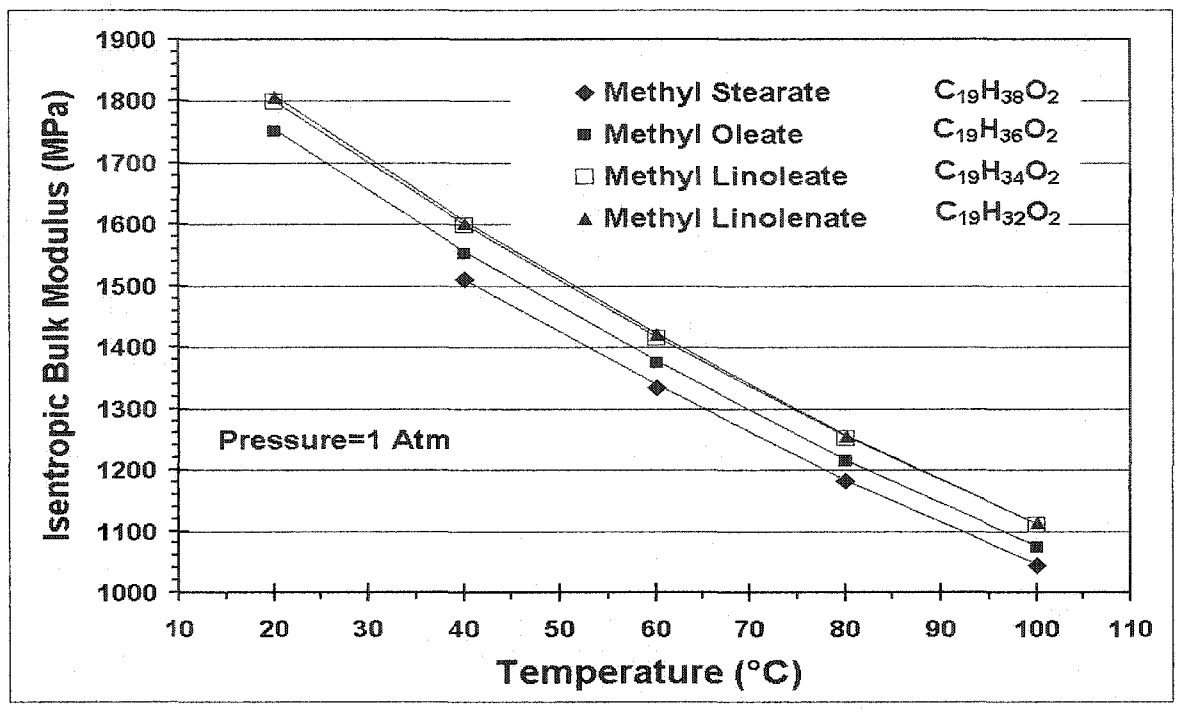

Figure 5.4. Temperature dependent saturation effect on isentropic bulk modulus at atmospheric pressure

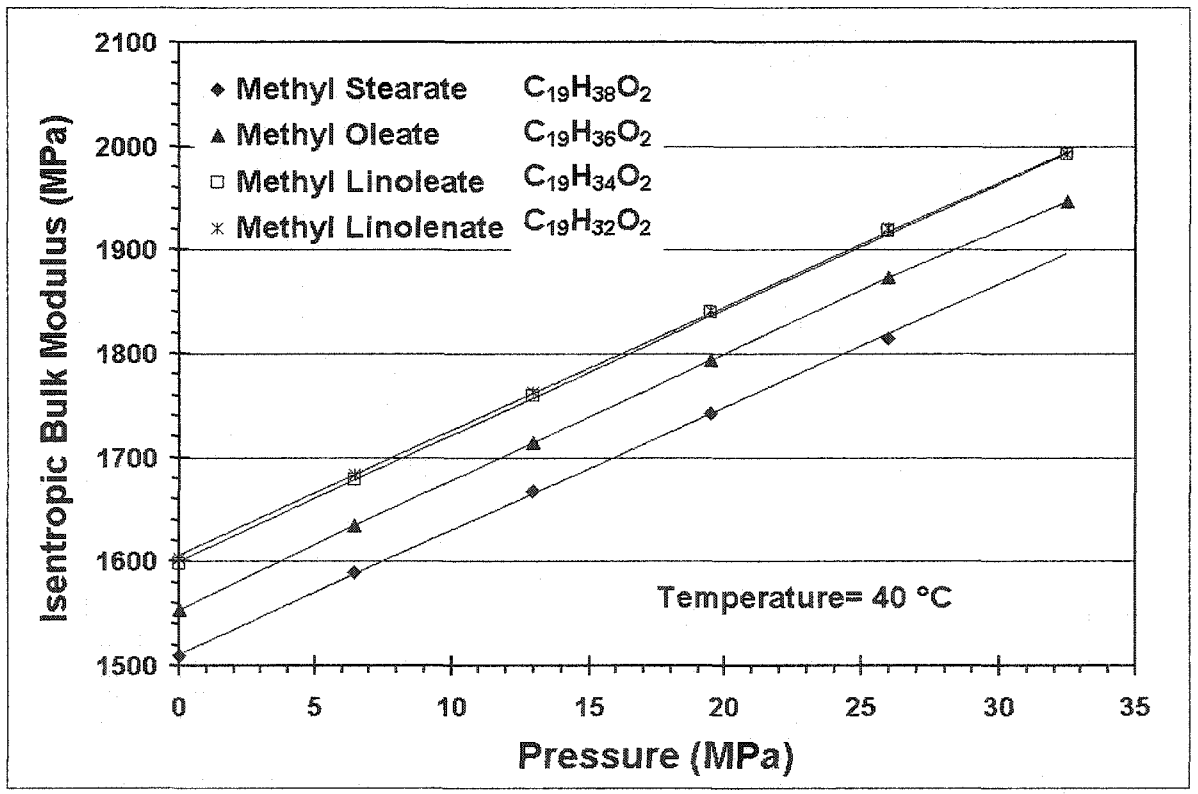

Figure 5.5. The effect of saturation on the isentropic bulk modulus at elevated pressures and 40°C

The property data for methyl butyrate, methyl laurate, methyl palmitate, and methyl stearate are provided in Figures 5.6 - 5.11 to show the effect of fatty acid chain length. These data demonstrate that the speed of sound and isentropic bulk modulus increase as the chain length increases, which supports the observation made for hydrocarbons in reference [87]. However, the density showed different characteristics than the speed of sound and the isentropic bulk modulus. The density increased with shorter chain length and the slope with temperature changes with chain length.

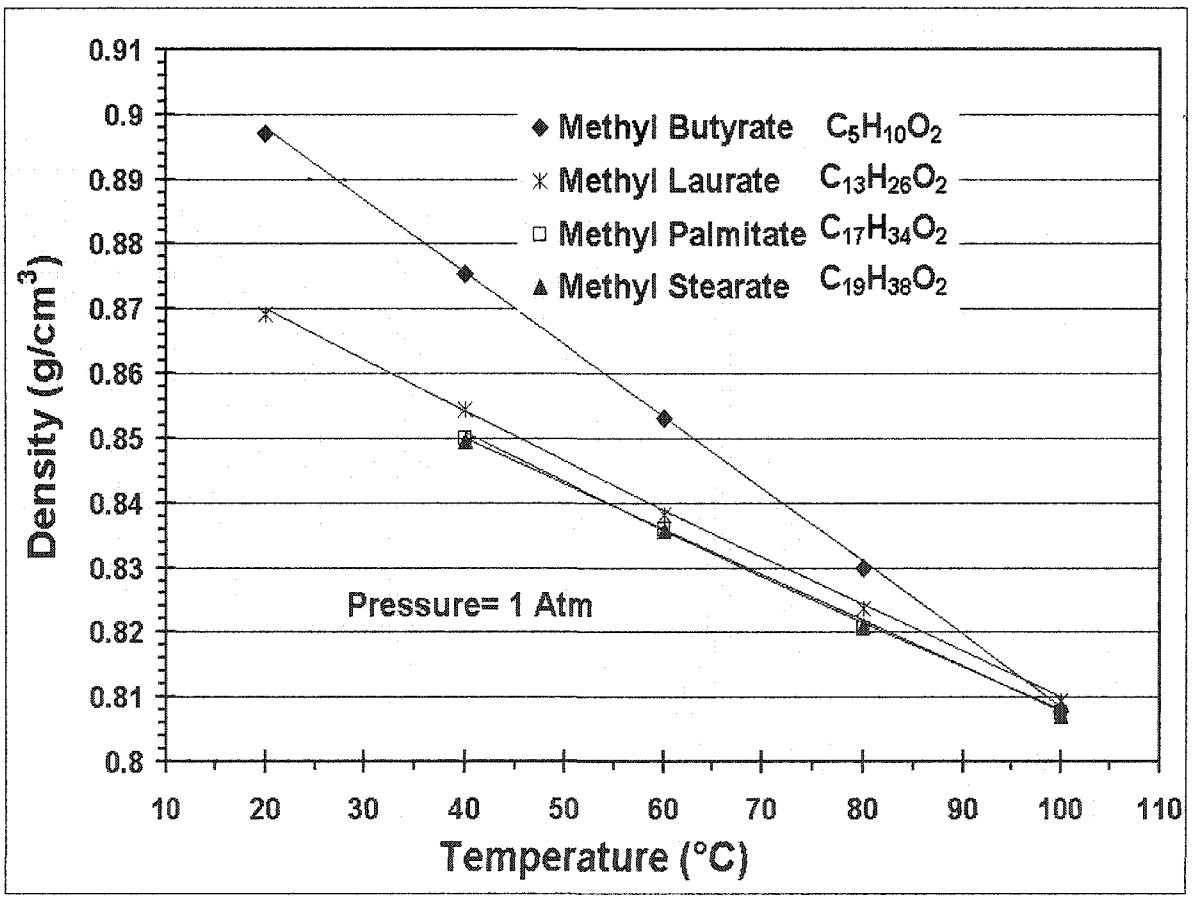

Figure 5.6. The effect of chain length and temperature on density at atmospheric pressure.

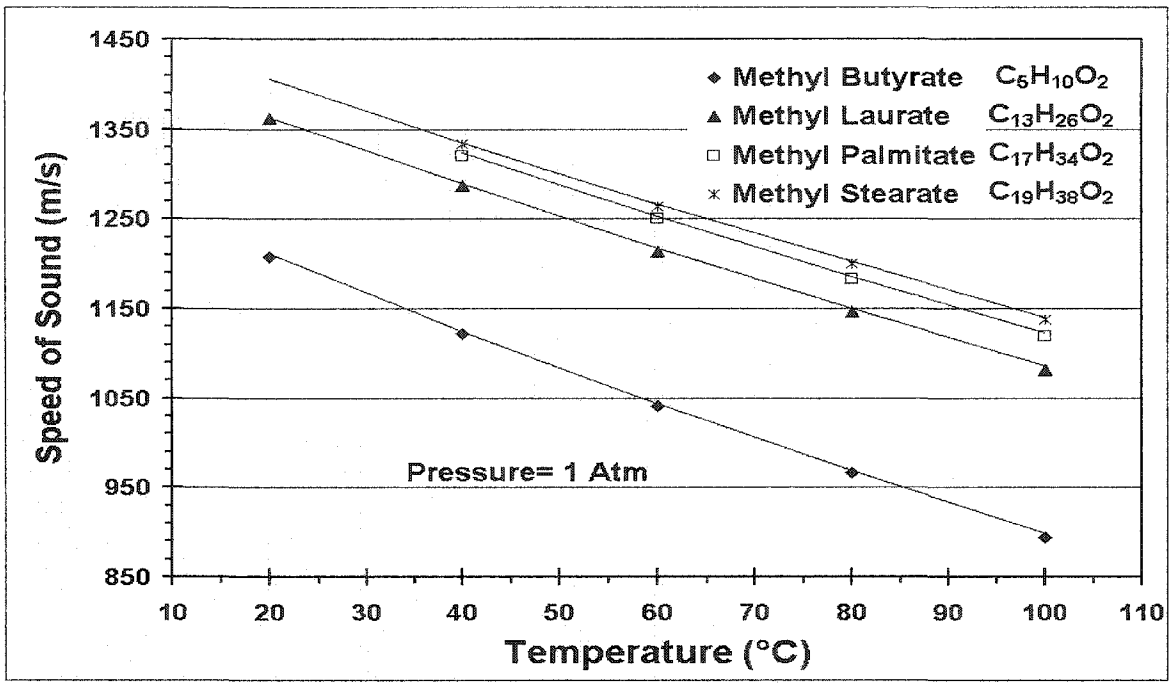

Figure 5.7. The effect of chain length on the speed of sound at atmospheric pressure.

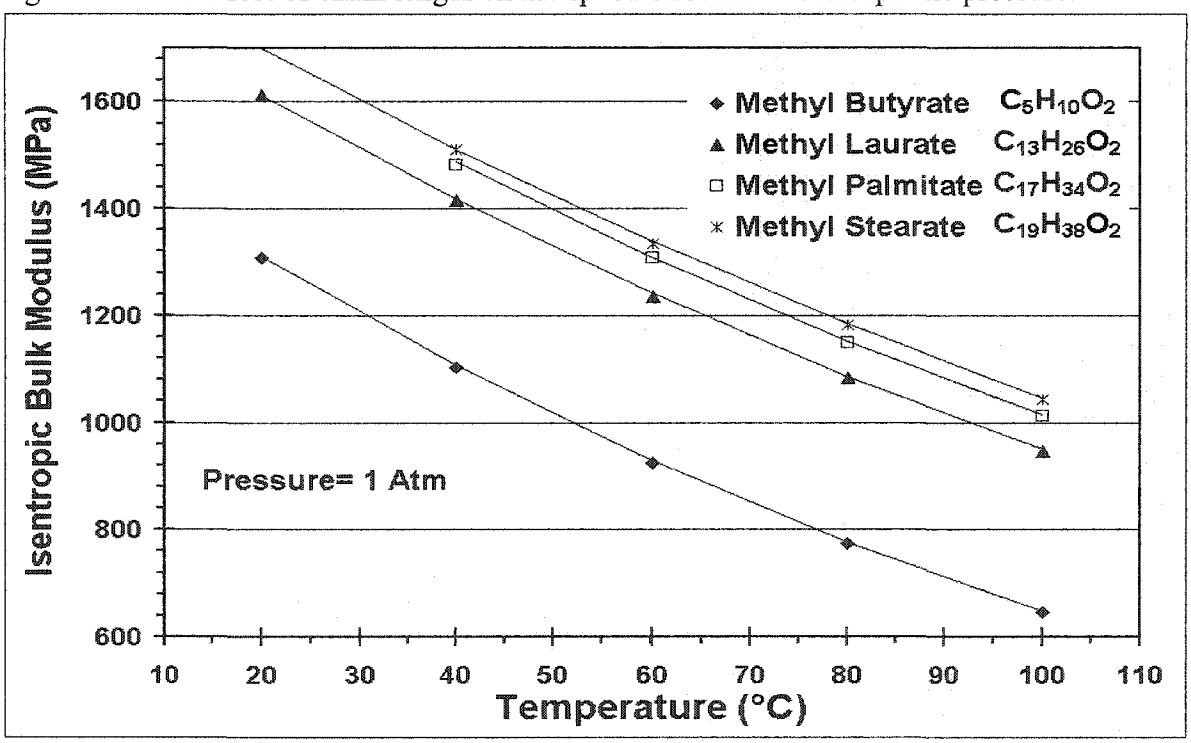

Figure 5.8. The effect of chain length on the isentropic bulk modulus at atmospheric pressure.

Figures 5.9 to 5.11 show the effect of pressure on the density, speed of sound, and isentropic bulk modulus for different chain length esters at 40 °C. It is clear that there is an approximately linear change in the properties with pressure.

The effect of temperature on the density, speed of sound, and bulk modulus of soy methyl ester, soy ethyl ester, emissions certification grade No. 2 diesel fuel (Cert D2), and dodecane is shown in Figures 5.12 - 5.14. Although these measurements were conducted independently with samples from another source (Colorado School of Mines) the data are consistent with the measurements presented in Figures 5.1-5.3. However, those were limited to a single temperature of 21°C. The soy methyl ester is approximately 0.5% more dense than ethyl soy ester and 5% more dense than the Cert D2.

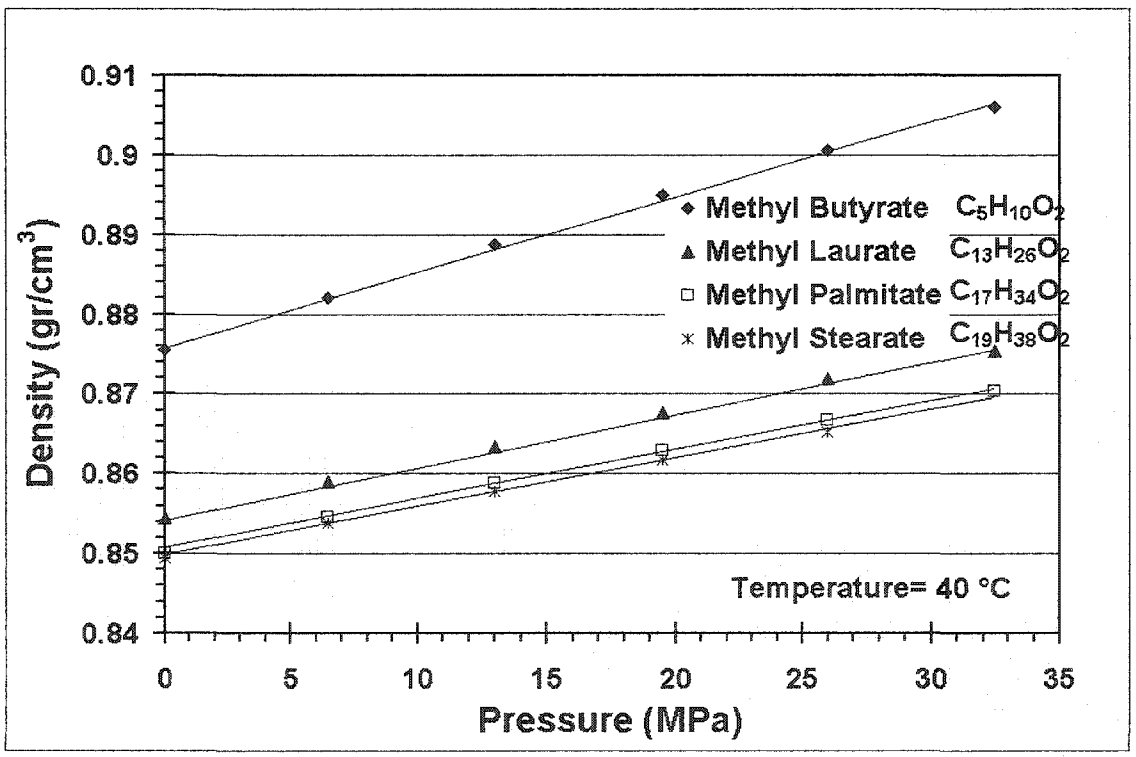

Figure 5.9. The effect of chain length on density at elevated pressures and 40 °C

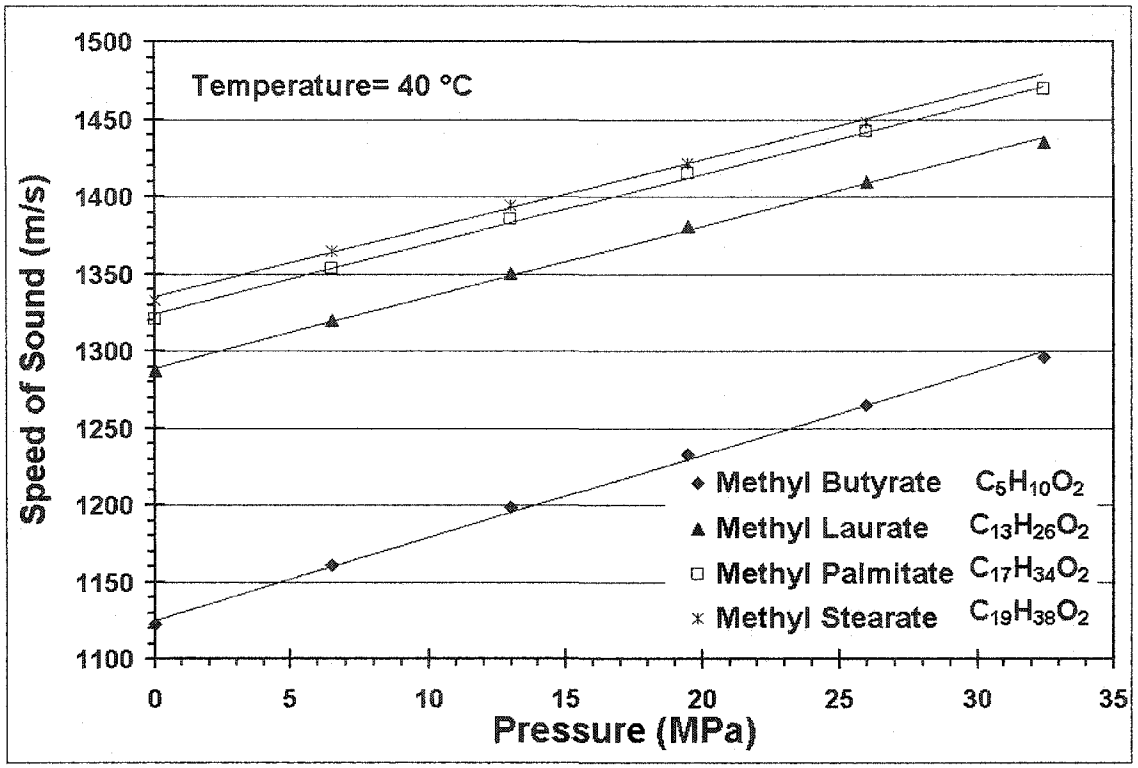

Figure 5.10. The effect of chain length on the speed of sound at elevated pressures and 40 °C

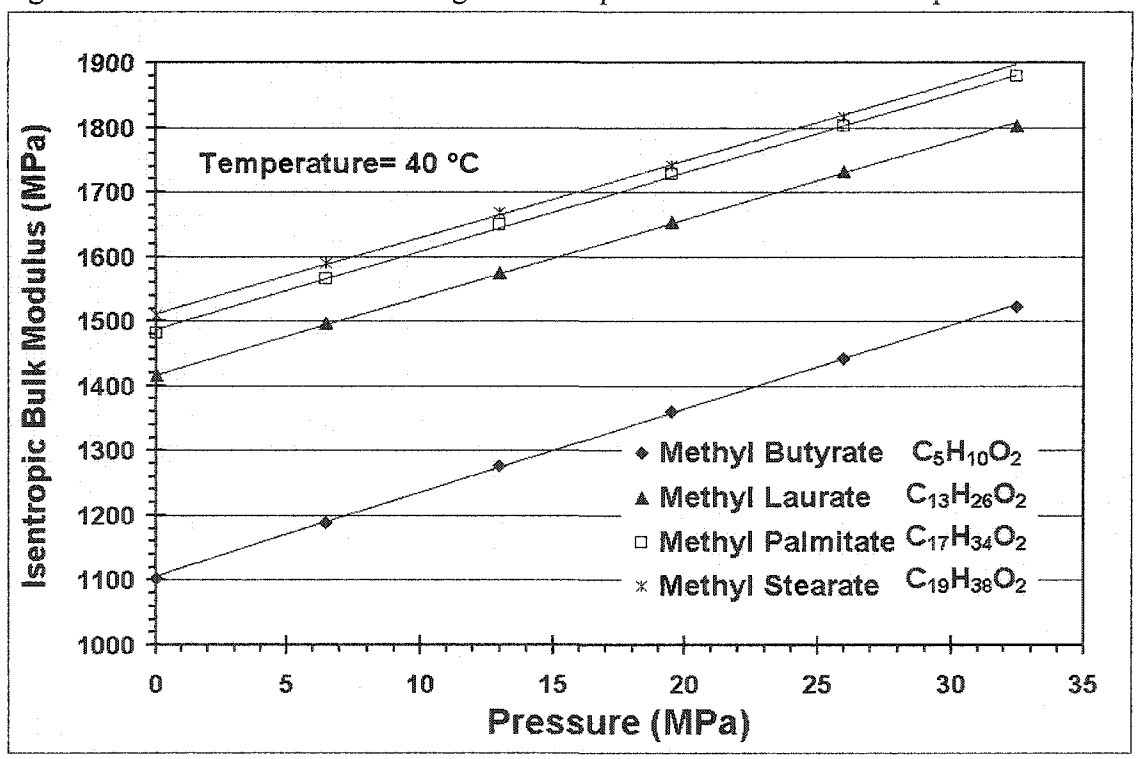

Figure 5.11. The effect of chain length on the isentropic bulk modulus at elevated pressures and 40 °C

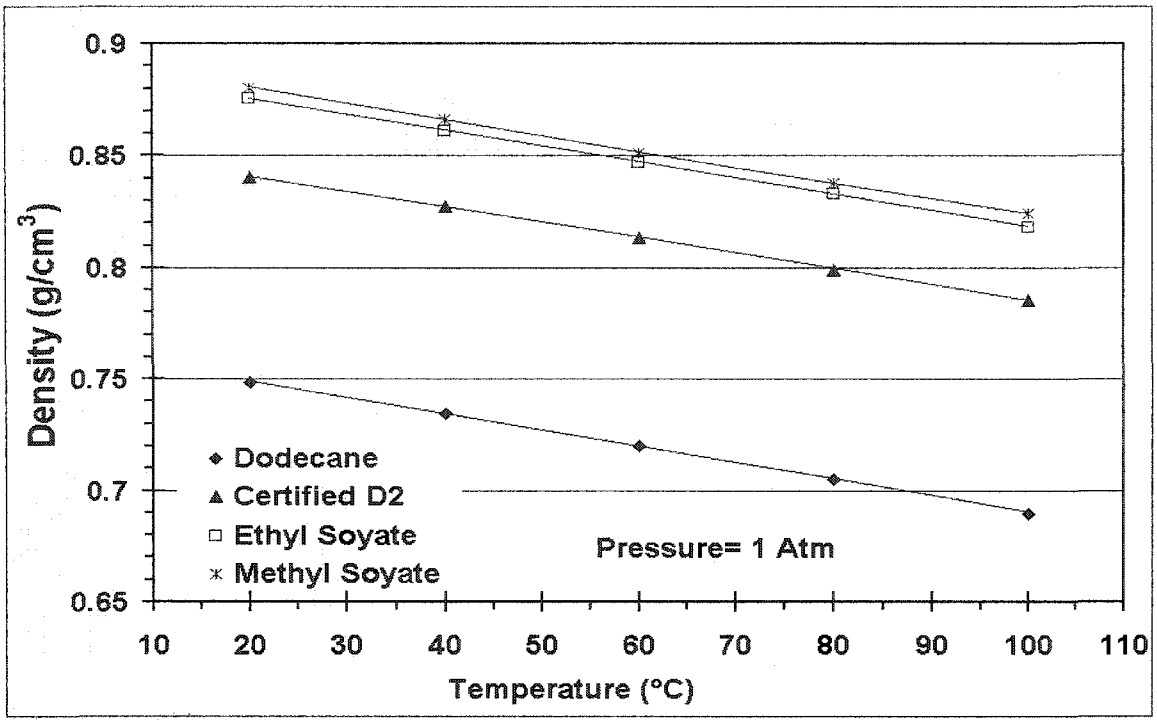

Figure 5.12. The density of methyl soyate, ethyl soyate, certified D2 diesel fuel and dodecane at atmospheric pressure.

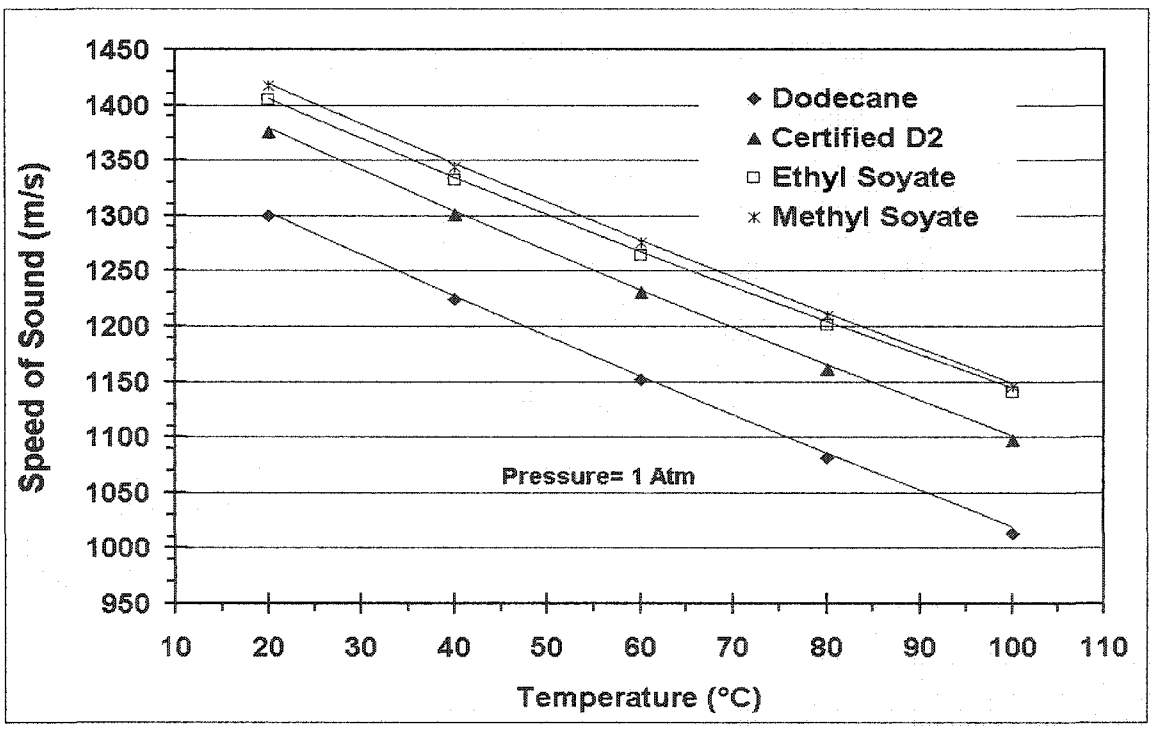

Figure 5.13. The speed of sound of methyl soyate, ethyl soyate, certified D2 diesel fuel and dodecane at atmospheric pressure.

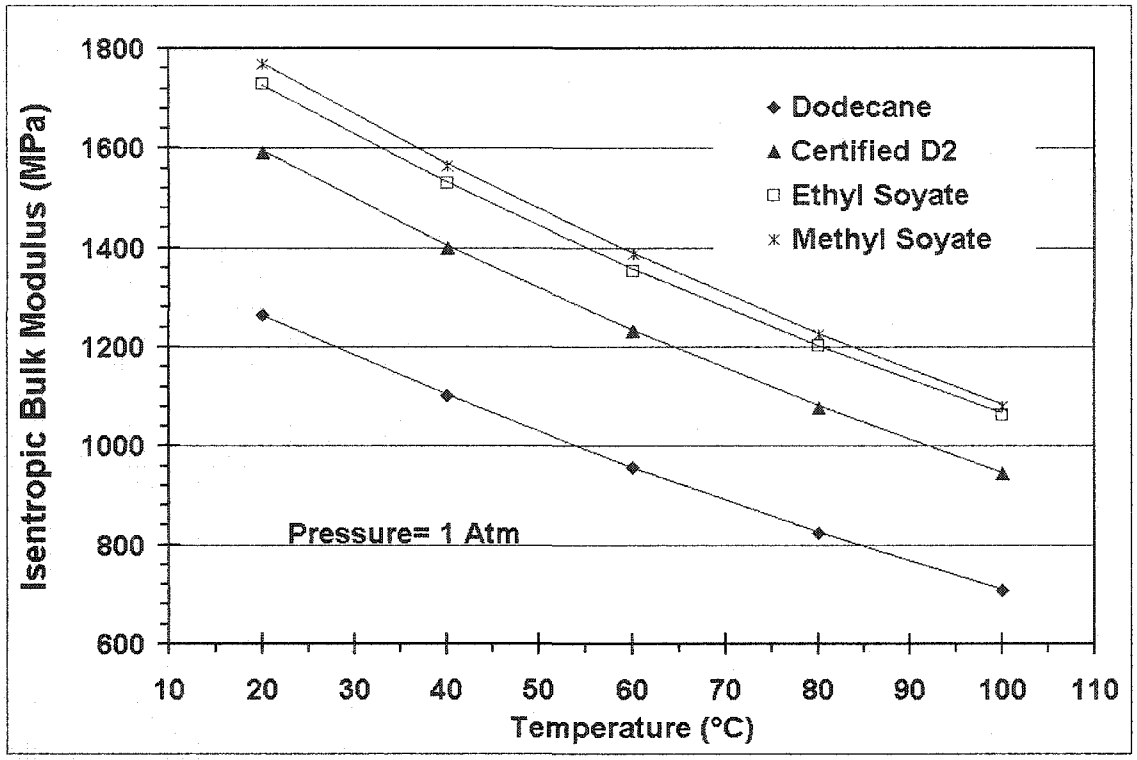

Figure 5.14. The isentropic bulk modulus of methyl soyate, ethyl soyate, certified D2 diesel fuel and dodecane at atmospheric pressure.

The speed of sound in the soy methyl ester is about 0.7% faster than the soy ethyl ester and 2.8% faster than the Cert D2. The calculated isentropic bulk modulus of the methyl soy ester was 1% higher than that of the ethyl soy ester and 10% higher than the Cert D2. The higher bulk modulus means that biodiesel will experience a more rapid pressure rise than petroleum-based diesel fuel as the injection pump displaces a fixed volume. This will result in earlier injection for biodiesel and may be part of the reason of biodiesel's higher NOx emission.

5.2.3. Blend Measurement of Biodiesel and Diesel Fuels

Another objective of this study was the investigation of the effect of biodiesel-diesel fuel blend level on the density, speed of sound, and isentropic bulk modulus at higher pressures and at temperatures of 20 °C and 40 °C.

When the biodiesel-diesel fuel blend level was varied, and the pressure was increased, the density, speed of sound, and isentropic bulk modulus of the fuel samples showed approximately linear increases with pressure at the two temperature levels that were investigated, 20 and 40 °C. A polynomial that was linear in temperature, pressure, and blend percentage was used to fit the density and isentropic bulk modulus data. This general equation is shown as Equation 5.2.

$$y = C_1T + C_2P + C_3B + C_4 \qquad (5.2)$$

where y is the density or the isentropic bulk modulus of the blends of No. 1 and No. 2 diesel fuel with biodiesel fuel, T is the temperature in °C, P is the pressure in MPa, B is the biodiesel percentage in the blend, and C_i, $i=1, 4$ are the regression constants given in Tables 5.5 and 5.6. The R^2 values and the standard errors for y calculated by an Excel spread sheet are also shown in the tables. It should be noted that since measurements were taken at only two values of temperature, the exact nature of the temperature effect cannot be determined. However, the assumption that the effect is linear is expected to be reasonable based on the more comprehensive measurements that have been presented for biodiesel itself.

A more complex three variable polynomial was used to fit the speed of sound data. The general form of this equation is shown in Equation 5.3.

$$y = C_1T + C_2P + C_3B + C_4TP + C_5PB + C_6P^2 + C_7B^2 + C_8 \qquad (5.3)$$

The coefficients C_i, $i=1, 8$ are given in Table 5.7. The density, speed of sound, and isentropic bulk modulus of the biodiesel-No. 2 diesel fuel blends at 20 °C have been presented in publication [88].

Table 5.5. Density regression constants.

Samples	$C_1 \times 10^4$	$C_2 \times 10^4$	$C_3 \times 10^4$	$C_4 \times 10$	R^2	$Se_y \times 10^4$
No. 2 Diesel Fuel Blends	2.6324	5.8574	-6.5302	8.6671	0.9983	5.5
No. 1 Diesel Fuel Blends	5.9030	6.1040	-6.5757	8.3318	0.9991	7.2
Density (g/cm3) = $C_1 \times T(°C) + C_2 \times P(MPa) + C_3 \times B$(Biodiesel Percentage) + C_4						

* Se_y: the standard error for the y estimate

Table 5.6. Isentropic bulk modulus regression constants.

Samples	C_1	$C_2 \times 10^{-1}$	C_3	$C_4 \times 10^{-3}$	R^2	Se_y
No. 2 Diesel Fuel Blends	1.1927	1.2170	-9.7434	1.8384	0.9985	6.8
No. 1 Diesel Fuel Blends	2.7763	1.2206	-9.6579	1.6727	0.9983	8.1
Isentropic Bulk Modulus (MPa) = $C_1 \times T(°C) + C_2 \times P(MPa) + C_3 \times B$(Biodiesel Percentage) + C_4						

* Se_y: the standard error for the y estimate

Table 5.7. Speed of sound regression constants.

Sample	No. 2 Blends	No. 1 Blends
C_1	-3.5972	-3.7043
C_2	4.6849	5.0232
C_3 x 10	2.3682	6.5479
C_4 x 10^2	1.4412	1.4958
C_5 x 10^3	-3.9664	-6.9146
C_6 x 10^2	-1.6236	-1.7425
C_7 x 10^4	8.8429	11.8120
C_8 x 10^{-3}	1.4570	1.4147
R^2	0.9989	0.9990
Se_y	2.0	2.1
Speed of Sound (m/s) = $C_1 \times T(°C) + C_2 \times P(MPa) + C_3 \times B$(Biodiesel Percentage) + $C_4 \times T \times P + C_5 \times P \times B + C_6 \times P^2 + C_7 \times B^2 + C_8$		

* Se_y: the standard error for the y estimate

Only the isentropic bulk modulus of the samples will be presented here to demonstrate the type of data that were collected. The measured data and the predicted values are given in Figure 5.15. The data points shown on the figure are the averages of the measured values at each pressure level and the lines are the regression results calculated using Equation 5.2. The error bars represent the 90% confidence intervals. As can be seen in from the figure, the isentropic bulk modulus shows very linear behavior with blend percentage at each pressure level. Although not shown, the density data were also very linear. The speed of sound data were somewhat nonlinear which justified the use of the higher degree polynomial. The density, speed of sound, and isentropic bulk modulus data also showed very linear behavior with pressure. Results were similar at 40 °C to those at 20 °C.

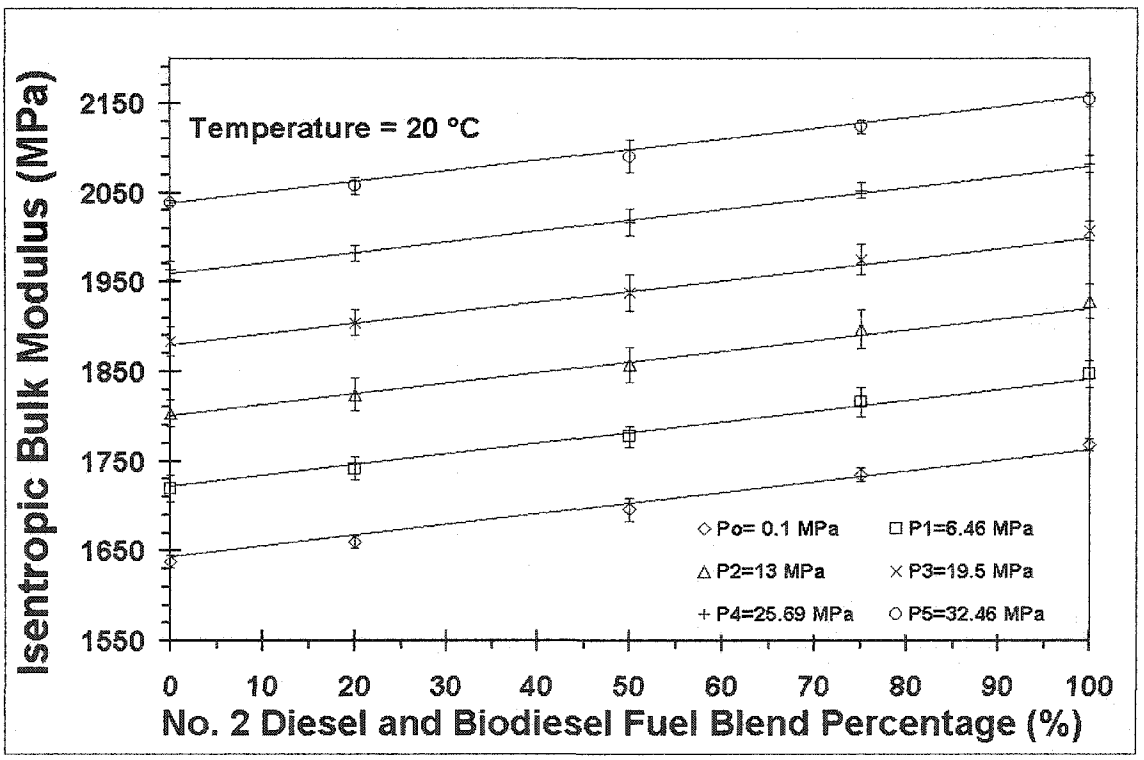

Figure 5.15. Isentropic bulk modulus comparison between measured data and regression equation (Lines are from the three variable regression Equation 5.2.)

5.3. Engine Test Results and Discussion

In this section, the test procedures defined in Chapter Three will be reviewed prior to presenting the experimental data. Each of the test matrices was targeted to investigate the effect of a specific fuel property on diesel engine combustion and biodiesel NOx emission. The first section will present the fuel properties of the biodiesel from soybean oil, biodiesel from yellow grease, and No. 2 diesel fuel with and without a cetane number enhancing additive. These fuels were chosen to investigate the fuel property effects on NOx emission. In Chapter Three, a four step test was proposed. However, in the final test matrices, steps 3 and 4 were combined into a single set of tests.

The test matrices, as introduced in Chapter 3, were designed in such a way that each test matrix targeted one portion of the concept map, explaining the interrelationships between the physical and chemical properties of biodiesel fuel and the higher NOx emission of biodiesel. The test matrices are discussed in three subsections. In the first section, the global effects of the fuel properties on emission and diesel combustion are discussed and compared. In the second section, the effects of biodiesel's lower heating value, higher density, speed of sound, and isentropic bulk modulus on the start of injection and the start of combustion are discussed and comparisons are made between the fuels. In the third section, the effect of biodiesel's higher cetane number and lower volatility on the combustion rate and on the BSNOx emission are discussed and comparisons are made between the fuels.

Biodiesel has a lower heating value, higher density, higher viscosity, higher speed of sound, higher isentropic bulk modulus, higher cetane number, and lower volatility than regular diesel fuel. In order to understand the global effect of these fuel properties, biodiesel fuels from soybean oil and yellow grease were compared with regular No. 2 diesel fuel at

steady state engine test conditions of 1400 rpm and 260 ft lbf (352.5 N m) of torque. The oxides of nitrogen (NOx), unburned hydrocarbons, carbon monoxide, and Bosch smoke number emissions were compared to determine the property effects on the start of injection, start of combustion, and the combustion rate of the fuels. This section was called the Investigation of the Global Effects of Biodiesel Fuel Properties.

Biodiesel has about 12% less heating value than regular diesel fuel by mass and about 8% less heating value by volume because biodiesel is about 3.4% more dense than regular diesel fuel. Diesel engine fuel management is handled by the diesel fuel injection pump. Inline- and distributor-type injection pumps control the engine load by varying the injection duration and injection timing. Distributor-type injection pumps such as the pump for the engine used in this study, increase the amount fuel injected to the cylinders by starting the injection earlier. The end of the injection is fixed at all injection conditions including all load conditions. Since the fuel measurement in the fuel injection pump is volumetric, biodiesel use causes about an 8% power loss. This power loss is compensated for by increasing the fuel amount, which causes the injection to start earlier. The higher speed of sound and isentropic bulk modulus of biodiesel are also expected to affect the start of injection, start of combustion, and NOx emission of the biodiesel fuels. In order to define and differentiate the lower heating value, or fuel quantity effect, from the higher speed of sound and isentropic bulk modulus effects, a test sequence was designed. In this test, biodiesel from soybean oil and regular No. 2 diesel fuels were compared. Each fuel was tested at 1400 rpm and at load conditions from 100% to 20% of the maximum torque level of each fuel. The tests were repeated three times. The test matrix was repeated with two different pumps, pump #1 and pump #2. The start of injection comparisons were made at the same power level and at the

same fuel volume per injection. At the same power level, we were able to see the total start of injection advancement due to the lower heating value (and resulting fuel flow increase) and the higher speed of sound and bulk modulus. It was possible to differentiate the effect of the higher speed of sound and isentropic bulk modulus of biodiesel by comparing the start of injection timings of the two fuels at the same volumetric rate per injection. The emissions, start of combustion, and combustion rates were compared and the property effects on these parameters will be discussed in the sections that follow.

Biodiesel has a higher cetane number that improves the diesel combustion by shortening the ignition delay period and restricting the combustion rate for the uncontrolled (premixed) portion of the diesel combustion. Therefore, it would be expected that the oxides of nitrogen emission of biodiesel should decrease. However, this has not been observed by most researchers. Also, the low volatility of biodiesel restricts the amount of fuel that vaporizes during the ignition delay period, reducing the amount of ignitable fuel in the cylinder and the premixed portion of the combustion. This decrease usually lowers the maximum temperature and the oxides of nitrogen emissions of biodiesel. Engine tests were conducted with biodiesel from soybean oil, biodiesel from yellow grease, and No. 2 diesel fuel with and without a cetane improver. To be able to make the comparisons of these fuels at the same start of combustion timing, the fuel injection pump was rotated and data were collected at five different levels of injection timing. Two different fuel injection pumps were used and two different sets of data were collected. Biodiesel from soybean oil and from yellow grease were compared to each other because both had the same volatility but different cetane numbers, so that it was possible to make inferences about the effect of cetane number on biodiesel combustion and oxides of nitrogen emission. To investigate the low volatility

effect, regular No. 2 diesel fuel, regular No. 2 diesel fuel with a cetane improver, and biodiesel from soybean oil were compared. The No. 2 diesel fuel with cetane improver had the same cetane number as the biodiesel from soybean oil so the ignition delay periods were the same. This allowed the determination of the effect of different volatilities at the same start of combustion on the diesel combustion rate and oxides of nitrogen. These results will also be discussed in the following sections.

5.3.1. Physical and Chemical Properties of Biodiesel and Diesel Fuels Used in the Engine Test Matrices

Before presenting the engine test results, the fuels that were used for the tests will be described. This section introduces the biodiesel fuels and regular diesel fuel that were specially chosen for the engine tests. The physical and chemical properties of the fuels are given in Tables 5.8 and 5.9. Regular No. 2 diesel fuel was purchased from a local supplier. Soybean oil methyl ester and yellow grease methyl ester were prepared at the Biomass Energy Conversion Center (BECON) facilities of the Iowa Energy Center in Nevada, Iowa. The fatty acid distributions of the soybean oil and yellow grease methyl esters are given in Table 5.9.

When the properties of the fuels are compared, it is seen that the chemical structure, sulfur content, molecular weight, cetane number, heating values, density, and viscosity are different. Biodiesel fuels contain about 11% oxygen, by weight, where regular diesel fuels contain none. Biodiesel fuels are composed of long straight chain fatty acid esters. Diesel fuel is a mixture of hydrocarbons including saturates, aromatics, and olefins. Biodiesel has almost no sulfur. The No. 2 diesel fuel has a sulfur content of 0.034% by weight of the fuel.

Table 5.8. The physical and chemical properties of No. 2 diesel fuel, soybean oil methyl ester, and yellow grease methyl ester

Test Property	*No 2 diesel fuel*	*Soybean Oil Methyl Ester*	*Yellow Grease Methyl Ester*
Carbon (% mass)[d]	86.66[a]	77.00	76.66
Hydrogen (% mass)[d]	12.98[a]	12.18	12.33
Oxygen (% mass)[d]	-	10.82	11.01
C/H Ratio	6.676	6.322	6.217
Sulfur (% mass)[a]	0.034	<0.005	<0.005
Typical Formula	$C_{14.01}H_{25.00}$[b]	$C_{18.74}H_{34.51}O_2$[d]	$C_{18.40}H_{35.26}O_2$[d]
Average Molecular Weight	194.14[b]	291.73[d]	288.29[d]
Cetane Number (ASTM D613)[a]	42.2	50.4	62.6
Hydrocarbon Type, FIA (ASTM D1319)[a]			
Saturates	56.6	-	-
Olefins	1.6	-	-
Aromatics	41.8	-	-
Gross Heat of Combustion (Btu/lb)[a]	19419	17183	17252
Net Heat of Combustion (Btu/lb)[a]	18235	16072	16209
Specific Gravity[c]	0.8559	0.8796	0.8722
Kinematic Viscosity (@40°C, mm^2/s)[c]	2.8911	4.5926	5.9156
Total Glycerol (%)[c]	-	0.175	0.194

[a] Measured by Phoenix Chemical Laboratory Inc., Chicago, IL
[b] Calculated using UOP Method 375-86
[c] Measured at the Mechanical Engineering Department, Iowa State University
[d] Calculated from Fatty Acid Profile unless stated otherwise

Table 5.9. Fatty Acid Profiles for Biodiesel Fuels from Soybean Oil and Yellow Grease

*Profile**	*Soybean Oil Biodiesel*	*Yellow Grease Biodiesel*
C14:0 Tetradecanoic (Myristic)	<0.10	1.27
C14:1 Tetradecenoic (Myristoleic)	<0.10	0.43
C15:0 Pentadecanoic	<0.10	0.18
C16:0 Hexadecanoic (Palmitic)	10.81	17.44
C16:1 Hexadecenoic (Palmitoleic)	0.11	2.03
C17:0 Heptadecanoic (Margaric)	<0.10	0.51
C17:1 Heptadecenoic (Margaroleic)	<0.10	0.41
C18:0 Octadecanoic (Stearic)	4.54	12.38
C18:1 Octadecenoic (Oleic)	24.96	54.67
C18:2 Octadecadienoic (Linoleic)	50.66	7.96
C18:3 Octadecatrienoic (Linolenic)	7.27	0.69
C18:4 Octadecatetraenoic	<0.10	0.13
C20:0 Eicosanoic (Arachidic)	0.37	0.25
C20:1 Eicosenoic (Gadoleic)	0.32	0.52
C20:2 Eicosadienoic	<0.10	0.11
C22:0 Docosanoic (Behenic)	0.42	0.21
C24:0 Tetracosanoic (Lignoceric)	0.12	0.0
Unknown	0.32	0.81

* Measured by Woodson-Tenent Laboratories, Inc., Des Moines, IA.

Biodiesel fuels have much higher cetane numbers than diesel fuel, which has a significant effect on the diesel combustion. Ten points of cetane number increase makes about 1° degree advancement in combustion timing [65]. The soybean oil and yellow grease methyl esters had 50.5 and 62.6 cetane numbers, respectively, while the No. 2 diesel fuel had a cetane number of 42.2. The cetane numbers of biodiesel from soybean oil and yellow grease were about 10 and 20 cetane numbers higher than the cetane number of regular No. 2 the diesel fuel. The lower heating value of biodiesel is 12% lower than for regular diesel fuel but biodiesel fuels are about 3.5% more dense than regular diesel fuel. Therefore, a volume-based heating value comparison shows that biodiesel has about 8% less heating value than

diesel fuel. The viscosities of soybean oil and yellow grease methyl esters are about 60 and 100% higher than regular diesel fuel, respectively.

The soybean oil methyl ester included only about 15% saturated fatty acids while the yellow grease methyl ester contained about 30% saturated fatty acids. The most common saturated fatty acids are palmitic (C16:0) and stearic (C18:0). It should be noted that the biodiesel fuel from yellow grease has a much higher cetane number than the biodiesel fuel from soybean oil and this is related to the amount of saturated fatty acid compounds [89].

Biodiesel from soybean oil and yellow grease were chosen because both fuels have about the same volatility and physical property characteristics, but have significantly different cetane numbers, which permits an investigation of the cetane number effect on the biodiesel combustion and biodiesel oxides of nitrogen emission. In addition, for the investigation of the effect of low volatility, a cetane improver was used to increase the cetane number of No. 2 diesel fuel to the same level as the soybean biodiesel. This permitted a test matrix that includes two fuels with the same cetane number and thus, the same ignition delay period, but with different volatility levels. 2-ethylhexyl nitrate was used as the cetane improver.

5.3.2. Investigation of the Global Effects of Biodiesel Fuel Properties (on Diesel Engine Performance and Emissions)

In this section, biodiesel from soybean oil, biodiesel from yellow grease, and No. 2 diesel fuel are compared at standard timing. These three fuels were specifically chosen because of their properties. The two biodiesel fuels had the same heating values, chemical characteristics, volatility, and physical properties, but different cetane numbers. However, when both biodiesel fuels were compared to No. 2 diesel fuel, the biodiesel fuels had lower

heating values, higher cetane numbers, and different physical properties. When the engine was run with the fuels, it was possible to see the global effects of the biodiesel fuel properties on the diesel engine.

5.3.2.1. Emission Comparison of the Fuels

The global effects of biodiesel fuel properties on the performance and emissions of a diesel engine will be discussed in this section. The start of injection, start of combustion, and the combustion rates of No. 2 diesel fuel and the biodiesel fuels from soybean oil and yellow grease will be compared. The higher NOx emissions of biodiesel will be presented and the reasons for the observed changes will be discussed. The data in this section were obtained using pump #2 only.

A steady state engine test matrix was applied. The operating condition was 352.5 N-m (260 ft-lbf) of torque and 1400 rpm. The engine emissions reported in these sections are presented on a brake specific basis (g/kW-h) at this operating condition. Carbon monoxide (CO), carbon dioxide (CO_2), unburned hydrocarbons (HC), oxides of nitrogen (NOx), and the Bosch Smoke Number (SN) were recorded. The test matrix was repeated three times for each fuel. Therefore in the figures, the average of the three measurements is shown and the error bars represent the maximum and the minimum of the three measurement for each fuel. In order to see the differences between the biodiesel and No. 2 diesel fuel emissions, a statistical analysis called "Tukey Grouping" was performed on the data and the ANOVA tables are presented in the Appendix. In Tukey Grouping, if two or more variables have the same letter, it means that there is no statistically significant difference between the variables. A confidence interval of 95% (α=0.05) was used.

The brake specific fuel consumption (BSFC) and the percentage change in the brake specific fuel consumption of biodiesel from soybean oil, yellow grease, and No. 2 diesel fuel are presented in Figure 5.16. The BSFC is defined as the amount of fuel consumption per hour per unit of brake power. The Tukey grouping of BSFC for the fuels is given in Table 5.10. As seen in Figure 5.16, the biodiesel fuels had about 12% higher BSFC than regular diesel fuel. The increase in BSFC is a result of biodiesel having a lower heating value that is about 12% lower than regular diesel fuel. The heating values of No. 2 diesel fuel, soybean biodiesel, and yellow grease biodiesel are 18,235, 16,072, and 16,209 Btu/lb, respectively. The BSFC values for the two biodiesel fuels are about the same and this is expected since their heating values are close. These results align with the observations published earlier by other researchers, including Canakci [90], Monyem [82], and McDonald et al. [91].

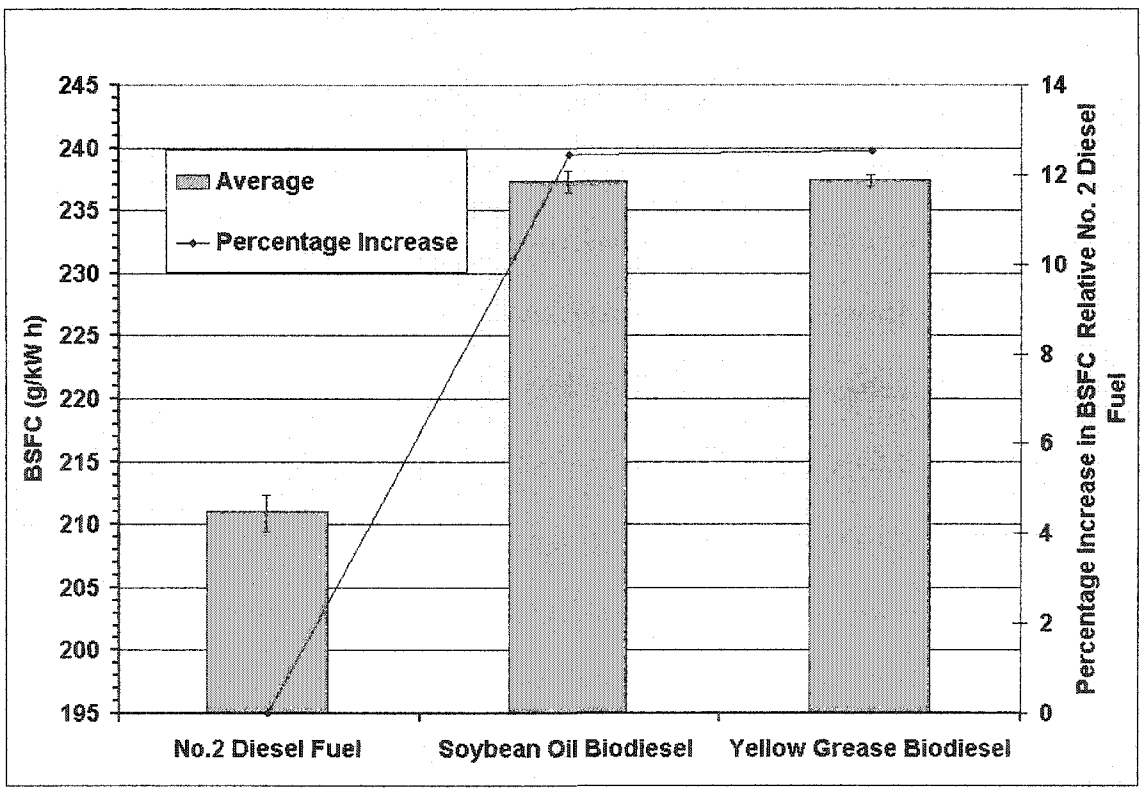

Figure 5.16 Comparison of brake specific fuel consumption

Table 5.10. Tukey Grouping for BSFC

Sample	*Tukey Grouping*	*Mean*
No.2 Diesel Fuel	A	211.06
Soybean Oil Biodiesel	B	237.30
Yellow Grease Biodiesel	B	237.48

Oxides of nitrogen (NOx) are the emission of primary interest for this research and the brake specific oxides of nitrogen (BSNOx) values are given in Figure 5.17. The percentage increase in BSNOx emissions of the biodiesel fuels relative to No. 2 diesel fuel is also shown in Figure 5.17. It is clear that the BSNOx emission was increased with biodiesel from soybean oil, but there was no significant difference between the BSNOx of biodiesel from yellow grease and No. 2 diesel fuel as indicated by the Tukey grouping data in Table 5.11.

A detailed discussion of the NOx results will be given at the end of the section after the combustion parameters have been discussed. While most researchers have found that soybean oil-based biodiesel gave higher NOx emissions [42], Canakci [90], and Mittelbach and Tritthart [92] also found significantly higher NOx emission with biodiesel from yellow grease than diesel fuel, unlike our results. McCormick et al [43] showed that the molecular structure of biodiesel can have a significant effect on diesel engine emission. They found that increasing the number of double bonds can be correlated with increased NOx emission and more saturated feedstocks gave lower NOx than less saturated feedstocks.

Table 5.11. Tukey Grouping for BSNOx

Sample	*Tukey Grouping*	*Mean*
No.2 Diesel Fuel	A	8.54
Soybean Oil Biodiesel	B	9.75
Yellow Grease Biodiesel	A	8.61

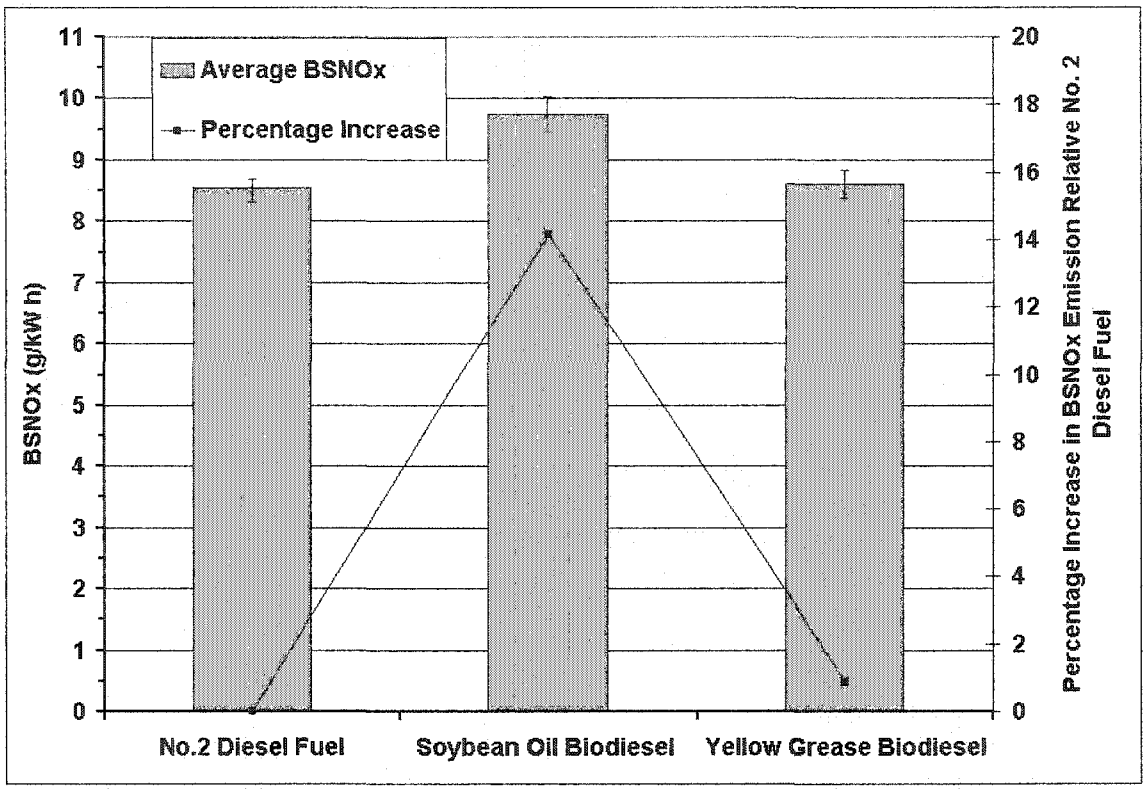

Figure 5.17. Comparison of brake specific oxides of nitrogen (BSNOx)

The brake specific hydrocarbon (BSHC) emissions of the fuels are compared in Figure 5.18. Biodiesel fuels showed very significant reductions of about 50% in BSHC emissions relative to No. 2r diesel fuel. Table 5.12 indicates that there was no significant difference between the BSHC emission of the two biodiesel fuels. Canakci [90] and Monyem [82] also found reductions in BSHC of 50%.

Table 5.12. Tukey Grouping for BSHC

Sample	*Tukey Grouping*	*Mean*
No.2 Diesel Fuel	A	0.147
Soybean Oil Biodiesel	B	0.074
Yellow Grease Biodiesel	B	0.069

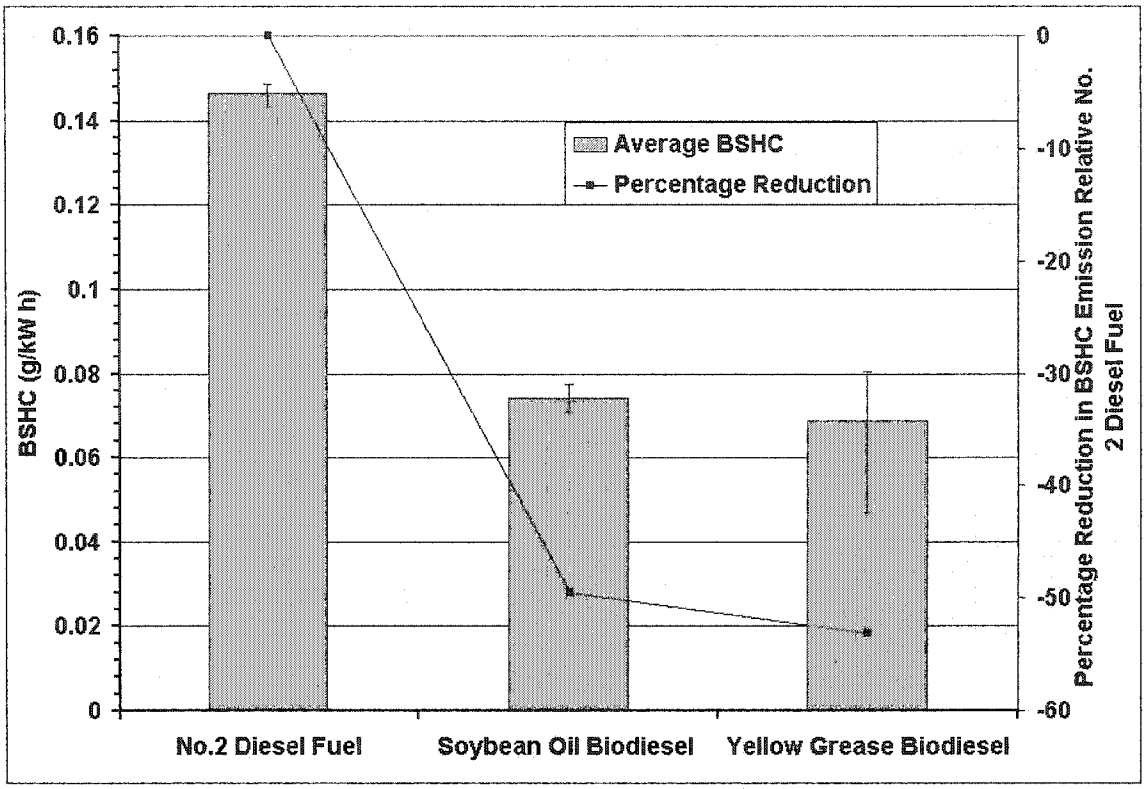

Figure 5.18. Comparison of brake specific hydrocarbon (BSHC)

The brake specific carbon monoxide (BSCO) emissions of the fuels are compared in Figure 5.19. Biodiesel from soybean oil and yellow grease show 33 and 26% reductions in BSCO relative to No. 2 diesel fuel and there was no significant difference between the biodiesel fuels as shown in Table 5.13.

Table 5.13. Tukey Grouping for BSCO

Sample	*Tukey Grouping*	*Mean*
No.2 Diesel Fuel	A	1.314
Soybean Oil Biodiesel	B	0.885
Yellow Grease Biodiesel	B	0.965

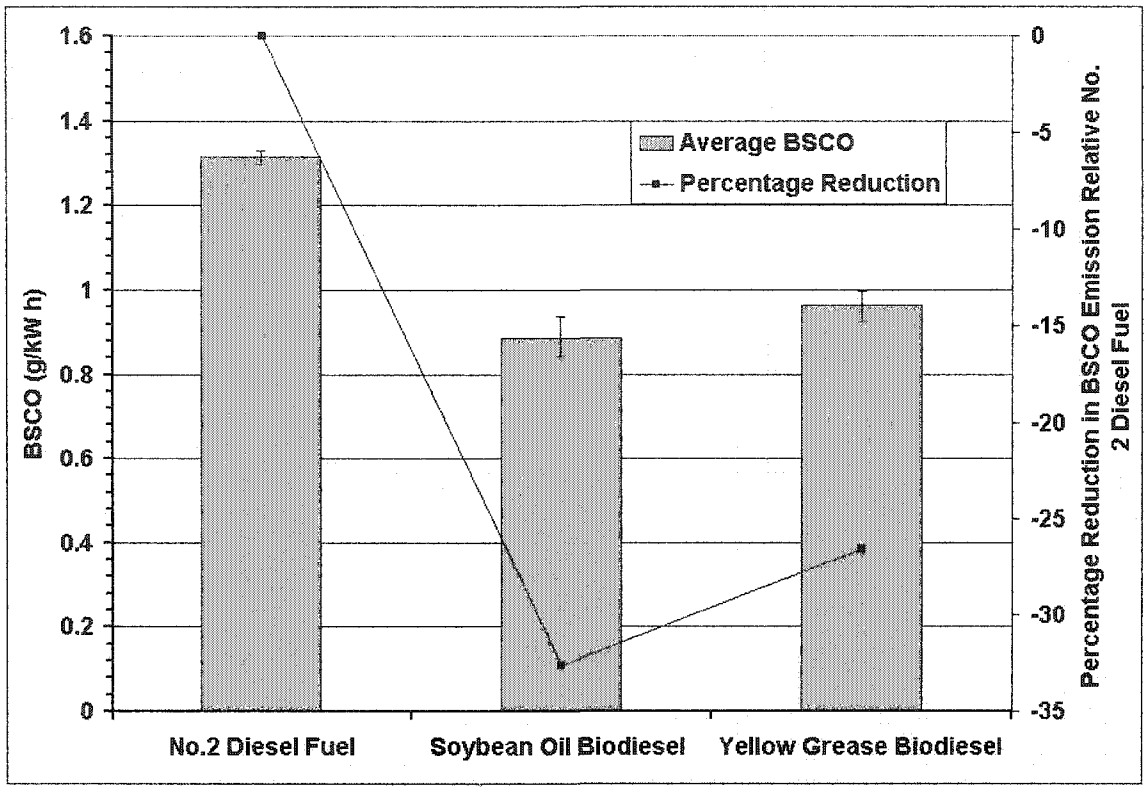

Figure 5.19. Comparison of brake specific carbon monoxide (BSCO)

Bosch Smoke Numbers (SN) for the biodiesel fuels are compared to No. 2 diesel fuel in Figure 5.20. Biodiesel from soybean oil and yellow grease showed SN reduction of 43 and 39%, respectively. These reductions are somewhat lower than the 60 and 57% observed by Canakci [90] and Monyem [82]. Statistically there was no significant difference between the biodiesel fuels, as shown in Table 5.14

Table 5.14. Tukey Grouping for Bosch Smoke Number

Sample	*Tukey Grouping*	*Mean*
No.2 Diesel Fuel	A	2.68
Soybean Oil Biodiesel	B	1.51
Yellow Grease Biodiesel	B	1.62

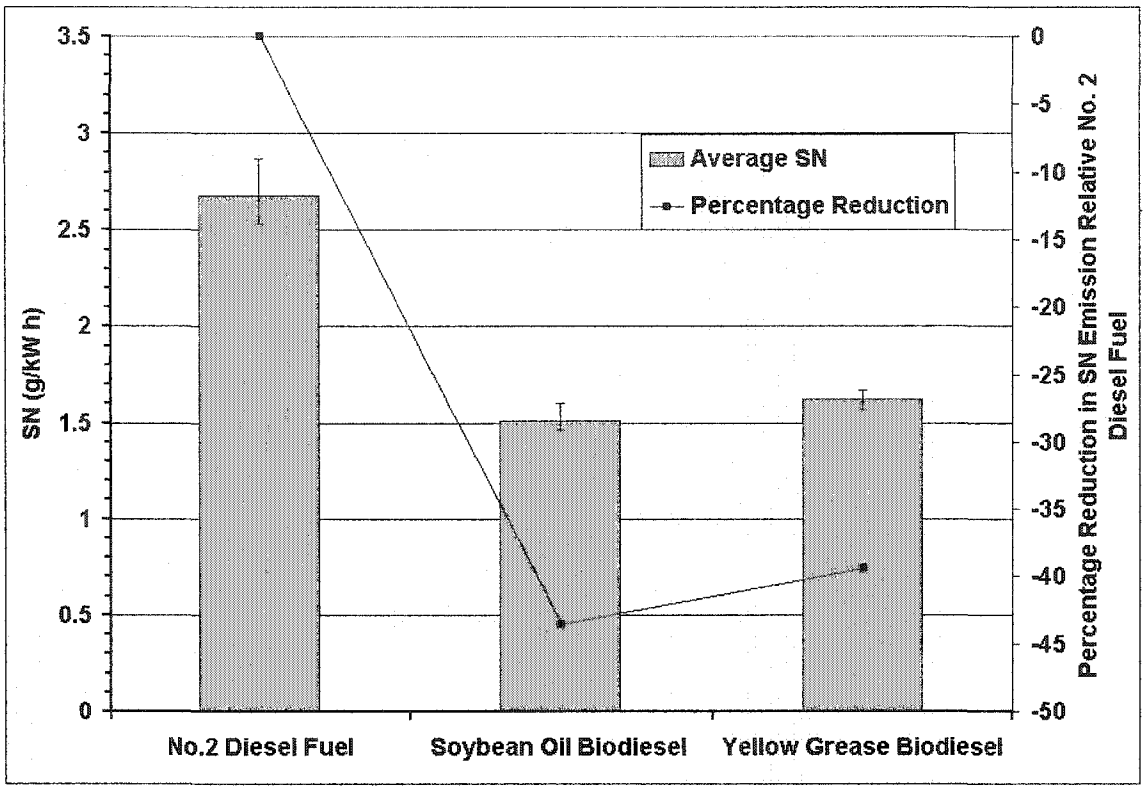

Figure 5.20. Comparison of brake specific Bosch Smoke Numbers (SN)

5.3.2.2. Combustion Comparison of the Fuels

Heat release analysis comparisons for the three fuels at the baseline condition are shown in Figure 5.21. Calculated quantities such as the start of injection and the ignition delay, that have been determined from the heat release curves, are shown in Table 5.15. The start of heat release for the yellow grease biodiesel was advanced about 2 degrees, and about 1.5 degrees for soybean biodiesel, relative to No. 2 diesel fuel. As shown in Table 5.15, the premixed combustion portion for the No. 2 diesel fuel includes about 9% of the total heat release. The premixed combustion is the initial period of rapid combustion that follows ignition. It involves fuel that was prepared to burn during the ignition delay period. High levels of premixed combustion are often associated with high exhaust NOx levels because the combustion occurs early and at high temperature and pressure. For soybean oil and

yellow grease biodiesel, the premixed combustion percentages were only 6.75 and 4.5%, respectively, showing less premixed combustion. This lower amount of premixed combustion is expected to be a result of a shorter ignition delay, which provides less time for the preparation of premixed fuel, and slower fuel vaporization due to biodiesel's low volatility.

The ignition delay period for No. 2 diesel fuel was 4.3 degrees, given in Table 5.15. The ignition delay periods for soybean and yellow grease biodiesel fuels were 3.5 and 3.0 degrees, respectively. The source of the higher NOx level with biodiesel is not readily apparent, since the biodiesel premixed combustion is less, but it is likely to be a result of the earlier combustion timing (compared with diesel fuel). The soybean-based biodiesel had higher NOx levels than the yellow grease-based biodiesel. The slightly higher premixed combustion for the soybean-based biodiesel than the yellow grease-based biodiesel may still be the cause of the higher NOx levels for soybean biodiesel.

Table 5.15 shows that the percentage of fuel burned in the premixed mode depends on more than just ignition delay. Diesel fuel's ignition delay is 37% longer than the ignition delay for soybean biodiesel and the percentage of fuel burned as premixed increased by a similar 33%. However, when diesel fuel is compared with yellow grease biodiesel, its ignition delay is 57% longer, while its fraction of fuel burned as premixed is 98% larger. This would indicate that the diesel fuel's greater volatility may be contributing to a greater rate of fuel preparation during the ignition delay. However, when soybean biodiesel and yellow grease biodiesel are compared with each other, the ignition delay of soybean biodiesel is only 15% longer while it has 50% more premixed combustion. Since all of the compounds

in biodiesel from both sources have similar boiling points, the difference in the fraction of fuel burned as premixed cannot be attributed solely to volatility differences.

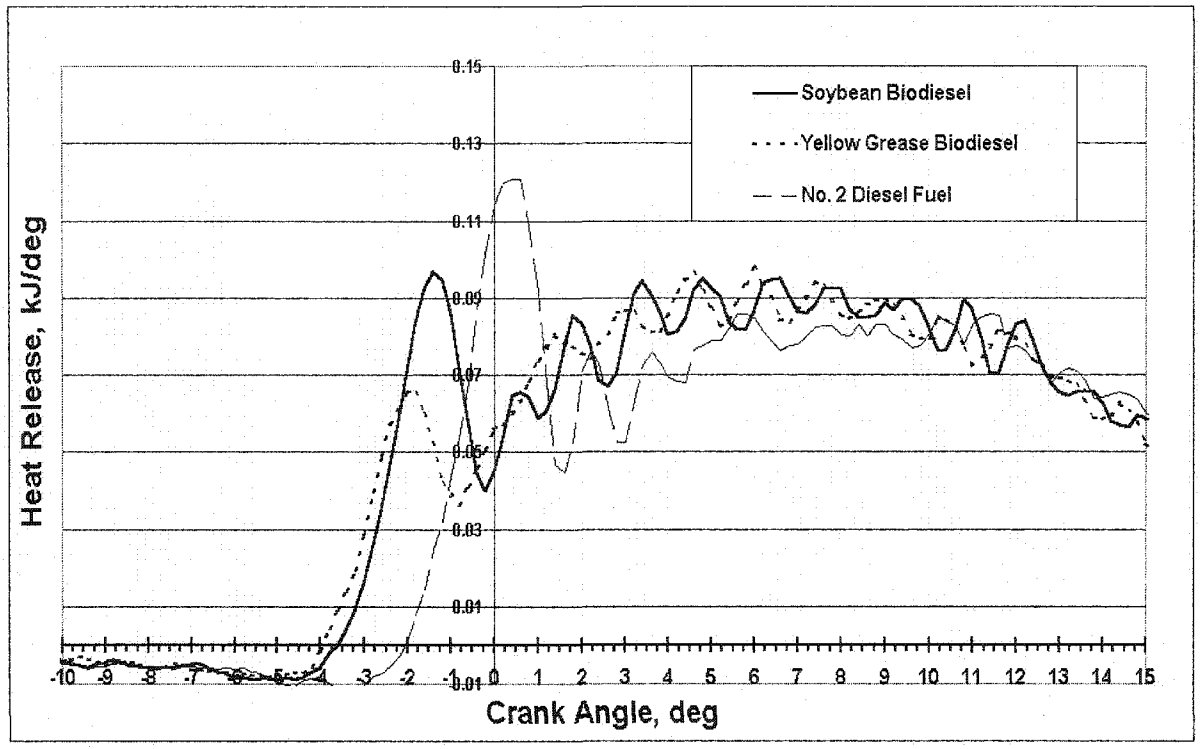

Figure 5.21. Heat release analysis comparison at 352.5 N-m and 1400 rpm with pump #2

Table 5.15. Combustion characteristics of No. 2 diesel, soybean, and yellow grease biodiesel fuels at 352.5 N-m and 1400 rpm, with pump #2.

Combustion Characteristics	***No. 2 Diesel Fuel (DIE)***	***Soybean Biodiesel (SBB)***	***Yellow Grease Biodiesel (YGB)***
Start of Injection, deg	-6.34	-7.13	-7.00
Start of Combustion, deg	-2.04	-3.61	-3.94
Ignition Delay, deg	4.28	3.50	3.05
Total of fuel energy released per injection, kJ/inj-cyl	2.756	2.720	2.760
Percent of fuel energy burned as premixed, %	8.92	6.73	4.5
Comparisons	***Ratios of Ignition Delay***		***Ratios of Percent Energy Release Rates as Premixed***
DIE/SBB =	1.37		1.33
DIE/YGB =	1.57		1.98
SBB/YGB =	1.15		1.5

5.3.3 Investigation of the Effects of Lower Heating Value and Higher Physical Properties of Biodiesel (Step 2, with pump #1).

In this section, the test matrix was completed with both pump #1 and pump #2. This test matrix was targeted to investigate the impact of biodiesel's 8% lower heating value (by volume) and the 11% lower compressibility of soybean oil biodiesel fuel than No. 2 diesel fuel. The effect of the lower heating value and less compressibility of biodiesel can be observed on the power and the start of injection timing. The lower heating value of biodiesel fuels causes 8% less power, or, for the same power level, an 8% greater volume of fuel must be consumed. This extra amount of fuel sent to the engine by the fuel injection pump causes an advance in the start of injection timing. Besides this, the lower compressibility (higher isentropic bulk modulus) of the biodiesel fuels was also expected to affect the start of injection timing by early injection for the same volume of fuel. It was mentioned earlier in the concept map discussion that early injection and combustion timing have a very significant effect on the NOx generation. Therefore, in this test matrix, soybean oil biodiesel and No. 2 diesel fuel's start of injection were compared both at the same power and the same volumetric fuel consumption level. The engine emissions, start of combustion, and ignition delays were also compared at the same power level. The engine was run at load conditions of 100, 95, 90, 80, 70, 60, 50, 40, 30, 20% of the maximum power that could be obtained from each fuel.

5.3.3.1 Investigation of Lower Heating Value and Bulk Modulus Effects on Fuel Injection Timing

Figure 5.22 presents the start of injection timing comparison of soybean-based biodiesel and No. 2 diesel fuel from 100% of maximum load to 20% light load conditions. It is clearly shown that, for pump #1, the biodiesel fuel injection timing is more advanced than for regular diesel fuel at the same BMEP, and the advancement is about 1.34° at the intermediate load level of 7.67 bar. This is the total timing advancement due to both the lower heating value and higher bulk modulus of biodiesel.

It is understood that when the engine load decreases, the start of injection is retarded until the light load advancement system in the pump is activated and the timing is advanced. It can be seen that the light load advancement system came on earlier with regular diesel (about 5 bar) than with biodiesel fuel (about 3 bar). This should have a significant effect on the light load emissions of the engine. This may explain the lower NOx emissions observed by some researchers using light load chassis dynamometer tests [43, 44, 45]. From these data, we are not able to discriminate the relative significance of the two property effects on the timing. However, when the comparisons are made based on volume it is easier to separate the effects.

Figure 5.23 presents the start of injection timing versus fuel delivery (cc/inj) data for both fuels. From this comparison it can be seen that the start of injection of biodiesel from soybean oil was advanced about 0.68° relative to No. 2 diesel fuel when the same volume of fuel was injected. This comparison is made at the same value of intermediate load (7.67 bar) that was examined earlier.

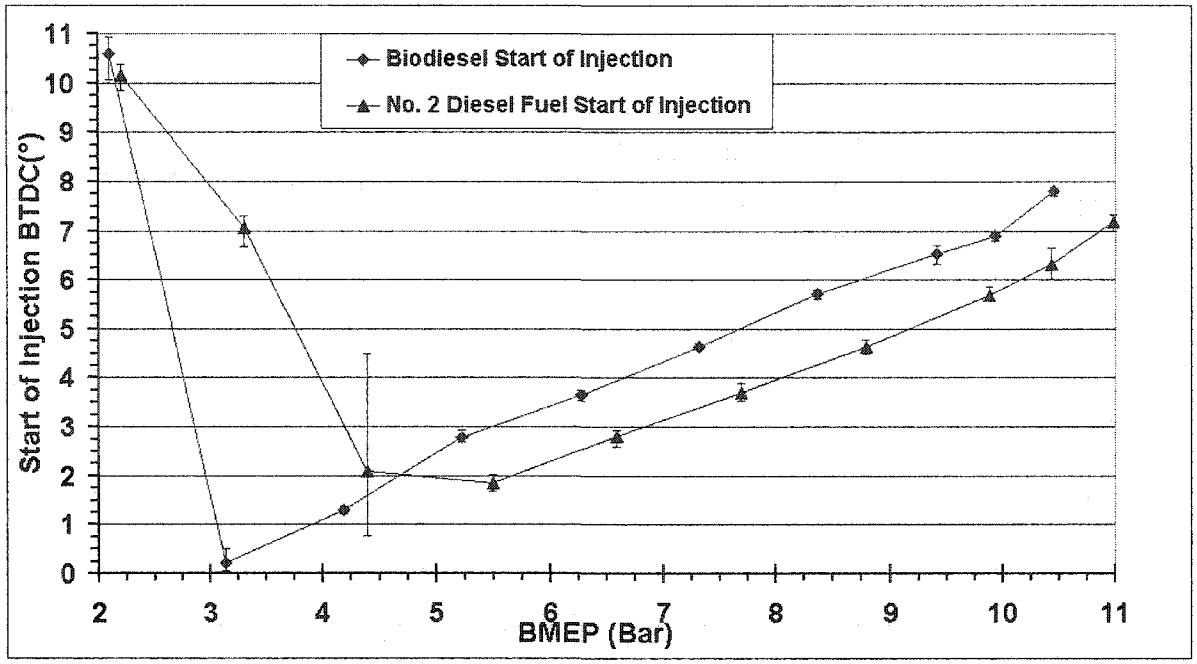

Figure 5.22. Start of injection comparison of soybean oil biodiesel and No. 2 diesel fuel at varying the load conditions from 100% to 20%, at 1400 rpm and with pump #1.

As explained above, the start of injection is retarded as the volume of fuel is reduced. For the same volume of fuel, the difference of 0.68° was initially assumed to be purely due to the effect of the speed of sound and isentropic bulk modulus. Therefore, 1.34° - 0.68° = 0.66° is proposed as the effect of the lower heating value of biodiesel on the start of injection timing due to fuel injection pump advancement at constant torque. Other inferences to be made are that the start of injection timing curves are parallel to each other until the light load advancement system in the pump comes on earlier with diesel fuel than biodiesel. It should also be noted that later work to be presented in this dissertation indicate that the 0.68° difference may not be solely due to speed of sound and isentropic bulk modulus effects. Viscosity and density differences may also be responsible for the variation in timing.

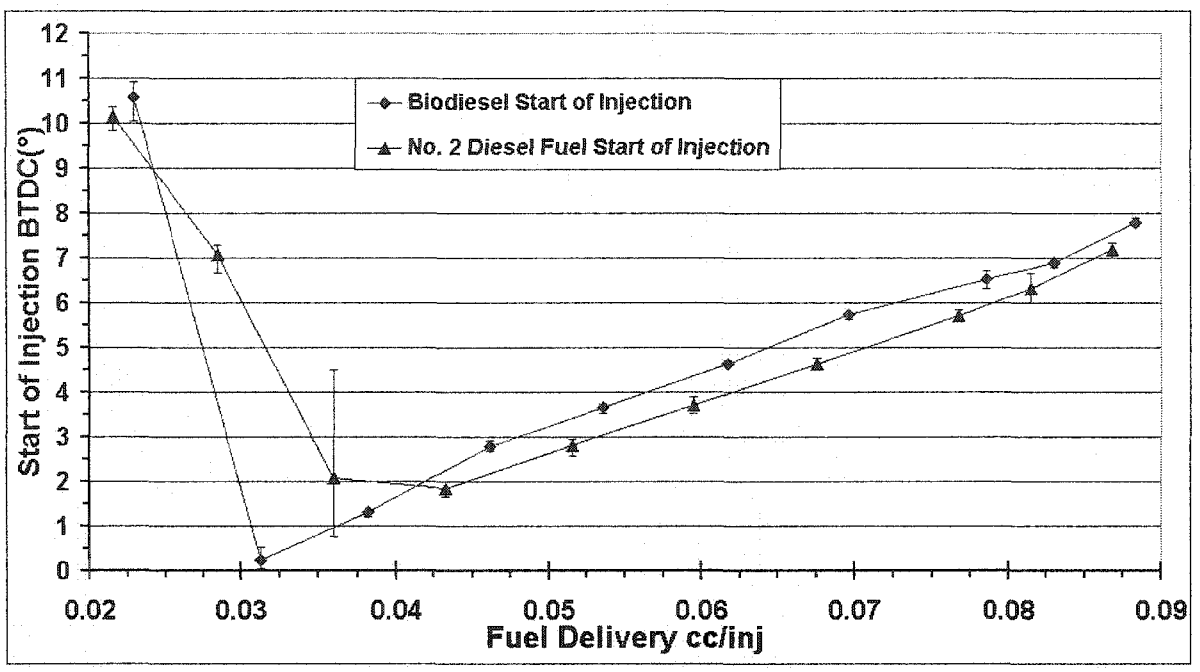

Figure 5.23. Volumetric comparison of the fuel delivery versus start of injection of Biodiesel and No. 2 Diesel fuels at varying the load conditions from 100% to 20%, at 1400 rpm and with pump #1.

5.3.3.2 Investigation of Lower Heating Value and Bulk Modulus Effects on Diesel Combustion with pump #1

In this section, the start of combustion timings are compared as a function of engine load for biodiesel from soybean oil and No. 2 diesel fuel. Figure 5.24 shows the start of combustion timings of both fuels as a function of load conditions. The start of combustion timings are presented in crank angle degrees and negative numbers represent degrees before TDC (top dead center), zero is TDC, and positive numbers represent degrees after TDC. It is observed that the start of combustion timing also reflects the start of injection timing trends, which means ignition delays are relatively constant at each load conditions. It is possible to see the light load advancement difference between the two fuels at about 2-4 bar BMEP. Start of injection, start of combustion, and ignition delay comparisons were made at the

intermediate load condition of 7.67 bar. This load condition was chosen for the comparison because it was a representative engine condition and it is a point where the measured values were relatively consistent. Biodiesel's start of combustion timing was advanced 2.38° crank angle relative to diesel fuel at 7.67 bar. When the ignition delay periods of biodiesel and diesel fuel were compared it was found that biodiesel had a shorter ignition delay period at all load conditions than diesel fuel. It was also found that the ignition delay periods were longer as the load decreased and the difference between biodiesel and diesel fuel increased until the light load advancement was engaged. The ignition delay difference between the two fuels at 7.67 bar BMEP was 1.06°. When added together, the lower heating value effect of 0.66°, the higher speed of sound and isentropic bulk modulus effect of 0.68°, and the shorter ignition delay period of 1.06° due to higher cetane number, the total start of combustion advances 2.38° which matches closely what we observe in Figure 5.24.

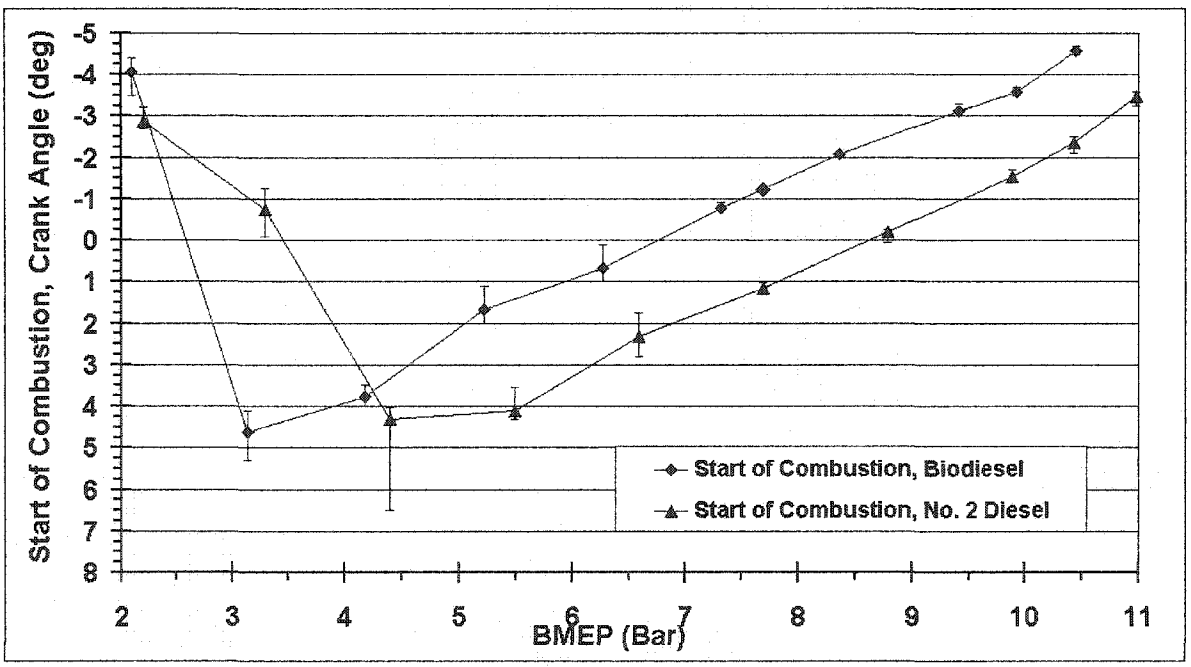

Figure 5.24. Comparison of the start of combustion timings of Biodiesel and No. 2 Diesel fuels at varying load conditions from 100% to 20% at 1400 rpm and with pump #1

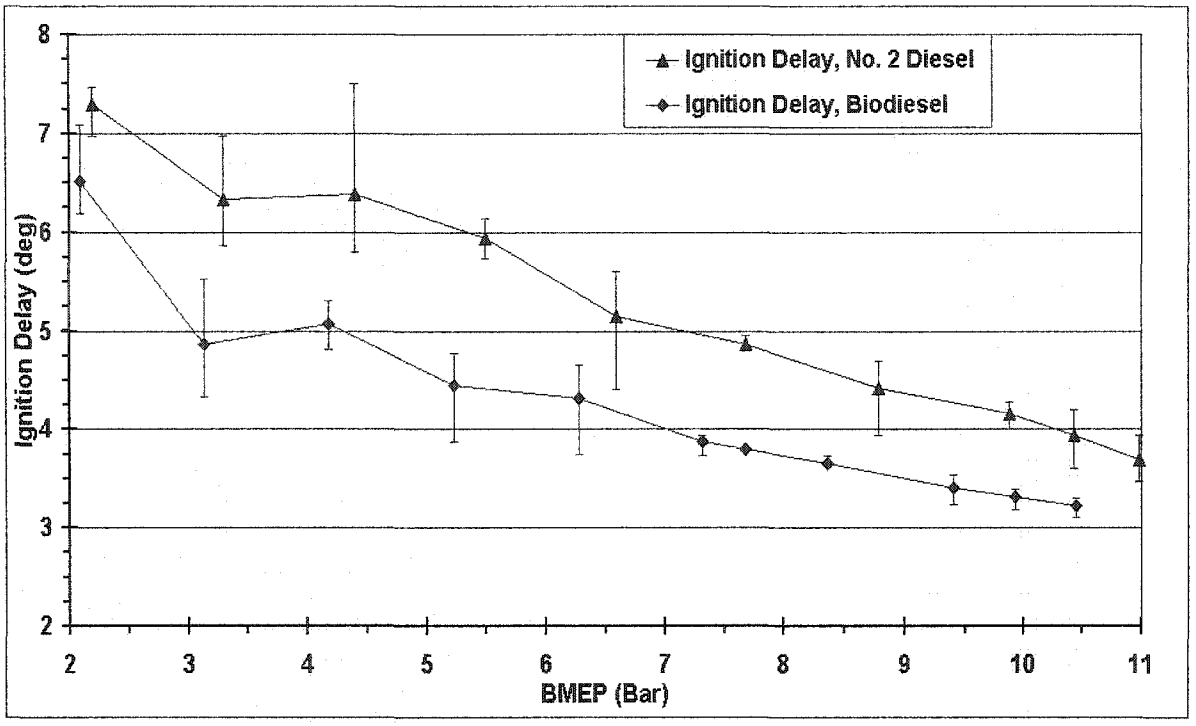

Figure 5.25. Comparison of the ignition delay period of Biodiesel and No. 2 Diesel fuels at varying load conditions from 100% to 20% at 1400 rpm and with pump #1

Heat release analysis of both fuels is compared at 100, 70, 40% and 40, 30 and 20% load conditions in Figures 5.26 and 5.27, respectively. Advancement of the start of combustion is clearly observed with the biodiesel fuel. It is also seen that the premixed combustion portion of the biodiesel combustion is also less than with diesel fuel. The premixed combustion corresponds to the initial peck, or spike, in the combustion that occurs immediately after ignition. When the engine load is reduced, the premixed portion of the combustion becomes a more significant fraction of the overall combustion in the engine. Especially at light load conditions, the biodiesel fuels' premixed combustion is much less than for diesel fuel.

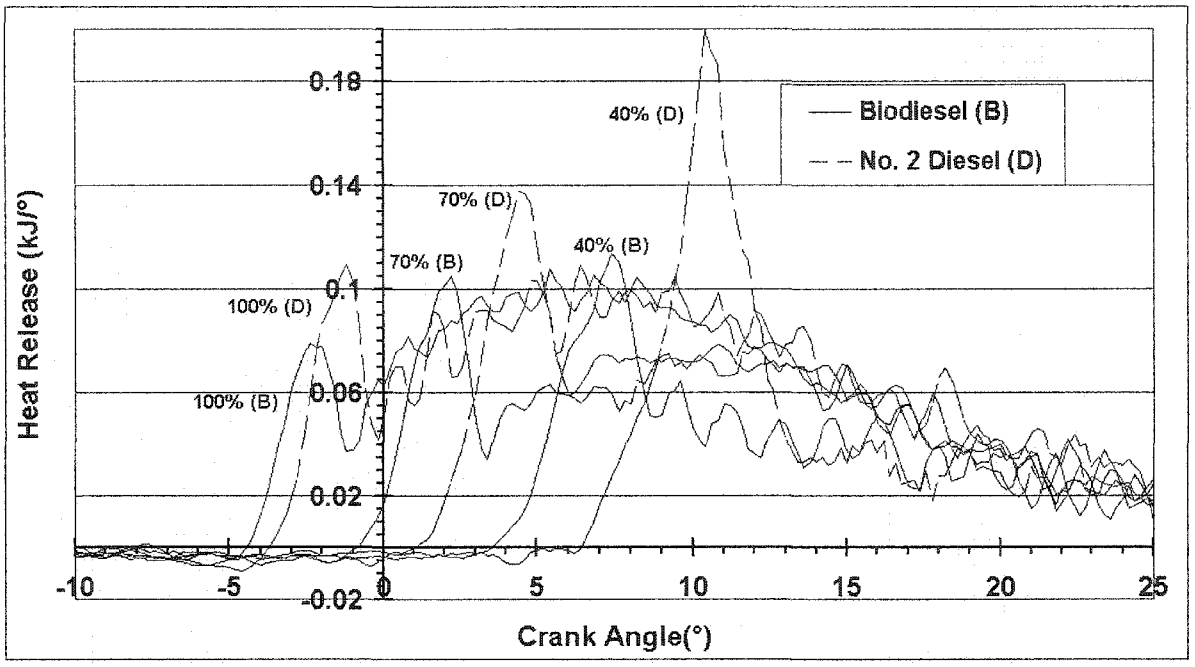

Figure 5.26. Comparison of the heat release analysis of biodiesel and No. 2 diesel fuels at 100%, 70%, and 40% load conditions at 1400 rpm and with pump #1

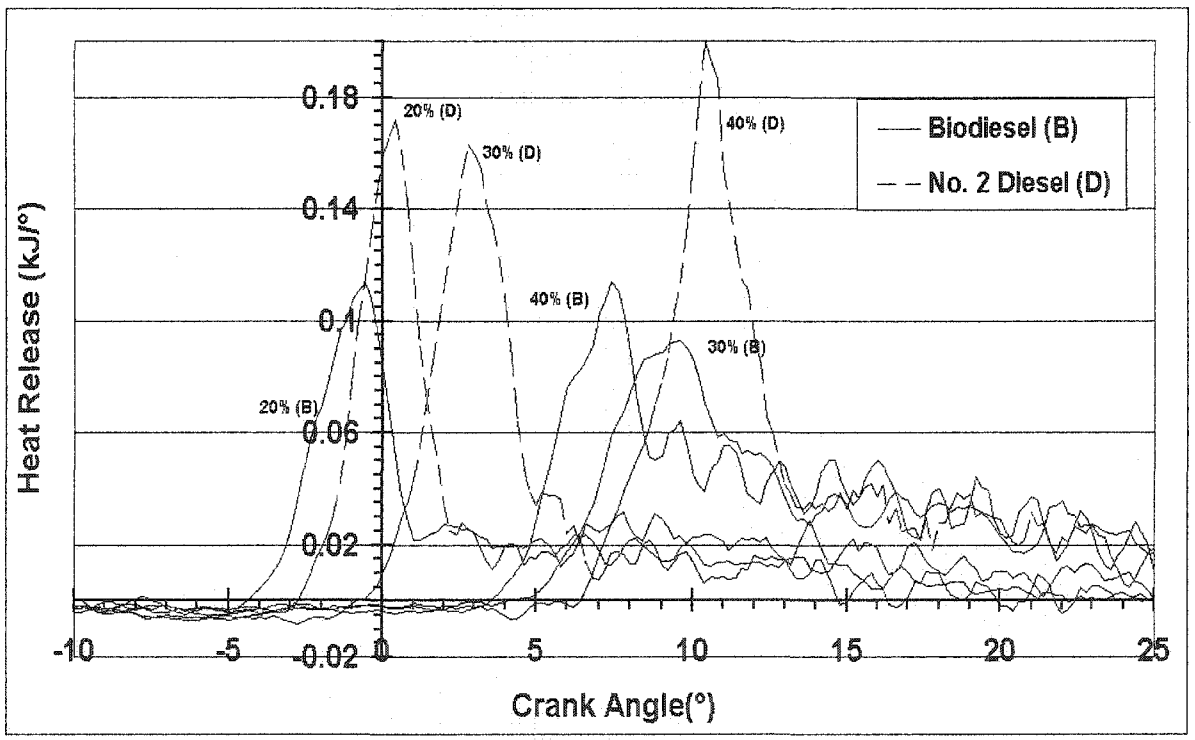

Figure 5.27. Comparison of the heat release analysis of biodiesel and No. 2 diesel fuels at 40%, 30%, and 20% conditions at 1400 rpm and with pump #1

5.3.3.3 Investigation of Lower Heating Value and Bulk Modulus Effects on Diesel Emission

The brake specific oxides of nitrogen emission (BSNOx) of biodiesel from soybean oil and No. 2 diesel fuels are compared in Figure 5.28. It is seen that at the maximum load condition corresponding to a BMEP of 10.5 bar, the biodiesel produced about 16% more NOx than the diesel fuel and as the load decreased, and the injection timing was retarded, the NOx difference between the two fuels also decreased. The effect of the light load advance system can be seen on the BSNOx emission results. When the light load advance system was engaged for No. 2 diesel fuel at between 4 and 5 bar, the No. 2 diesel fuel started to produce more the BSNOx than the biodiesel and the difference was increased until the light load advancement system engaged for biodiesel. Even after the system was engaged and the biodiesel start of injection was slightly more advanced, the BSNOx emission of biodiesel was less than for the No. 2 diesel fuel. This might explain the lower biodiesel NOx emission results obtained by Peterson et al. [44, 44, 45]. Reviewed in Section 2.4.3, Peterson et. al. conducted EPA chassis dynamometer engine tests. It is well known than in chassis dynamometer tests, the engine load conditions are much less that engine dynamometer tests. Therefore, the difference in the engagement conditions for the light load advancement for both fuels may explain the lower NOx and higher particulate emission of the test.

Figure 5.29 presents the brake specific unburned hydrocarbon (BSHC) emissions as the load varied. The BSHC emissions of both fuels increased as the load decreased. The BSHC emission of biodiesel is less than No. 2 diesel fuel at most of the load conditions, and at the maximum load condition, the BSHC emission is about 30% less than that of diesel fuel.

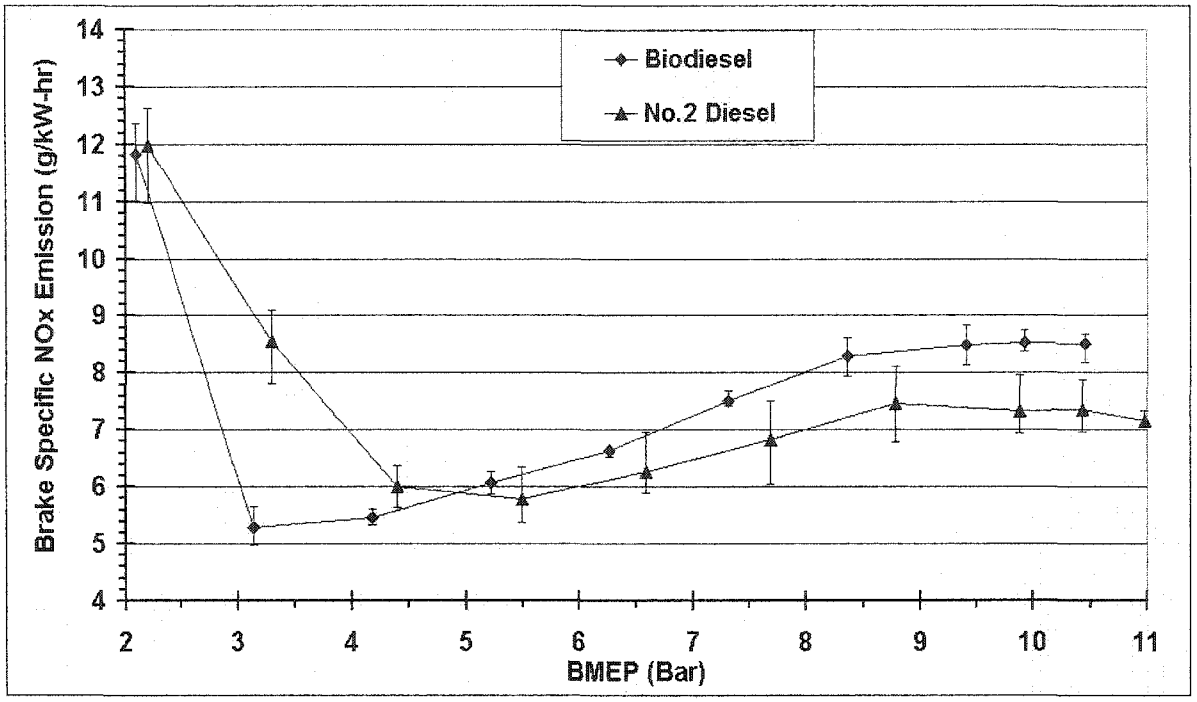

Figure 5.28. Comparison of the brake specific oxides of nitrogen (BSNOx) of biodiesel and No. 2 diesel fuel at varying the load conditions from 100% to 20% at 1400 rpm and with pump #1

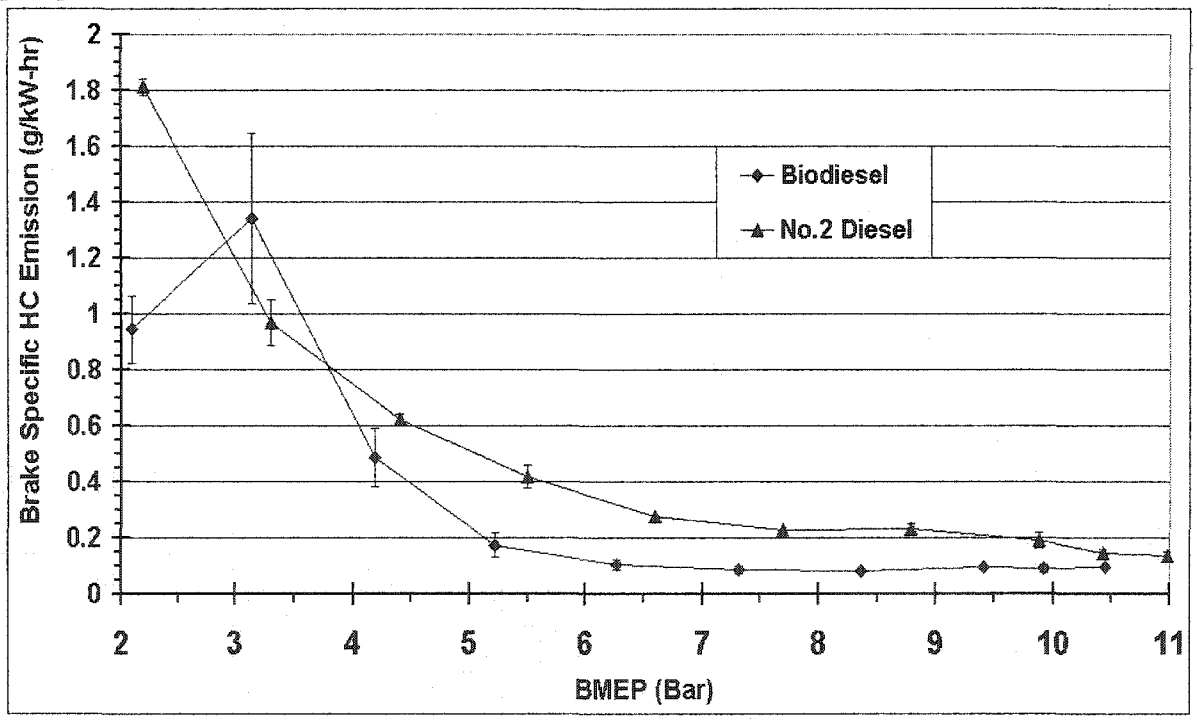

Figure 5.29. Comparison of the brake specific hydrocarbon (BSHC) of biodiesel and No. 2 diesel fuels at varying load conditions from 100% to 20% at 1400 rpm and with pump #1

It can be seen that the difference in BSHC emission increases as the load is reduced, until about 4 bar of BMEP. At this point, the effect of the light load advancement system can be observed. Right before the light load advancement was engaged for the biodiesel, the biodiesel's BSHC emission becomes higher than regular diesel fuel. This lasts until the light load advancement is engaged and the BSHC emission of biodiesel is much less than diesel fuel again. When the BSHC emissions of No. 2 diesel and biodiesel fuels are compared, it appears that the BSHC emission of No. 2 diesel fuel was not affected by the light load engagement timing although the BSHC emissions from the biodiesel were affected. This means that the BSHC emissions of No. 2 diesel fuel may be a stronger function of load rather than combustion timing. On the other hand, the BSHC emissions of biodiesel significantly increased as the load decreased, and the combustion timing was retarded, but as soon as the light load system was engaged, the BSHC emission dropped lower than diesel fuel and its level before the advancement.

Figure 5.30 shows the comparisons of the brake specific carbon monoxide (BSCO) emission of the fuels. Just like the BSHC emission results, the BSCO emission of biodiesel is less than the BSCO emission of No. 2 diesel fuel at almost all load conditions. However, the rate of BSCO emission of biodiesel increases very significantly at light load and heavy loads.

In Figure 5.31, the Bosch Smoke Numbers (SN) of the fuels are compared. The SN of biodiesel is considerably less than for No. 2 diesel fuel at all load conditions. Biodiesel's SN is about 50% less than diesel fuel's and the difference decreases as the load decreases to 2 bars, which is 20% of the maximum power, where the smoke numbers for the two fuels are

about equal. As was noted for the BSNOx, BSHC, and BSCO emissions of the fuels, the effect of the light load advancement timing can be observed on the SN.

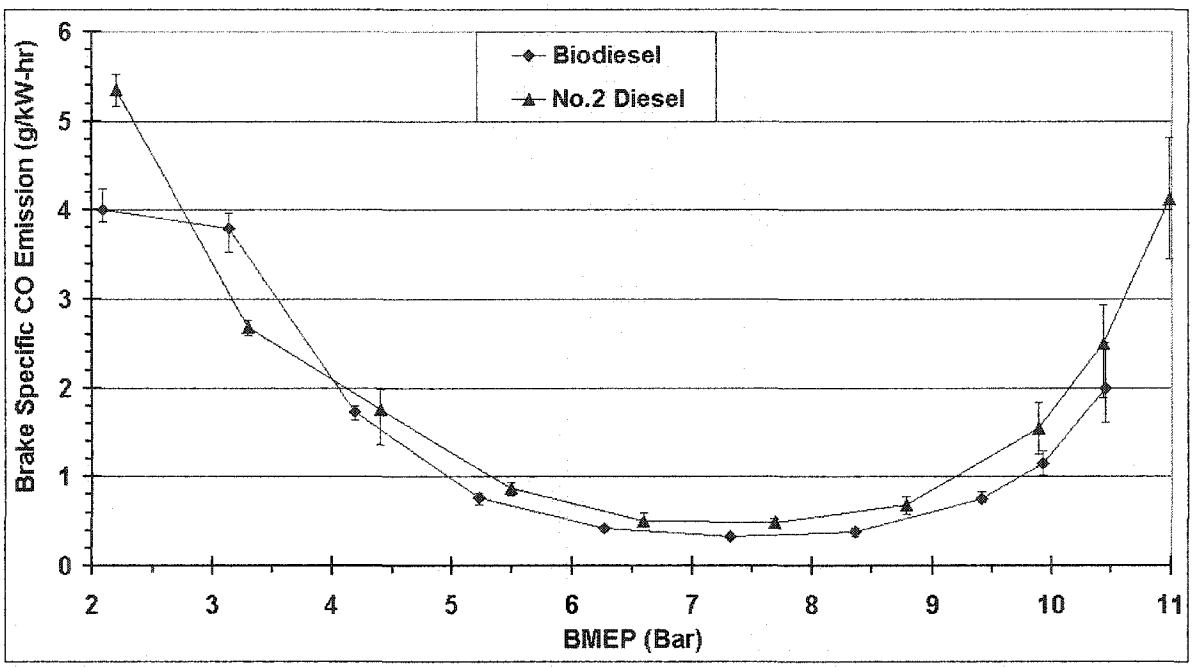

Figure 5.30. Comparison of the brake specific carbon monoxide (BSCO) of biodiesel and No. 2 diesel fuels at varying load conditions from 100% to 20% at 1400 rpm and with pump #1

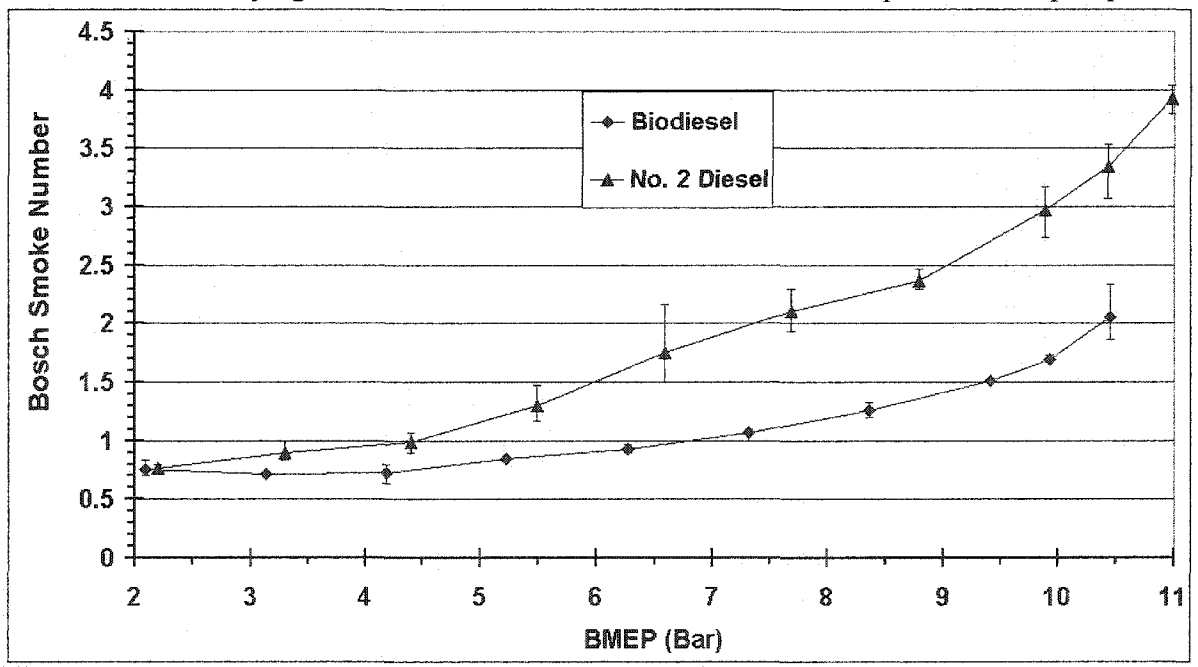

Figure 5.31. Comparison of the brake specific Bosch Smoke Numbers (SN) of biodiesel and No. 2 diesel fuels at varying load conditions from 100% to 20% at 1400 rpm and with pump #1

5.3.3.4. Investigation of Lower Heating Value and High Physical Properties Effects on Diesel Emission with Pump #2

After an accident mentioned earlier, pump #1 was removed and it was replaced with a pump donated by the John Deere Product Engineering Center. This pump matched the characteristics of the engine but was a different part number than the original pump. The pump was called pump #2 and after minor calibration of the pump, it was used to complete the rest of the test matrix. The test matrix mentioned earlier in this section to determine the effect of the lower heating value and higher bulk modulus of biodiesel on the diesel combustion and emission was repeated with pump #2.

The start of injection timing versus load level obtained with pump #2 is presented in Figure 5.32. It is observed that the start of injection timing of biodiesel is advanced about 0.6° compared with diesel fuel at a BMEP of 7.67 bar. It should be noted that this is the same condition that gave a difference of 1.34° in Figure 5.22 for pump #1. In Figure 5.33, the start of injection timing versus fuel delivery in cc/inj is presented for the same fuels. As shown in this figure, when the same volume of both fuels was injected, the start of injection timing was the same, unlike the results obtained with pump #1. This means that the higher speed of sound and isentropic bulk modulus of biodiesel appear to have no effect on the start of injection in contrast to what was observed with pump #1. This was not expected.

Up to this point, the effect of fuel viscosity was assumed to be negligible. However, as a result of these significant differences between the two pumps, it was speculated that the fuel viscosity might have an effect on the fuel injection timing, also.

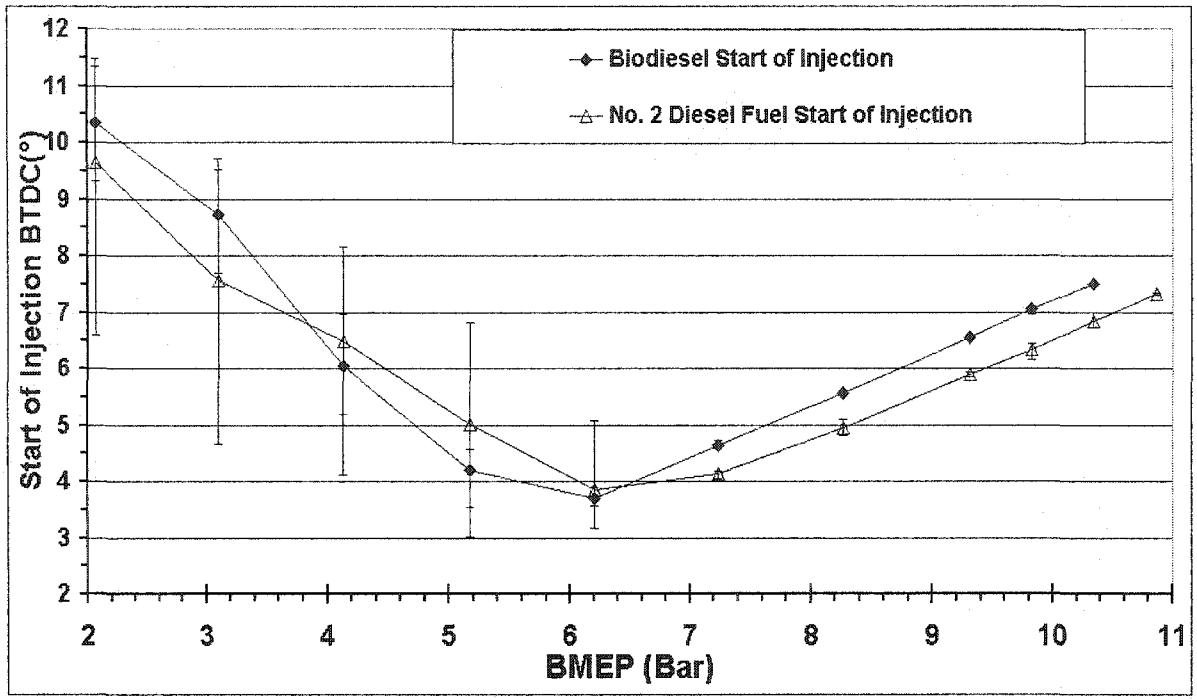

Figure 5.32. Start of injection comparison of soybean oil biodiesel and No. 2 diesel fuel at varying load conditions from 100% to 20%, at 1400 rpm and with pump #2

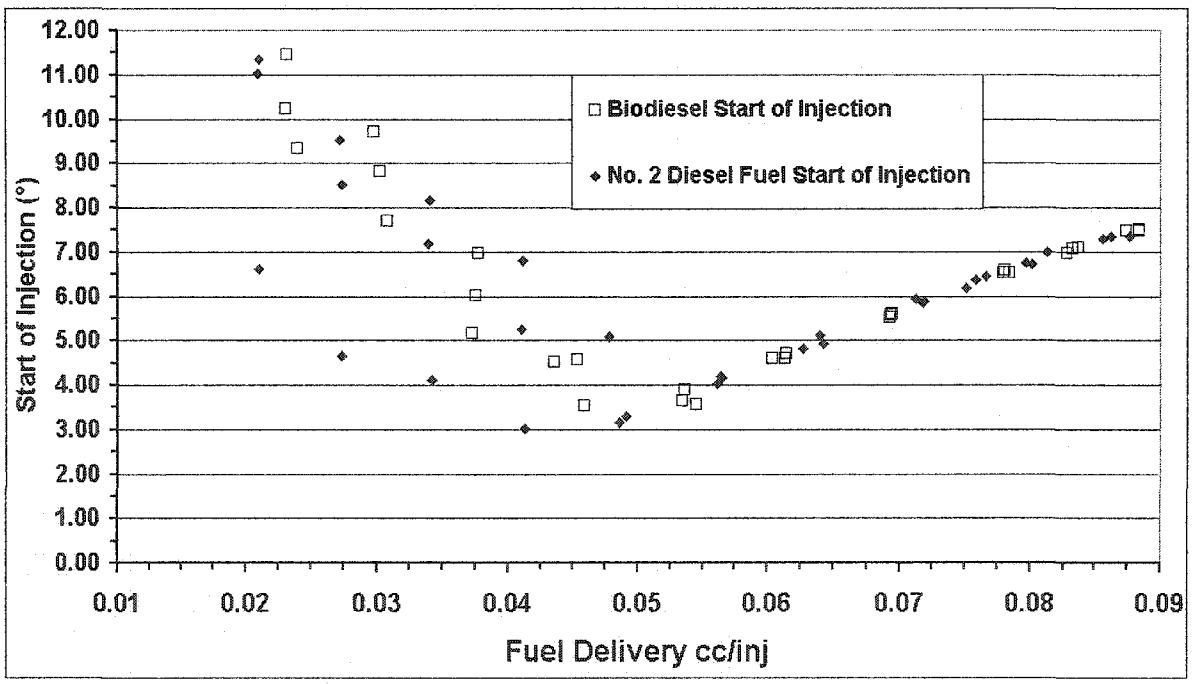

Figure 5.33. Volumetric comparison of the fuel delivery versus start of injection of biodiesel and No. 2 diesel fuels at varying load conditions from 100% to 20% at 1400 rpm with pump #2

Fuels are used as lubricants and coolants in the pump, and the amount of delivered fuel may be significantly affected by the leakage of fuel past the plungers. It was also thought that the physical property effect on the fuel injection timing could be a function of the pump speed. Therefore, viscosity and pump speed effects on the injection timing were investigated. These data will be discussed in the following section.

It was also observed with pump #2 that the light load advancement system was engaged at much earlier load conditions than for pump #1. In Figures 5.32 and 5.33, it is seen that the error bars that show the minimum and maximum points of the measurements are very large below 6 bar BMEP and 0.05 cc/inj. It appeared that there was some kind of mechanical problem with the light load regulation system. It was also noticed that the regulation problem was more severe with the diesel fuel.

The brake specific oxides of nitrogen (BSNOx) emission comparison with pump #2 is given in Figure 5.34. It is seen with pump #2 that the biodiesel BSNOx emission is still higher than diesel fuel. However, this time the difference is not as high as was observed with pump #1. The BSNOx emission of both fuels clearly follows the start of injection timing curves. The timing change associated with the light load advancement is very clear from the BSNOx graphic. The percentage of BSNOx change goes to negative right after the light load advancement system engages.

5.3.3.5 Speed Effect on Start of Injection and Fuel Delivery

After the emission tests with pump #2 it was believed that the lack of an effect of fuel type on the injection timing shown in Figures 5.33 might be a result of the interaction of viscosity and the other fuel properties. It was postulated that viscosity effects should be speed dependent because leakage in the pump should be less significant at higher speeds.

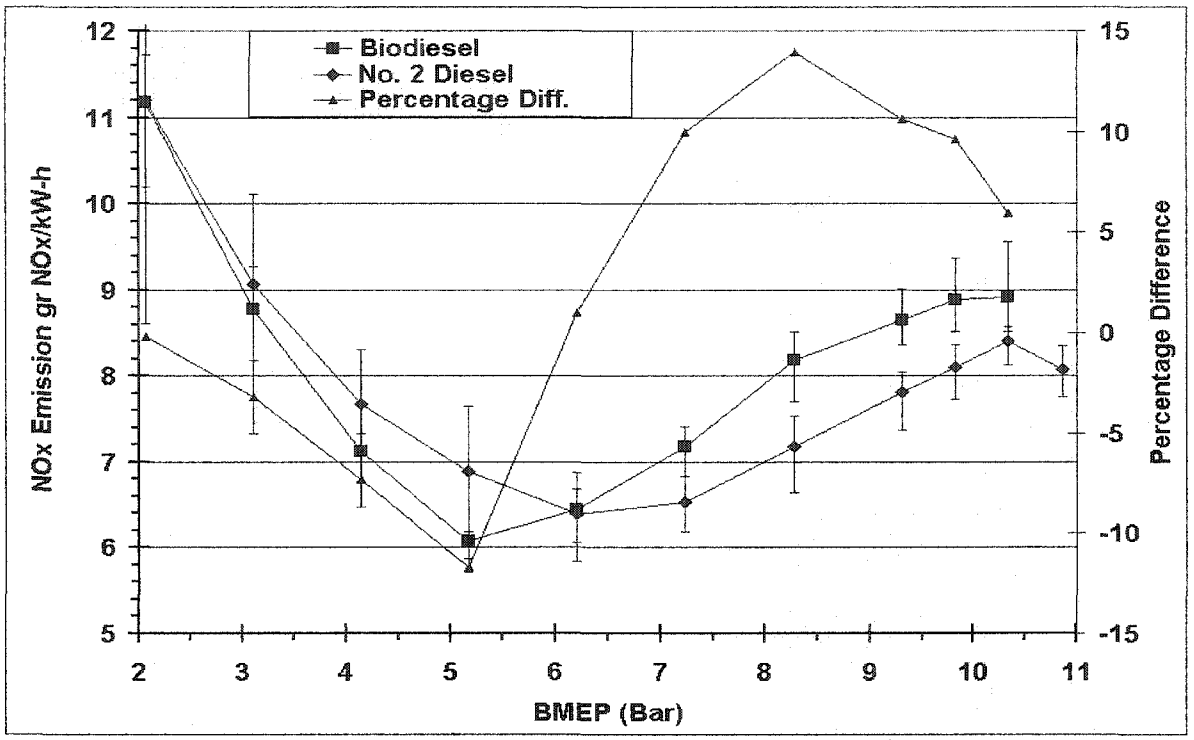

Figure 5.34. Comparison of the brake specific oxides of nitrogen (BSNOx) of biodiesel and No. 2 diesel fuel at varying load conditions from 100% to 20% at 1400 rpm and pump #2.

To investigate this, start of injection timing and fuel delivery comparisons were made at different engine speeds of 1000, 1400, 1800, and 2100 rpm. Pump #2 start of injection results for these speeds are presented in Figures 5.35 to 5.38. For pump #2, both fuels had the same start of injection timing for the same amount of fuel delivery at 1000 and 1400 rpm engine speeds. However, at 1800 rpm it is observed that the light load advancement system engaged with diesel fuel much earlier than with biodiesel. At 2100 rpm, the No. 2 diesel fuel timing was totally advanced and was virtually constant at about 9.5° BTDC for all values of fuel delivery. However, the start of injection of biodiesel was only advanced to 7° BTDC. The different behavior of the pump between the fuels was attributed to the higher viscosity of biodiesel. The viscosity of No. 2 diesel was at 40 °C 2.9 cSt while the viscosity of biodiesel was 4.6 cSt. It was also judged that the light load advancement system of pump #2 was not

working properly because the pump timing at light loads was extremely variable causing large differences between repetitions.

A new pump was purchased from a fuel injection pump service, designated pump #3, and was tested for fuel injection timing and fuel delivery values for the same fuel and speed conditions. The test results of pump #3 are also given in Figures 5.35-5.38. The start of injection timing was the same for both fuels at the same fuel delivery at all engine speed conditions, even though the injection timing varied at different speed levels. While the differences between fuels do not seem to be affected by speed, it was still believed that viscosity effects were a potential source of the differences between pump #1 and the subsequent pumps. The control systems in the diesel fuel injection system can be affected by the high viscosity of biodiesel. Based on these observations the viscosity effect on the fuel injection timing was also investigated and is discussed in the next section.

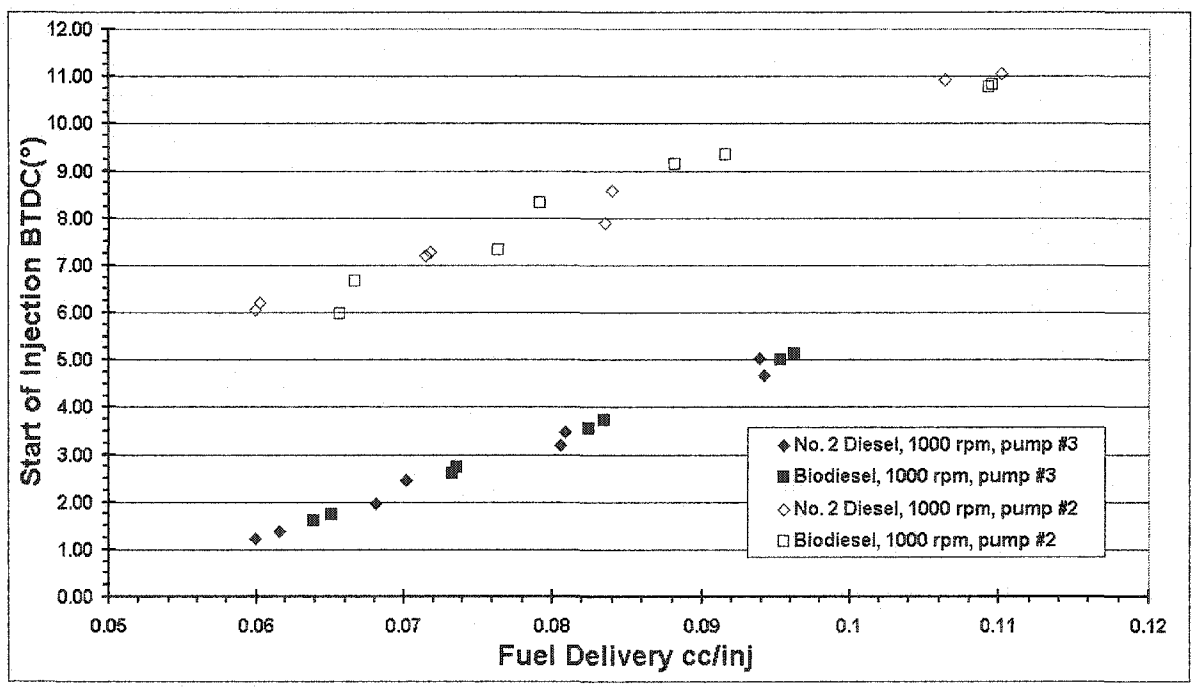

Figure 5.35. Start of injection and fuel delivery comparisons at 1000 rpm with pump #2 and pump #3.

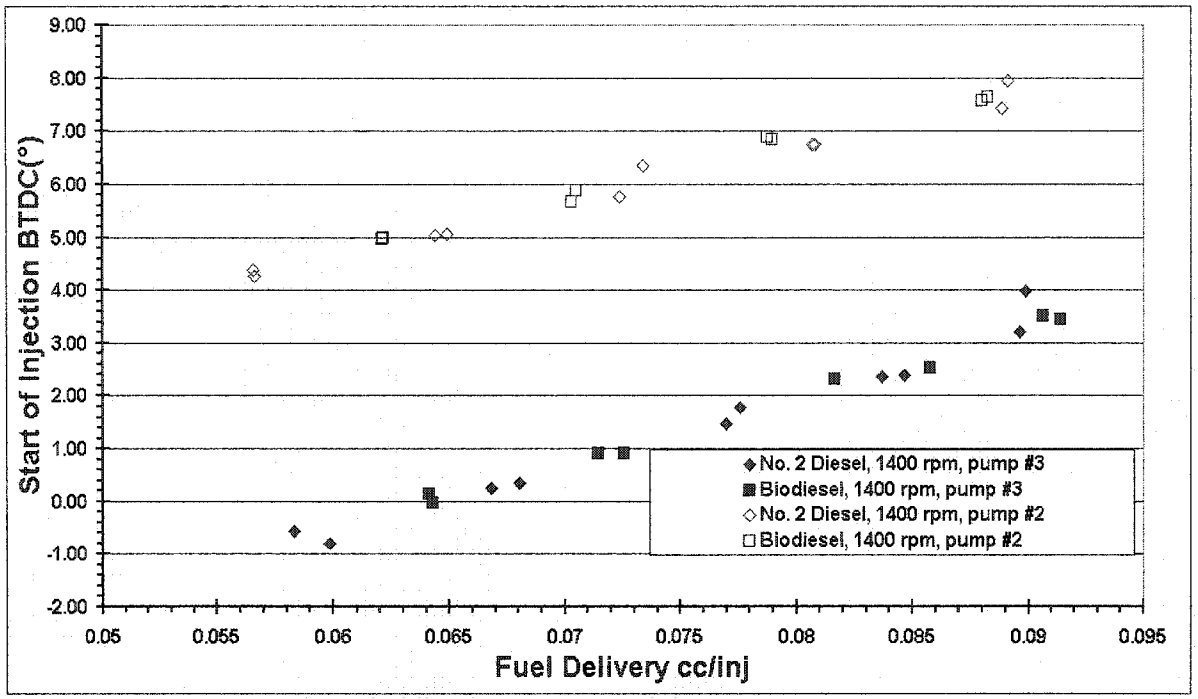

Figure 5.36. Start of injection and fuel delivery comparisons at 1400 rpm with pump #2 and pump #3.

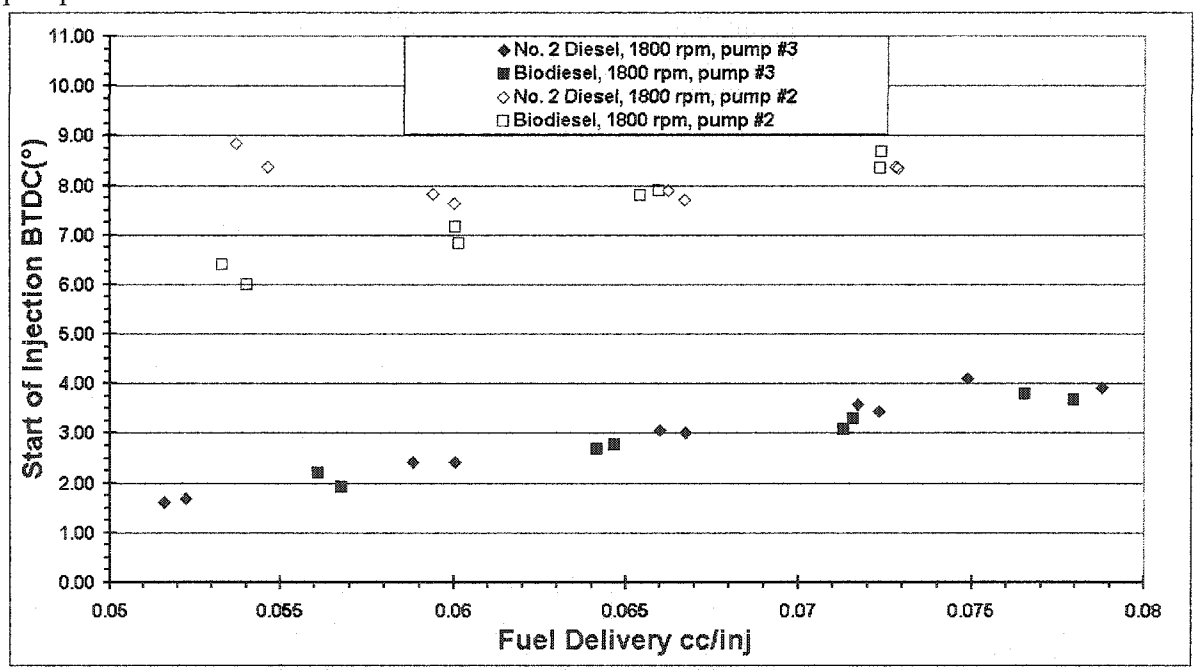

Figure 5.37. Start of injection and fuel delivery comparisons at 1800 rpm with pump #2 and pump #3.

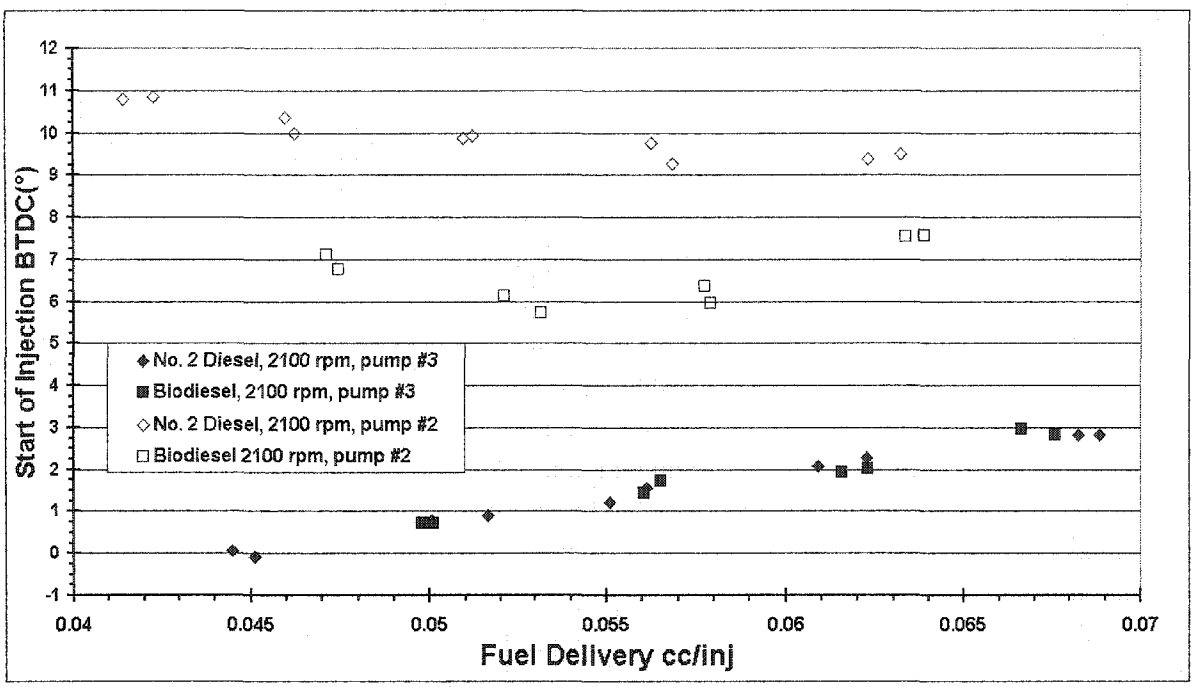

Figure 5.38. Start of injection and fuel delivery comparisons at 2100 rpm with pump #2 and pump #3.

Before investigating the effect of viscosity on the fuel delivery and timing, the timing adjustment mechanism on the distributor-type fuel injection pump should be explained. As shown in Figure 5.39, the cam ring that controls the fuel injection events can be rotated through limited angle. A lever projects up from the cam ring that can be moved by a set of pistons. The piston on the right is the speed advance piston. When the engine speed increases, a positive-displacement fuel transfer pump supplies a higher fuel pressure to the speed advance piston that pushes the cam ring in the advance direction. At high loads, a counter-acting flow of high pressure fuel is supplied to the piston on the left that resists the rotation, and resulting timing advance.

At heavy load and low speed conditions, the transfer pump pressure on the speed advance piston is greater than the pressure on the low load advance piston causing timing advancement. The fluctuations observed with pump #2 may have been due to the fact that

the pump was used and had set for a considerable period of time before it was installed for this project. Corrosion and varnish deposits could cause the timing adjustments to stick and be more dependent on fuel viscosity.

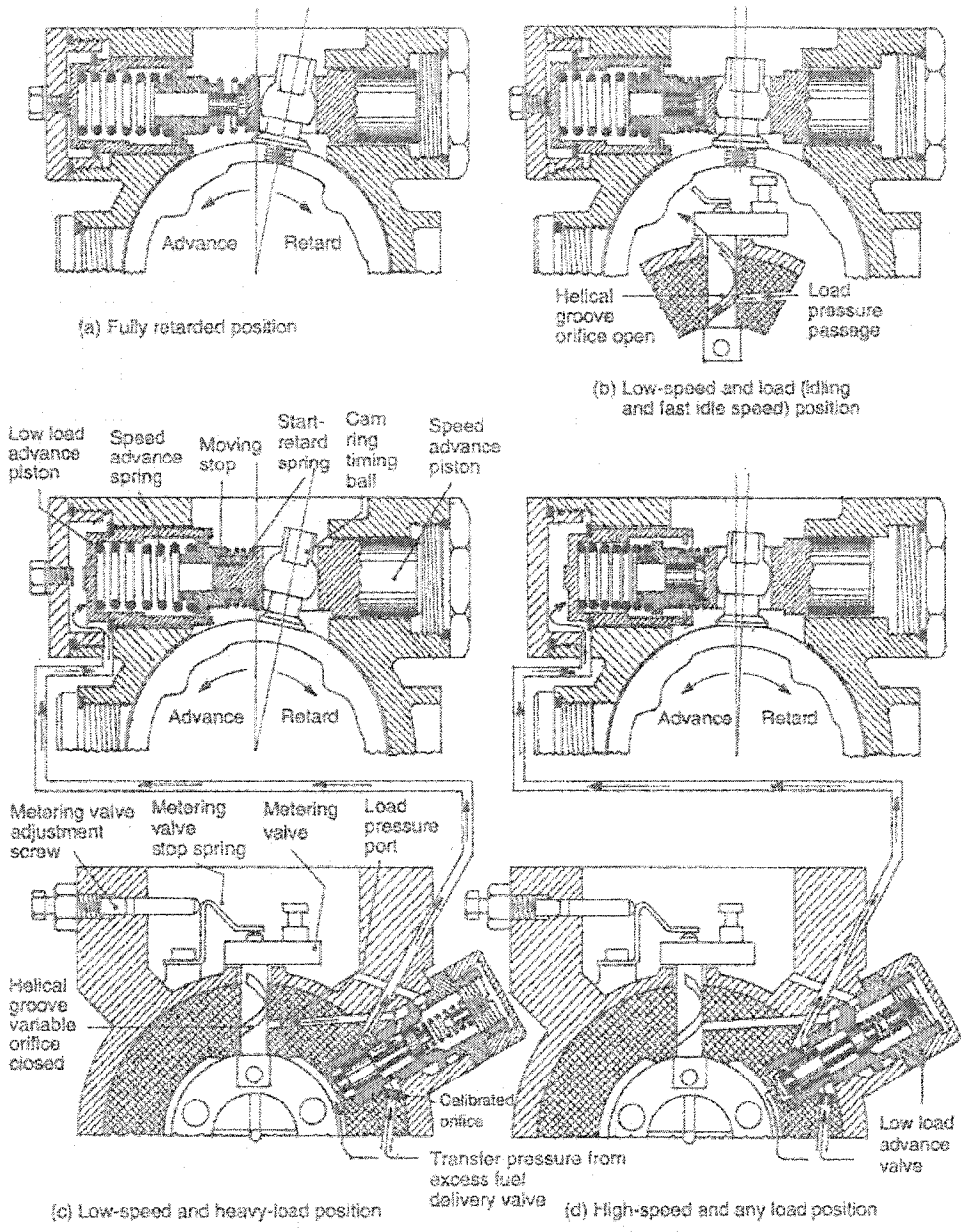

Figure 5.39. Low load advance by metering valve control [93]

5.3.3.6. Viscosity Effect on the Start of Injection and Fuel Delivery

In Section 5.3.3.2, the start of injection timing was investigated with pump #1 and it was found that the start of injection timing of biodiesel, for the same volume of fuel, was advanced about 0.68° compared with No. 2 diesel fuel. When the same tests were completed with pump #2, no timing difference was found between the two fuels, as described in Section 5.3.3.4. The speed effect was investigated on pump #2 and pump #3 in Section 5.3.3.5 and it was concluded that there was no effect on the start of injection timing. At all speeds there was no difference in the start of injection timing between the fuels with pump #3 and while there was some difference between the fuels at some speeds in tests with pump #2, it was judged that the speed and load advance systems were not working properly. In this section, the effect of viscosity on the amount of fuel delivery and the fuel injection timing are discussed. The leakage between the plunger and the cylinder becomes important especially with lower viscosity fuels and this is believed to be the primary impact of viscosity on the pump's performance.

The viscosity of biodiesel is about twice that of diesel fuel. During fuel compression a small amount of fuel is permitted to leak past the plunger for lubrication and the amount of this leakage fuel is directly correlated with the fuel viscosity and the clearance between the cylinder and the plunger. The more viscous the fuel, the less the amount of fuel that will leak. The amount of the leakage fuel is sufficiently important that the temperature of the fuel has a significant impact on the engine power. The start of injection timing can also be affected by the amount of fuel leakage. The amount of fuel leakage can advance or retard the injection timing. During the compression stroke, the amount of leakage can impact the pressure rise and the start of injection. Therefore, a new engine test matrix was designed to

investigate the effect of viscosity on the start of injection. Viscosity is a strong function of temperature and temperature easily can be correlated back to viscosity with correlations available in the literature [7].

The engine was run at fuel temperatures of 25, 30, 40, 50, and 55°C using soybean biodiesel and No. 2 diesel fuel. The engine was run at wide open throttle (wide open metering) at 1400 rpm so that the fuel injection pump was trying to send the maximum and equal volumes for both fuels. Since the viscosities of the fuels were different, the leakage was different and this causes differences in the fuel delivery. Both pump #2 and pump #3 were tested. Due to damage in the accident mentioned earlier, pump #1 could not be tested

Temperature versus fuel delivery of both fuels with both pumps are given in Figure 5.40. At all temperatures, a greater volume of biodiesel was injected compared with diesel fuel. At 40°C, the temperature at which fuel is usually supplied to the engine during our tests, about 1.2 and 3.2% more biodiesel was injected than No. 2 diesel fuel with pump #2 and pump #3, respectively. It is also noticed that the fuel delivery of No. 2 diesel fuel was twice as sensitive to viscosity change as fuel delivery of biodiesel. This is based on the observations that the slope of No. 2 diesel is approximately twice the slope of the biodiesel. At 40 °C, the No. 2 diesel fuel delivery is about 0.087 cc/inj for both pumps. However, the biodiesel fuel delivery is 0.0885 cc/inj with pump #2 and 0.0900 cc/inj with pump #3. Therefore, 0.0015 cc/inj and 0.003 cc/inj more biodiesel was injected with pump #2 and pump #3, respectively, compared to diesel fuel. Using the data presented in Figure 5.23, an increase in the volumetric fuel delivery of 0.0015 cc/inj and 0.003 cc/inj is expected to 0.2° to 0.5° advance in the start of injection timing with pump #2 and pump #3, respectively. The kinematic viscosities of the fuels at each temperature were calculated using data from

reference [7] and a plot of viscosity versus fuel delivery was prepared. This plot is shown as Figure 5.41. It should be noted that even at the same fuel viscosity and metering valve position (wide open), the quantity of fuel delivered is not the same for the two fuels. However, at the same fuel viscosity, the quantity of diesel fuel delivered is higher than for biodiesel.

When the fuel temperature and the start of injection timings of fuels were compared in Figure 5.42, it was found that, at the same fuel temperature, both the fuels had the same start of injection timings. This confirms our observations from Figure 5.33.

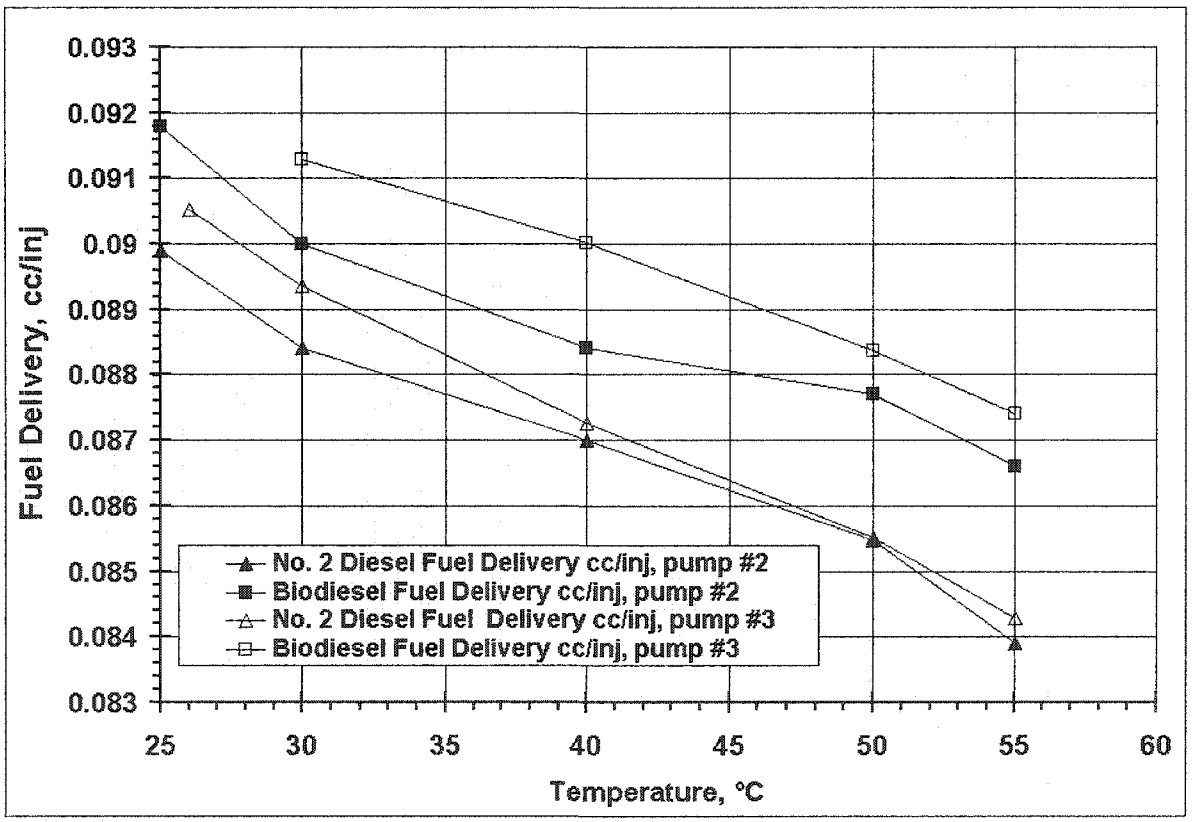

Figure 5.40. Fuel viscosity and fuel delivery comparison for biodiesel and diesel fuel with pump #2 and pump #3.

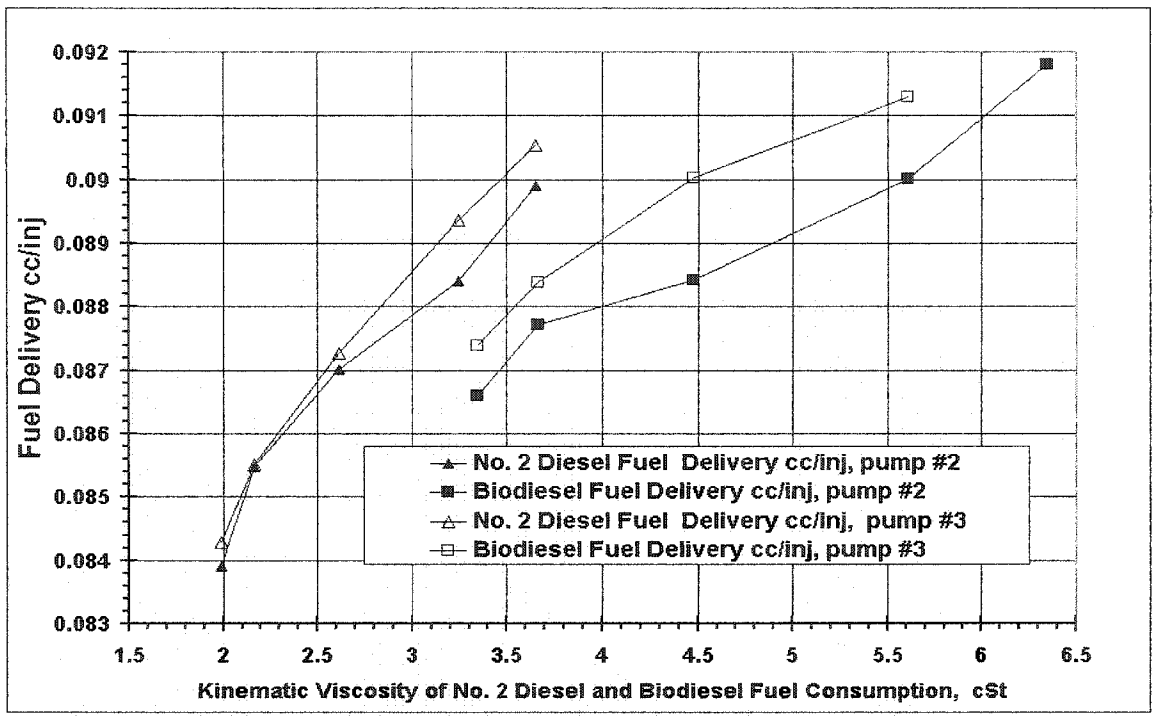

Figure 5.41. Fuel viscosity and fuel delivery comparison for biodiesel and diesel fuel with pump #2 and pump #3

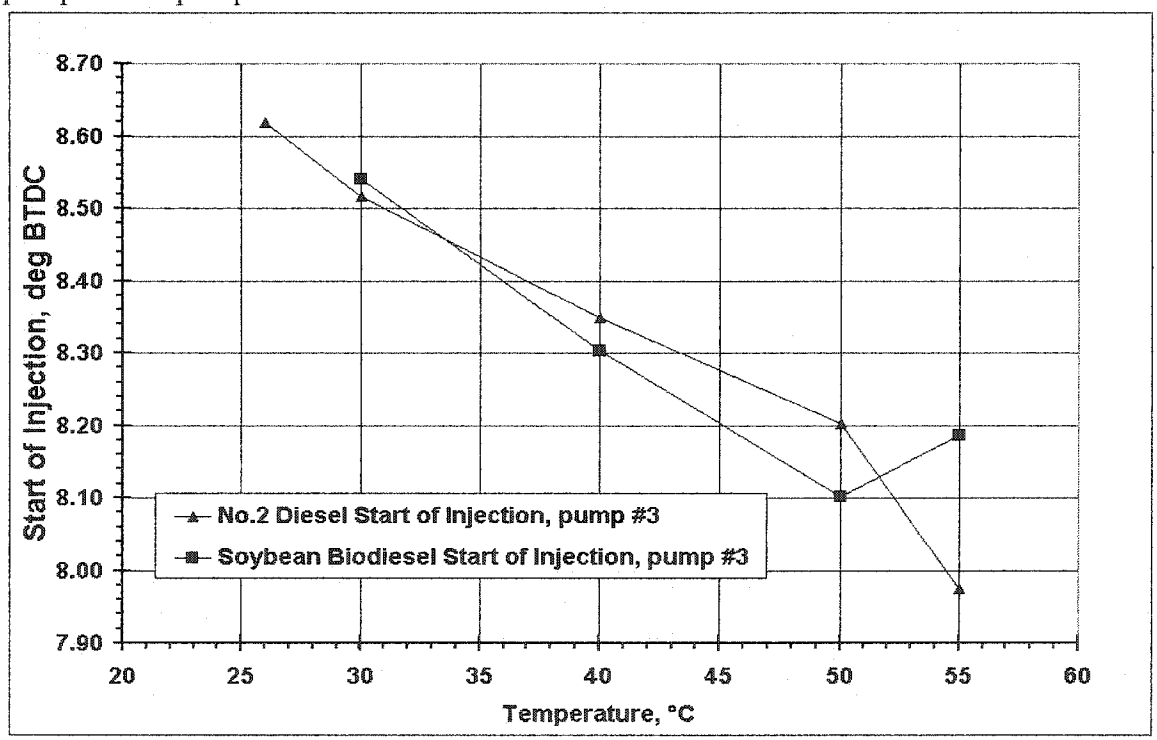

Figure 5.42. Fuel temperature and fuel start of injection comparison for biodiesel and diesel fuel with pump #3

The fuel delivery and the start of injection are compared at wide open throttle in 5.43. It is interesting that the start of injection for No. 2 diesel fuel was advanced about 0.25° relative to the biodiesel fuel. The leakage flow between the cylinder and the plunger under high pressure can be considered as a laminar flow between two flat plates and the governing equation would be Equation 5.4.

$$q = \frac{2 * h^3 * \Delta p}{3 * \mu * l} \tag{5.4}$$

where q is the flow rate, h is the half distance between the plates, Δp is the pressure difference, l is the length of the plates and μ is the viscosity. For this case, all of the variables are the same for both fuels except the viscosity.

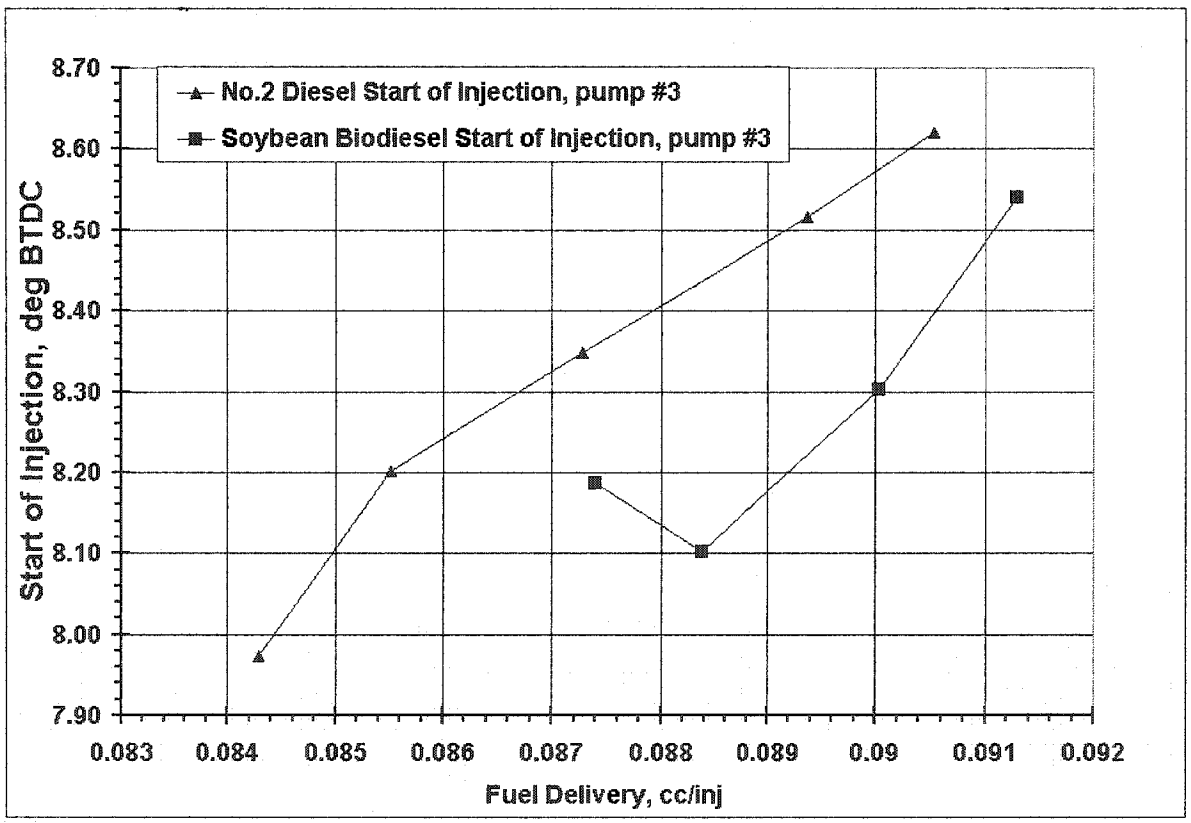

Figure 5.43. Fuel delivery and start of injection comparison for biodiesel and diesel fuel with pump #3

Using Equations 5.5 and 5.6, the amount of relative fuel leak as a function of viscosity can be estimated.

$$\frac{q_{biodiesel@40\ ^{\circ}C}}{q_{diesel@40\ ^{\circ}C}} = \left(\frac{\mu_{diesel@40\ ^{\circ}C}}{\mu_{biodiesel@40\ ^{\circ}C}} \right) = \frac{2.67\,cSt}{4.47\,cSt} = 0.58 \tag{5.5}$$

$$\frac{q_{biodiesel@55\ ^{\circ}C}}{q_{biodiesel@25\ ^{\circ}C}} = \left(\frac{\mu_{biodiesel@25\ ^{\circ}C}}{\mu_{biodiesel@55\ ^{\circ}C}} \right) \tag{5.6}$$

The relative increase in diesel fuel leakage at 40 °C is estimated to be 58% more than that for biodiesel. It is also estimated that the fuel temperature change in biodiesel from 25 to 55 °C, will increase the amount of leakage fuel by 52%. These calculations show that the viscosity of the fuels has a very significant effect on the amount of the leakage fuel. This is the primary reason for the change in fuel delivery as the fuel temperature changes that was shown in Figure 5.40. It is interesting to see from Figure 5.40 that, at the same viscosity level, the pump delivers more No. 2 diesel fuel than biodiesel fuel at wide-open throttle. Therefore, it is found that their flow is not only effected by viscosity, but is also probably affected by the fuel density. Equation 5.7 shows the equation that describes the flow of liquids through an orifice. It is clear that less dense fuels have more flow through orifices at the same pressure drop. Equation 5.7 can be reduced to Equation 5.8 at the same pressure difference when diesel fuel at 26 °C and biodiesel fuel at 52 °C are compared. The density of biodiesel at 52 °C is 0.863 g/cc and the density of diesel at 26 °C is 0.836 g/cc. It is found that the diesel flow rate is about 1.6% more than biodiesel fuel.

This explains the higher fuel delivery at the same viscosity and also explains the start of injection advance that occurs with diesel fuel presented in Figure 5.43.

$$q = C_D A_2 \sqrt{\frac{2*(P_1 - P_2)}{\rho*\left[1-(A_2/A_1)^2\right]}} \tag{5.7}$$

$$\frac{q_{diesel@26\ ^\circ C}}{q_{biodiesel@52\ ^\circ C}} = \sqrt{\frac{\rho_{biodiesel@52\ ^\circ C}}{\rho_{diesel@26\ ^\circ C}}} \tag{5.8}$$

It should be noted that the 0.2° and 0.5° of advance is very significant compared to the 0.63° increase in the start of injection due to the higher speed of sound and bulk modulus of biodiesel that was identified with pump #1. Note that these tests have tried to separate the effects of pump advance with load from the bulk modulus / speed of sound effect by comparing at the same volume of fuel injected. Now that the effect of viscosity is included, it cannot be separated as easily. The effect of leakage in the pump will be such that the pump will be trying to inject a larger quantity of fuel than is actually injected, and will have the earlier start of injection timing that corresponds to this greater quantity of fuel, but will actually have a lower volume of fuel delivered due to leakage. So, the technique proposed earlier of separating the timing advance into its two major components by comparing at the same volume of fuel delivered is not necessarily valid because the viscosity effect cannot be separated from the pump advance that corresponds to the greater fuel delivery needed to compensate for fuel biodiesel's lower energy content. The viscosity effect is also expected to be highly variable between the pumps due to variations in the factory tolerances which are different for each pump and any accumulated wear.

5.3.4 Investigation of High Cetane Number and Low Volatility Effect of Biodiesel with Pump #2 and Pump #3

The final two steps in the test matrix given in Chapter 3 were the investigation of the effect of the cetane number and volatility of biodiesel on combustion and NOx emission. This test matrix was targeted to make the emission and combustion comparisons at the same start of combustion timing of the fuels, which were No. 2 diesel, No. 2 diesel with cetane improver, soybean oil biodiesel, and yellow grease biodiesel. The fuels were tested at five different injection timing settings. The fuel injection pump was rotated for each fuel so that a 10° variation in the start of injection and combustion was obtained. The pump was rotated in two steps to about 5° advanced, to standard timing, and in two steps to 5° retarded.

This test matrix was used to investigate the relationships between the start of combustion, the combustion rate, and the biodiesel higher NOx emission. In particular, the NOx response to the start of combustion timing was sought. Therefore, the differences in the start of injection and the ignition delays, due to the fuel properties including the lower heating value, the higher speed of sound and bulk modulus, and the viscosity were canceled out when the comparisons were made. In this test matrix, the effect of higher cetane number and the lower volatility of biodiesel on the diesel combustion rate were investigated.

As was discussed in the concept map given in Chapter 3, higher cetane number shortens the ignition delay period and lowers the combustion rate. This lower combustion rate usually reduces the premixed burning and NOx emission. However, even though the cetane number of biodiesel is significantly higher than diesel fuel, biodiesel still has higher NOx emission. Biodiesel also has lower volatility than diesel fuel and the lower volatility of biodiesel should restrict the amount of fuel that is prepared for combustion during the

ignition delay period. The lesser amount of fuel prepared should also control and lower the premixed combustion, and so lower the NOx. However, the NOx emission of biodiesel is higher than that diesel fuel.

Therefore, this test matrix was designed so that the two biodiesel fuels (biodiesel from soybean oil and biodiesel from yellow grease) with the same volatility but different cetane numbers could be compared for the investigation of the cetane number effect on combustion and emissions at the same start of combustion timing. For the investigation of biodiesel's volatility effect on the combustion and emissions, the cetane number of regular No. 2 diesel fuel was increased to the same level as the soybean biodiesel cetane number using a cetane improver. The No. 2 diesel fuel with cetane improver, allowed the cetane number effect to be canceled and made possible an investigation of the volatility effect of biodiesel.

Biodiesel fuels have different cetane numbers based on the feedstocks used for biodiesel production. Biodiesel fuels that have more saturated fatty acid esters have higher cetane numbers relative to biodiesel fuels that have more unsaturated fatty esters. For example, the biodiesel fuels used in this study were obtained from soybean oil and yellow grease. Biodiesel obtained from soybean oil with about 83.5% unsaturated and 16.5% saturated fatty acids had a cetane number of 50. On the other hand, biodiesel from yellow grease with 67.5% unsaturated and 32.5% saturated fatty acid had a cetane number of 62.6. The 10 cetane number difference will have a significant effect on the diesel combustion and ignition delay. Therefore, biodiesel fuels from soybean oil and yellow grease were chosen to investigate the cetane number effect on biodiesel combustion. Biodiesel from soybean oil and biodiesel from yellow grease had essentially the same level of volatility but different

cetane numbers. At the same start of combustion, the emission and the combustion characteristics of the two fuels should give the effect of cetane number on biodiesel combustion and emission.

Biodiesel fuels have very different volatility characteristics than diesel fuels. Biodiesel consists of fewer chemical species than diesel fuel and the boiling points of these compounds are much higher than most of the species in diesel fuel. Its distillation curve is more like a straight line. Diesel fuel is composed of many different hydrocarbon molecules and distillation shows the boiling points of these compounds cover a range from 175 °C to 345 °C. To investigate the effect of volatility, biodiesel and No. 2 diesel fuel with the same cetane number as the biodiesel were compared. Both the cetane number and volatility have an effect on diesel combustion. In this portion of the test matrix, the emission and combustion comparisons were made at the same start of combustion and at the same cetane number. This test matrix was conducted using pump #2 first. After pump #3 was purchased this test matrix was expanded and repeated with pump #3. In the pump #3 tests, the cetane number of the No. 2 diesel fuel with additive was increased further by adding more additive to more closely match the cetane number of the biodiesel. With this change, the length of the ignition delay period of the No. 2 diesel fuel with additive became a little shorter and closer to the length of the biodiesel ignition delay period. This improved the volatility effect comparisons. Regular No. 2 diesel fuel without additive was also introduced to the test matrix. Having No. 2 diesel fuel without additive improved the inferences that could be derived from the diesel fuels with and without additive and with biodiesel.

5.3.4.1. High Cetane Number Effect on Biodiesel Combustion

The brake specific oxides of nitrogen (BSNOx) emissions of the biodiesel fuels from soybean oil and yellow grease obtained with pumps #2 and #3 are presented in Figure 5.44. Although obtained with different pumps, the two data sets for soybean-based biodiesel were very similar so a single regression line was fit to both sets. The same observation was true for the yellow grease. It is clear that the biodiesel from soybean oil produced higher BSNOx emission levels than biodiesel from yellow grease at all combustion timings.

Using the correlation equations given in Figure 5.44, it can be calculated that the BSNOx emission of soybean biodiesel was higher by about 9.4 to 12%, as the start of combustion was varied from -9° to +1°, than the BSNOx emission of the yellow grease biodiesel. The BSNOx increase with soybean oil follows the usual trend associated with cetane number at this point, because there is no difference in the volatility of the fuels. These two properties are assumed to have the greatest effect on NOx emissions.

Using the correlation equations given in Figure 5.44 at a standard timing of -4°, the BSNOx emission of yellow grease is 90.6% of the level of BSNOx for the soybean biodiesel. In other words, with the cetane number increase of 12 and with the same volatility level, the reduction in the BSNOx emission was about 9.4% of BSNOx emission of soybean biodiesel. Also, it should be noted that the two curves are parallel to each other and at -4° the slopes of biodiesel fuels from soybean and yellow grease are -0.70 and -0.71 (gNOx/kW-h)/° respectively, so they are equal. The combustion differences of the fuels will be further discussed in the Heat Release and Combustion Comparisons section of this chapter.

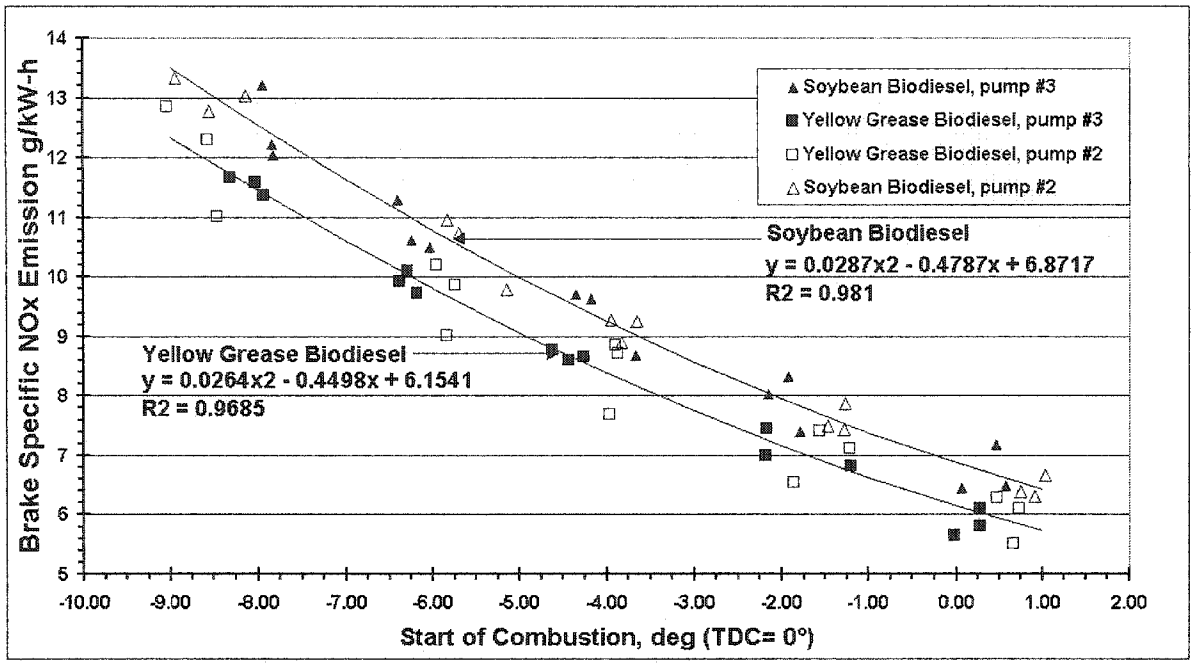

Figure 5.44. BSNOx emission comparisons for soybean and yellow grease biodiesel fuels at different combustion timing

5.3.4.2 Volatility Effect on Biodiesel Combustion

In order to identify the effect of volatility on the BSNOx emission and the combustion, the 2-ethyl hexyl nitrate additive was used to increase the cetane number of the No. 2 diesel fuel from 42 to 47 for the pump #2 tests and to 53.5 for the pump #3 tests. The main target was to match the ignition delay period of the diesel fuel to the soybean biodiesel fuel and compare the premixed portions of the combustion process for both fuels. The text matrix was initially conducted with pump #2, than the test matrix was changed by adding regular No. 2 diesel fuel without cetane improver to the test matrix and by increasing the amount of cetane improver in the cetane-enhanced No. 2 diesel fuel. This was done to the comparisons for the engine tests conducted with pump #3.

The brake specific oxides of nitrogen (BSNOx) emissions of biodiesel from soybean oil and No. 2 diesel fuel with a cetane number of 47 are presented in Figure 5.45. In this test,

pump #2 was used. In Figure 5.46, the BSNOx emissions of the same fuels are presented except that pump #3 was used and the cetane number of the No. 2 diesel fuel was increased to 53.5. In Figure 5.45, at the same start of combustion timing, the BSNOx emissions of biodiesel from soybean oil and No. 2 diesel fuel with 47 cetane number are about the same. A slight slope difference is still apparent. Also, when it is noted that the data points corresponding to biodiesel lead the data points for diesel it is clear that the biodiesel start of combustion was advanced about 1.2° relative to diesel fuel.

In Figure 5.46, at the same start of combustion timing, the BSNOx emissions of No. 2 the diesel fuel with a cetane number of 53.5 was less than the BSNOx of the soybean biodiesel. This had not been expected. Rather, it was expected that the No. 2 diesel fuel with the same cetane number and the same ignition delay would give more NOx than the diesel fuel. It was thought that the lower volatility of the biodiesel would restrict the amount of fuel in the premixed portion of the combustion and thus reduce the NOx production. In this case, volatility did not have this effect, and at the -4° standard injection timing, the BSNOx emission of No. 2 diesel with a cetane number of 53.5 was 5% less than the BSNOx emission of soybean biodiesel. This is the opposite of what was found by Monyem [82]. These figures show that when the injection timing effect due to different physical properties and with the same ignition delay is canceled, No. 2 diesel fuel still produces less BSNOx emission. The lower volatility of biodiesel did not have a significant effect on the BSNOx emission. Perhaps chemical differences between the fuels should be considered or that biodiesel may undergo chemical degradation under high pressure and temperature that changes its volatility. More detailed combustion comparisons will be given in the following section.

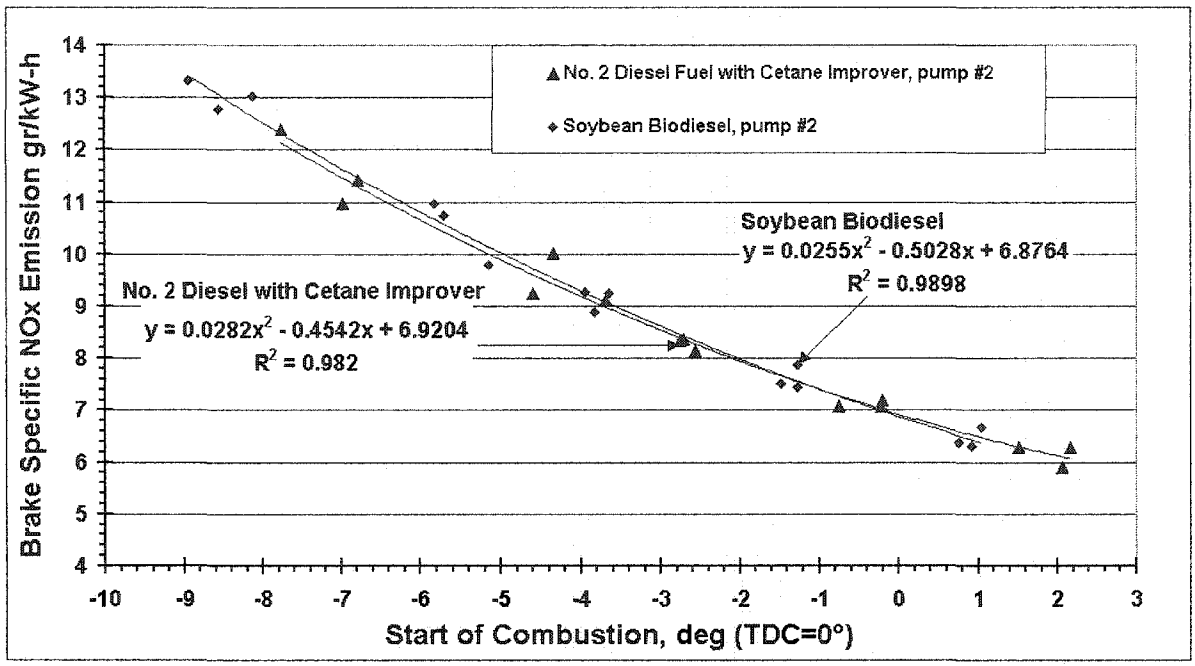

Figure 5.45. BSNOx emission comparisons for soybean biodiesel and No. 2 diesel fuel with additive, cetane # = 47 and pump #2.

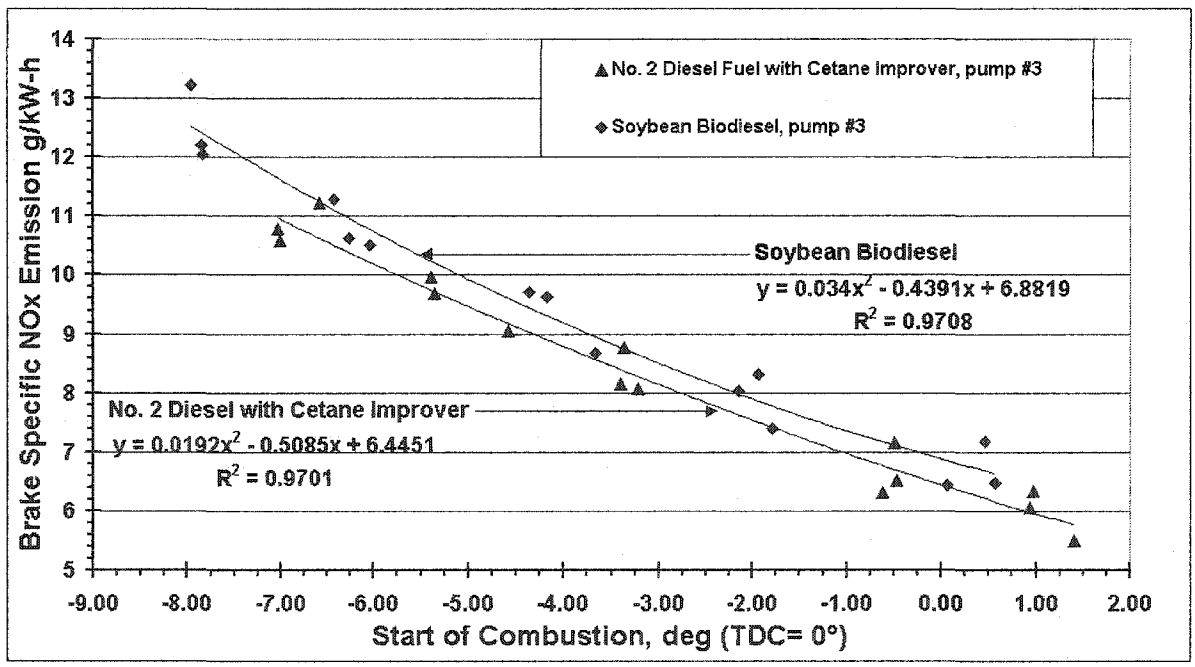

Figure 5.46. BSNOx emission comparisons for soybean biodiesel and No. 2 diesel fuel with additive, cetane # = 53.5 and pump #3.

5.3.4.3 Heat Release and Combustion Comparisons of Soybean Biodiesel and No. 2 Diesel Fuel.

In this section, the combustion characteristic of the fuels will be compared. The data are presented at the most advanced timing, at standard timing, and at the most retarded timing conditions. Prior to this discussion, the brake specific oxides of nitrogen (BSNOx) emissions of soybean oil biodiesel and regular No. 2 diesel fuel with cetane number of 42, without cetane improver, for pump #3 will be compared. In Figure 5.47, it is seen that the biodiesel and No. 2 diesel fuel had about the same level of BSNOx emission at the same start of combustion. However, it is also noticed that the combustion timings were significantly advanced, since the fuel injection pump was rotated to the same point for each advancement and retard setting. The slope of the BSNOx emissions for soybean biodiesel was slightly higher than the slope of the diesel fuel. When the polynomials were differentiated, it was found that the increase in the biodiesel slope was 20% at -8°, then the slope increase was reduced as the timing was retarded, until the start of combustion was equal to -1°. After -1°, the slope of biodiesel was less then diesel fuel and at 1° the biodiesel slope was 12% less than diesel fuel. It can be concluded that the BSNOx emissions of biodiesel are more sensitive to the start of combustion timing than for diesel fuel. This slope difference can also be noticed with the cetane enhanced diesel fuel.

Combustion characteristics and heat release analysis will be presented in the next sections. In the first section, the test matrix conducted with pump #2 will be discussed. Then, the same test matrix conducted with pump #3 will be presented and the differences between the two runs will be discussed.

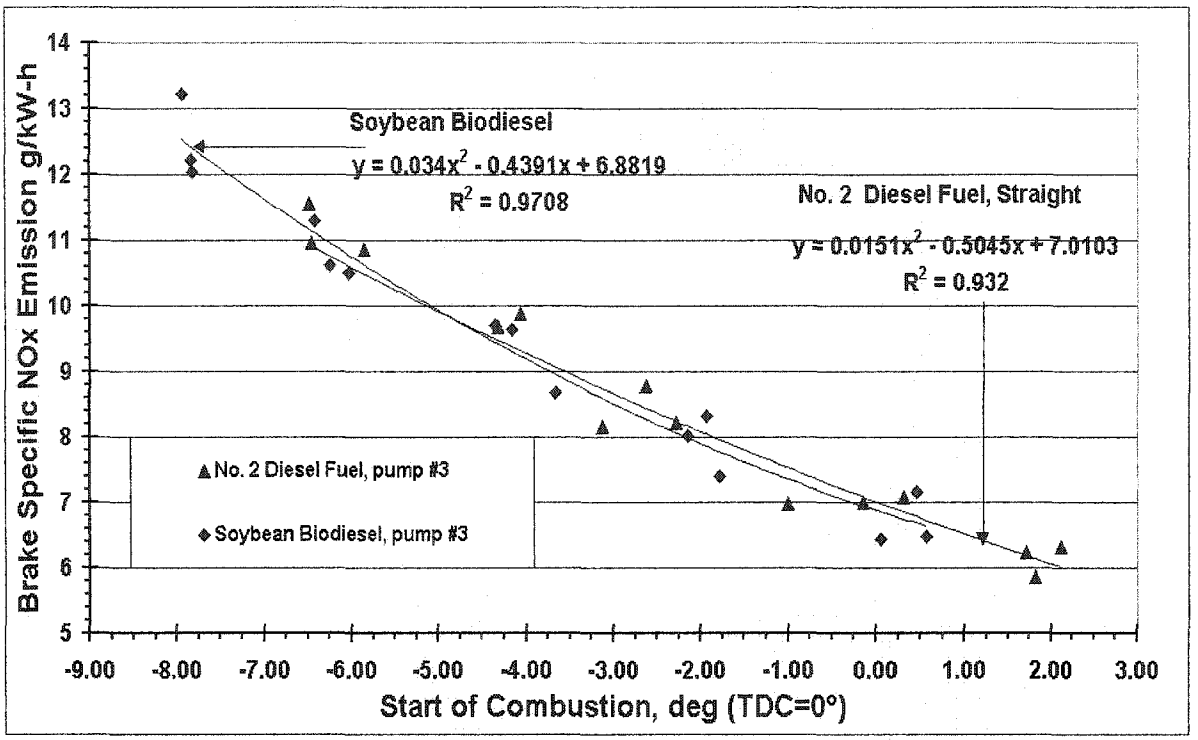

Figure 5.47. BSNOx emission comparisons for soybean biodiesel and No. 2 diesel fuel, 42 cetane number, pump #3.

5.3.4.3.1 Pump #2 Tests

In this section, the combustion characteristics and the heat release analysis are presented and compared at the standard, the most advanced, and at the most retarded timings using pump #2. In Tables 5.16 to 5.18, the combustion characteristics and in Figures 5.48 to 5.50, the heat release analysis are given for diesel fuel with cetane improver and biodiesel fuels from soybean oil and yellow grease.

In Figures 5.48 to 5.50, it is seen that increasing the cetane number of diesel fuel from 42 to 47 lowered the premixed portion of the diesel combustion to about the same level as the biodiesel fuel at all conditions. During the engine tests, the fuel injection pump might not be rotated to the same exact point as an earlier test, but when the start of combustion timings are compared, it is seen that the yellow grease biodiesel was the first and soybean biodiesel was

the second at all conditions. It is also seen that the premixed combustion of the yellow grease biodiesel was the lowest at all conditions. When the combustion characteristics in Tables 5.16-18 are compared, and the total energy released per injection is compared, it is seen that the amount of energy released for the same power level and at the same timing condition for all fuels were same. However, when the data are compared between the tables corresponding to different injection timings, it is seen that the total energy release per injection was increased as the timing was retarded. Because the combustion temperature and the efficiency were reduced, the amount of fuel and the energy needed to be increased to maintain the same power level. The total energy released per injection was calculated using the fuel amount per injection and the lower heating value of the fuel.

The percent of fuel energy burned in the premixed portion of the combustion was the highest at the most advanced timing condition for all the fuels. It was about 8.5% of the total energy for soybean biodiesel and No. 2 diesel fuel, and it was 6.38% of the total energy for the yellow grease at the most advanced timing. At the most retarded timing, No. 2 diesel with additive had 6.6% premixed combustion, biodiesel from soybean had 5.82%, and yellow grease biodiesel had 4.12% premixed combustion. At all timing conditions, the yellow grease biodiesel had the lowest percentage of premixed burning. These inferences can be confirmed from the heat release analysis shown in Figures 5.46-5.47. At most conditions, the premixed portion of the heat release analysis of biodiesel from soybean and the No. 2 diesel with 47 cetane number are about the same. This shows that the initial target of having the same level of premixed combustion for the two fuels was met and the BSNOx emission comparisons can be done sufficiently in Figure 5.46. It was expected that with the same

cetane number, biodiesel should give even less premixed combustion. To confirm this result, the cetane number was increased in the pump #3 test.

When the ratios of ignition delay periods and the percent energy releases are compared, it is seen that the ignition delay periods of the biodiesel fuels are about the same at all conditions and the No. 2 diesel fuel is only 10% longer than the biodiesel fuels. The fraction of energy released in the premixed portion of the combustion of the fuels are quite different from the ignition delay comparisons. The energy release in the premixed portion of the heat release analysis of the No. 2 diesel fuel with cetane improver was about 10% higher than that for soybean biodiesel, and a similar ratio was found for the ignition delay. However, the percent energy release in premixed combustion of the No. 2 diesel fuel is about 30 to 50% higher than for the yellow grease biodiesel.

5.3.4.3.2 Pump #3 Tests

The combustion characteristics and the heat release analysis are presented and compared at the standard, the most advanced, and at the most retarded timings, using pump #3. In this test matrix, the regular No. 2 diesel fuel with a cetane number of 42 was also tested. Also, the amount of cetane improver was increased in the No. 2 diesel with cetane improver to the higher level of 53.5.

The combustion characteristics of the samples are given in Tables 5.19 to 5.21, and the heat release analysis is presented in Figures 5.51 to 5.53. The heat release analysis is shown for the No. 2 diesel fuels with and without cetane improver and for the biodiesels from soybean oil and yellow grease. In Figures 5.51 to 5.53, it can be seen that increasing the cetane number of diesel fuel even further from 47 to 53.5, lowered the premixed portion of the diesel combustion to where it was even lower than the biodiesel premixed combustion.

Table 5.16. Combustion characteristics of No. 2 diesel with cetane improver (cetane #: 47), soybean, and yellow grease biodiesel fuels at 352.5 N-m and 1400 rpm and standard timing, with pump #2.

Combustion Characteristics	***No. 2 Diesel fuel with cetane improver (DIEWI)***	***Soybean Biodiesel (SBB)***	***Yellow Grease Biodiesel (YGB)***
Start of Injection, deg	-6.47	-7.26	-7.16
Start of Combustion, deg	-2.78	-3.95	-3.87
Ignition Delay, deg	3.69	3.30	3.29
Total of fuel energy released per injection, kJ/inj-cyl	2.76	2.77	2.74
Percent of fuel energy burned as premixed, %	7.04	6.15	4.65
Comparisons	***Ratios of Ignition Delay***	***Ratios of Percent Energy Release Rates as Premixed***	
DIEWI/SBB =	1.12	1.14	
DIEWI/YGB =	1.12	1.51	
SBB/YGB =	1.00	1.32	

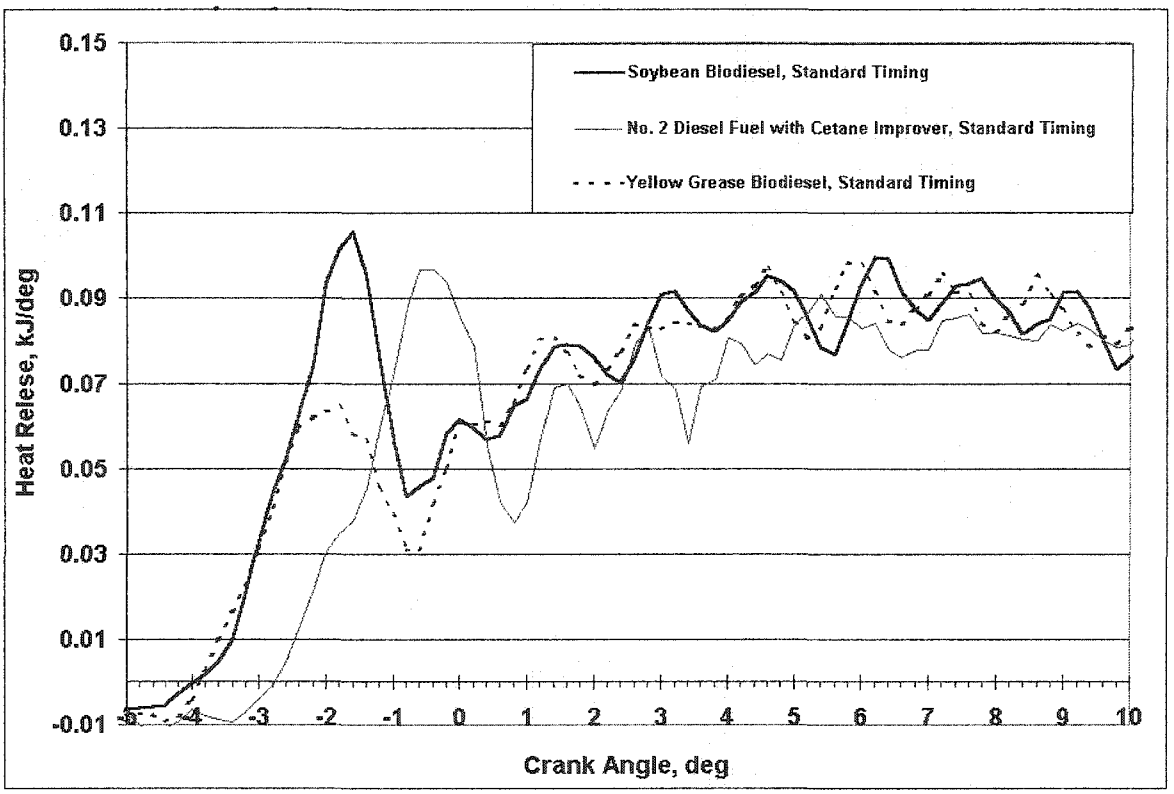

Figure 5.48 Heat release analysis comparisons at standard timing and 352.5 N-m, 1400 rpm, pump #2, and diesel fuel with cetane number increased to 47

Table 5.17. Combustion characteristics of No. 2 diesel with cetane improver(cetane #: 47), soybean, and yellow grease biodiesel fuels at 352.5 N-m and 1400 rpm and advanced timing with pump #2.

Combustion Characteristics	*No. 2 Diesel fuel with cetane improver (DIEWI)*	*Soybean Biodiesel (SBB)*	*Yellow Grease Biodiesel (YGB)*
Start of Injection, deg	-10.85	-11.99	-11.87
Start of Combustion, deg	-6.79	-8.14	-8.58
Ignition Delay, deg	4.06	3.85	3.30
Total of fuel energy released per injection, kJ/inj-cyl	2.71	2.70	2.72
Percent of fuel energy burned as premixed, %	8.55	8.56	6.38
Comparisons	***Ratios of Ignition Delay***	***Ratios of Percent Energy Release Rates as Premixed***	
DIEWI/SBB =	1.05	1.00	
DIEWI/YGB =	1.23	1.34	
SBB/YGB =	1.17	1.34	

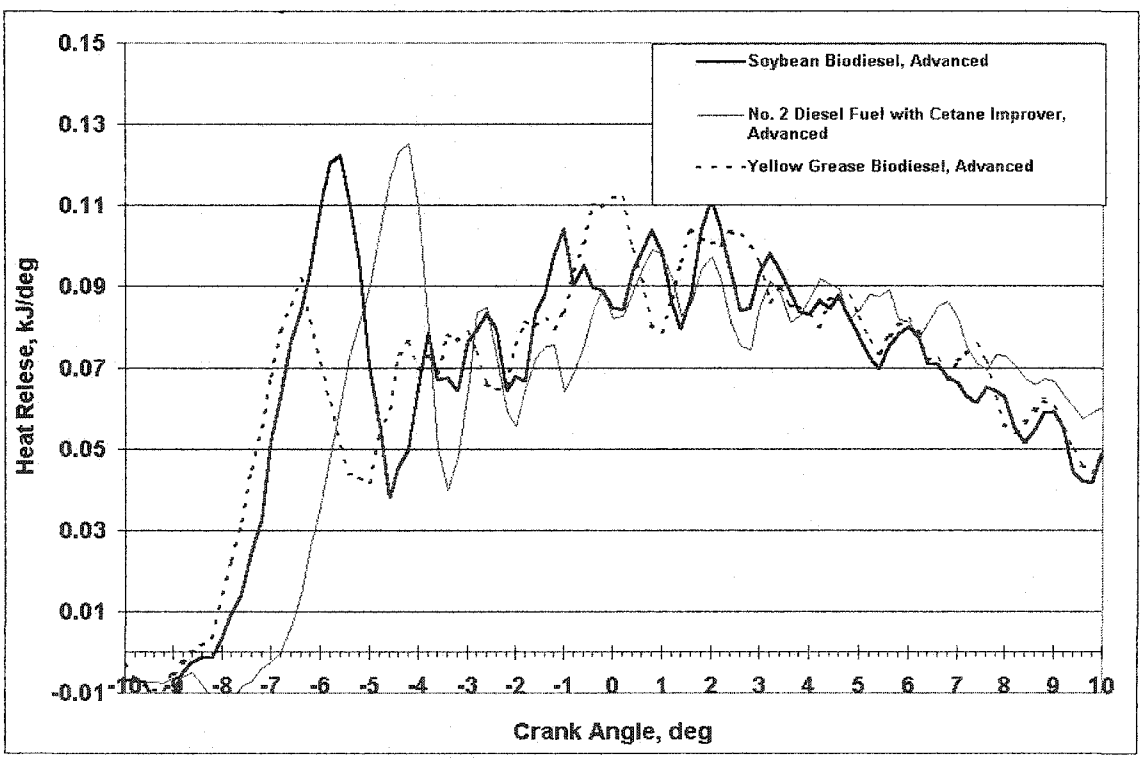

Figure 5.49 Heat release analysis comparisons at advanced timing and 352.5 N-m, 1400 rpm, pump #2, and diesel fuel with cetane number increased to 47

Table 5.18. Combustion characteristics of No. 2 diesel with cetane improver (cetane #: 47), soybean, and yellow grease biodiesel fuels at 352.5 N-m and 1400 rpm and retarded timing, with pump #2.

Combustion Characteristics	*No. 2 Diesel fuel with cetane improver (DIEWI)*	*Soybean Biodiesel (SBB)*	*Yellow Grease Biodiesel (YGB)*
Start of Injection, deg	-2.03	-2.48	-2.77
Start of Combustion, deg	1.50	0.75	0.47
Ignition Delay, deg	3.54	3.23	3.24
Total of fuel energy released per injection, kJ/inj-cyl	2.91	2.83	2.86
Percent of fuel energy burned as premixed, %	6.60	5.82	4.12

Comparisons	*Ratios of Ignition Delay*	*Ratios of Percent Energy Release Rates as Premixed*
DIEWI/SBB =	1.10	1.13
DIEWI/YGB =	1.09	1.60
SBB/YGB =	1.00	1.41

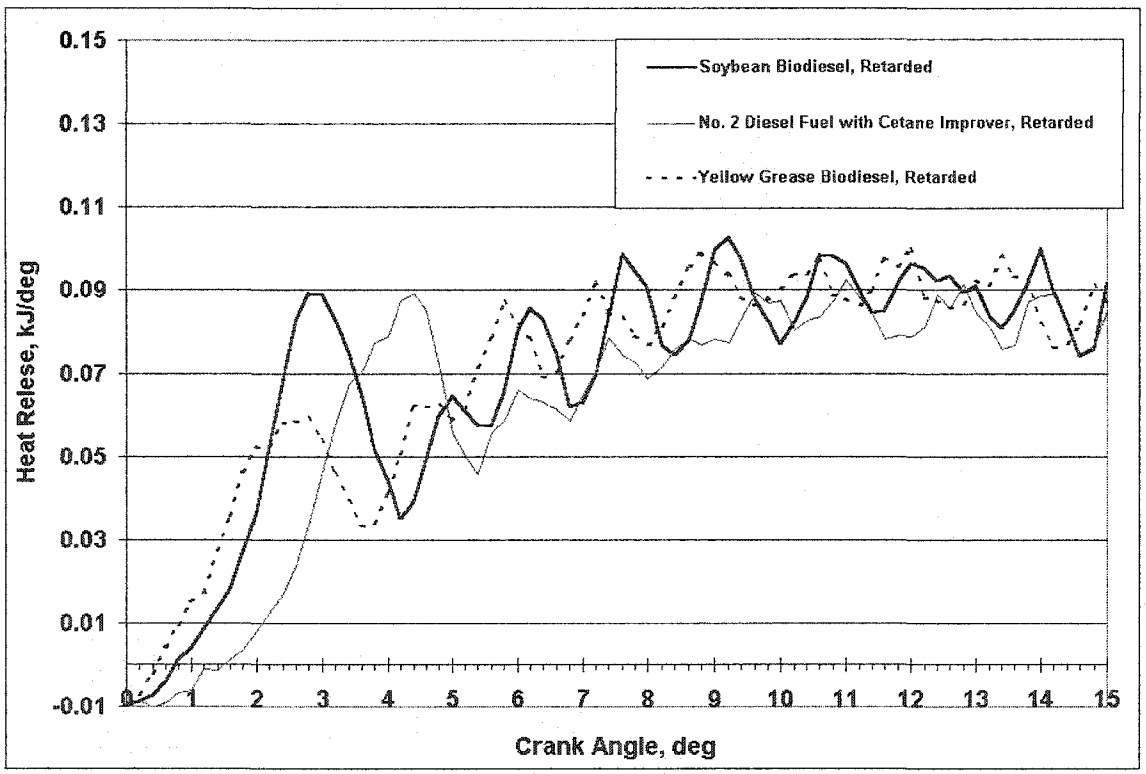

Figure 5.50 Heat release analysis comparisons at retarded timing and 352.5 N-m, 1400 rpm, pump #2, and diesel fuel with cetane number increased to 47

This explains the lower BSNOx emission of the No. 2 diesel fuel with cetane improver given earlier in Figure 5.46. Even though there might have been some minor mispositioning of the fuel pump, it is still clear that the start of combustion of the yellow grease biodiesel was the first, then biodiesel from soybean oil, No. 2 with the cetane additive, and the last one was regular No. 2 diesel fuel.

It is seen that the amount of energy released per injection for the same power level and at the same timing condition is the same for all of the fuels just like with the pump #2 tests. It is also observed that the total energy release per injection was increased as the timing was retarded. Because of less efficient combustion at the retarded timing, the combustion temperature and the efficiency were reduced, for the same power level, and the amount of fuel and the energy input were increased.

In the tables, it is found that the percent of fuel energy burned in the premixed portion of the combustion was the highest at the most advanced timing condition for all the fuels. No. 2 diesel fuel had a 30% longer ignition delay and 60% more premixed combustion than the No. 2 diesel fuel with the additive. No. 2 diesel fuel had a 40% longer ignition delay and 80% more premixed combustion than diesel fuel. When the regular No. 2 diesel fuel is compared with yellow grease biodiesel, the ignition delay of the No. 2 diesel fuel is about 50% longer and the premixed portion of the combustion is more than 200% higher at the standard timing. At this point it is possible to look back at the global effects of the biodiesel fuel properties on BSNOx emission, given in Section 5.3.2.1, and discuss the overall property effects on the higher BSNOx emission of biodiesel.

Table 5.19. Combustion characteristics of No. 2 diesel with cetane improver (cetane #: 53.5), soybean, and yellow grease biodiesel fuels at 352.5 N-m and 1400 rpm and standard timing, with pump #3.

Combustion Characteristics	*No. 2 Diesel fuel with cetane improver (DIEWI)*	*Soybean Biodiesel (SBB)*	*Yellow Grease Biodiesel (YGB)*	*No. 2 Diesel (DIE)*
Start of Injection, deg	-6.64	-7.32	-7.52	-6.90
Start of Combustion, deg	-3.41	-4.36	-4.63	-2.64
Ignition Delay, deg	3.23	2.97	2.89	4.25
Total of fuel energy released per injection, kJ/inj-cyl	2.76	2.74	2.76	2.74
Percent of fuel energy burned as premixed, %	5.95	5.30	4.50	9.47
Comparisons	***Ratios of Ignition Delay***		***Ratios of Percent Energy Release Rates as Premixed***	
DIEWI/SBB =	1.09		1.12	
DIEWI/YGB =	1.12		1.32	
SBB/YGB =	1.03		1.18	
DIE/DIEWI =	1.32		1.59	
DIE/SBB =	1.43		1.79	
DIE/YGB =	1.47		2.11	

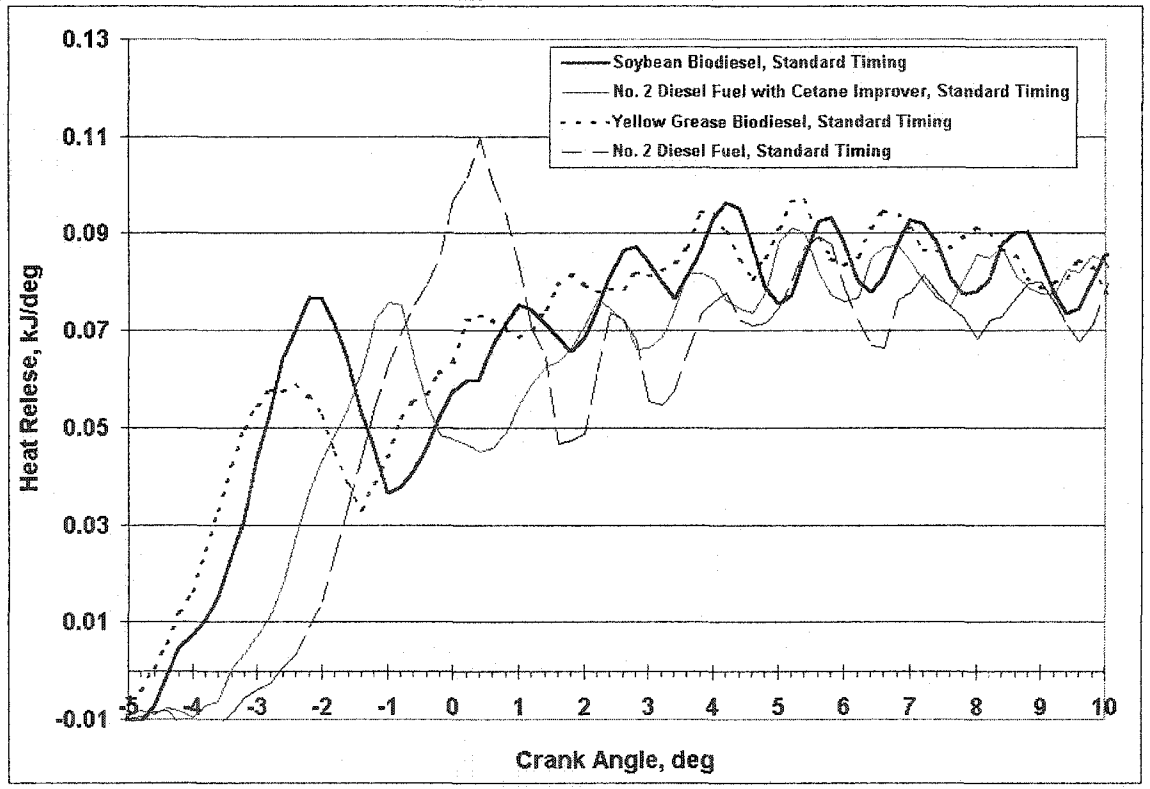

Figure 5.51 Heat release analysis comparisons at standard timing and 352.5 N-m, 1400 rpm, pump #3, and diesel fuel with cetane number increased to 53.5

Table 5.20. Combustion characteristics of No. 2 diesel with cetane improver (cetane #: 53.5), soybean, and yellow grease biodiesel fuels at 352.5 N-m and 1400 rpm and advanced timing with pump #3.

Combustion Characteristics	*No. 2 Diesel fuel with cetane improver (DIEWI)*	*Soybean Biodiesel (SBB)*	*Yellow Grease Biodiesel (YGB)*	*No. 2 Diesel (DIE)*
Start of Injection, deg	-10.35	-10.84	-11.33	-10.92
Start of Combustion, deg	-7.04	-7.84	-8.32	-6.49
Ignition Delay, deg	3.31	3.00	3.00	4.42
Total of fuel energy released per injection, kJ/inj-cyl	2.71	2.69	2.72	2.72
Percent of fuel energy burned as premixed, %	7.12	6.70	5.68	10.63
Comparisons	***Ratios of Ignition Delay***		***Ratios of Percent Energy Release Rates as Premixed***	
DIEWI/SBB =	1.10		1.06	
DIEWI/YGB =	1.10		1.25	
SBB/YGB =	1.00		1.18	
DIE/DIEWI =	1.34		1.49	
DIE/SBB =	1.47		1.59	
DIE/YGB =	1.47		1.87	

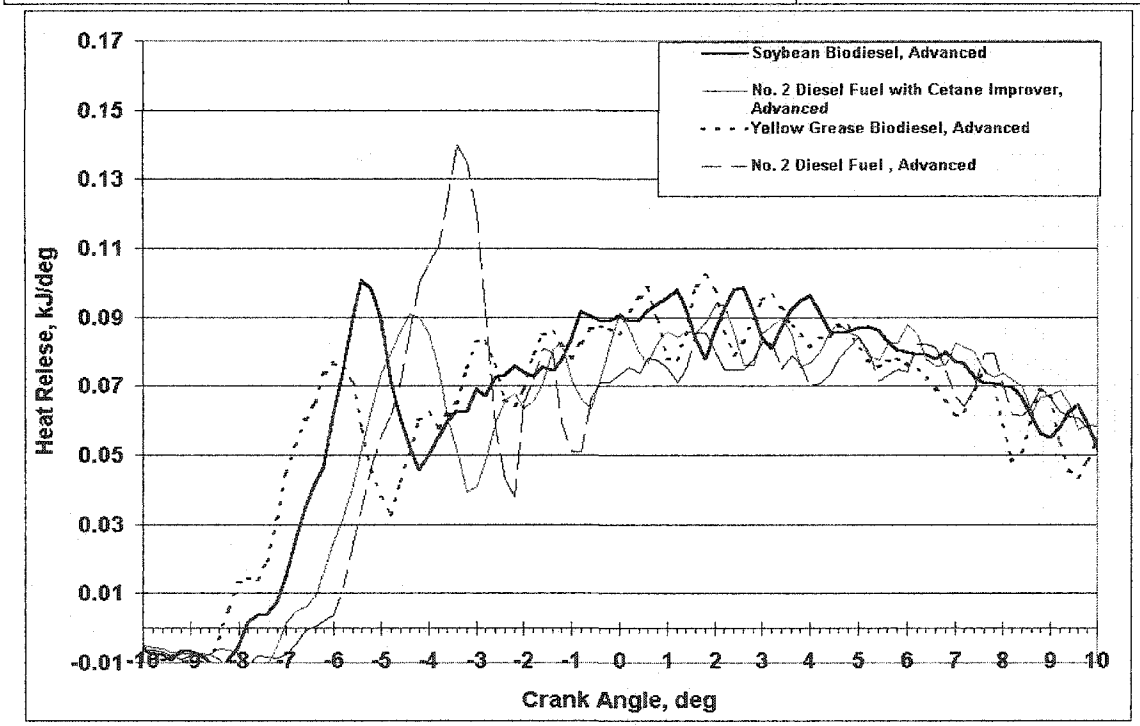

Figure 5.52 Heat release analysis comparisons at advanced timing and 352.5 N-m, 1400 rpm, pump #3, and diesel fuel with cetane number increased to 53.5

Table 5.21. Combustion characteristics of No. 2 diesel with cetane improver (cetane #: 53.5), soybean, and yellow grease biodiesel fuels at 352.5 N-m and 1400 rpm and retarded timing, with pump #3.

Combustion Characteristics	***No. 2 Diesel fuel with cetane improver (DIEWI)***	***Soybean Biodiesel (SBB)***	***Yellow Grease Biodiesel (YGB)***	***No. 2 Diesel (DIE)***
Start of Injection, deg	-1.85	-2.57	-2.50	-2.11
Start of Combustion, deg	1.40	0.57	0.28	2.11
Ignition Delay, deg	3.24	3.13	2.78	4.22
Total of fuel energy released per injection, kJ/inj-cyl	2.91	2.83	2.87	2.90
Percent of fuel energy burned as premixed, %	4.96	5.31	3.51	8.84
Comparisons	***Ratios of Ignition Delay***		***Ratios of Percent Energy Release Rates as Premixed***	
DIEWI/SBB =	1.03		0.93	
DIEWI/YGB =	1.17		1.41	
SBB/YGB =	1.13		1.51	
DIE/DIEWI =	1.30		1.78	
DIE/SBB =	1.35		1.66	
DIE/YGB =	1.52		2.52	

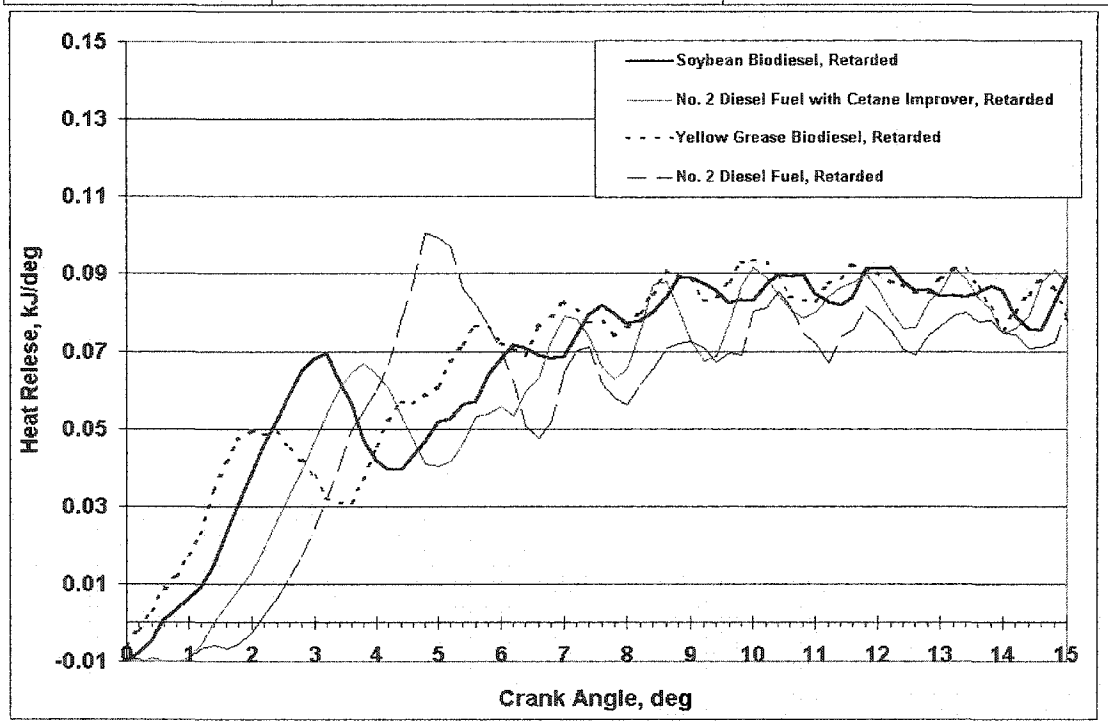

Figure 5.53 Heat release analysis comparisons at retarded timing and 352.5 N-m, 1400 rpm, pump #3, and diesel fuel with cetane number increased to 53.5

5.3.5 Discussion

At this point it is possible to examine the fuel property effects individually to estimate their effect on BSNOx emission. The first step engine tests, which were discussed in Section 5.3.2, will be analyzed first and some inferences will be made. When the start of combustion of regular No. 2 diesel fuel is read from Table 5.15 in Section 5.3.2.2, it is seen that the start of combustion for regular diesel fuel is 2° before TDC. Therefore, the BSNOx emission comparison analysis can be done at 2° BTDC. Using the quadratic regression equation given in Figure 5.44, the increase in the BSNOx emission of soybean biodiesel can be calculated as the start of combustion timing is advanced. The quadratic equation given in Figure 5.44 is used here because the equation was found using both pump #2 and pump #3 and therefore it is expected to be more reliable. If the soybean biodiesel start of combustion was 2° BTDC at the same load conditions where the data were collected, the BSNOx emission the soybean biodiesel is calculated to be 7.94 g/kW-h using the regression equation. If soybean biodiesel's start of combustion was advanced to 3°, 4°, and 5° BTDC, the BSNOx emission would increase by 7.8%, 16.4%, and 25.7% relative to 7.94 g/kW-h, respectively. In other words, 1°, 2°, and 3° advancements in the biodiesel combustion timing would cause 7.8%, 16.4%, and 25.7% increase in BSNOx emission.

When the start of combustion timings of soybean biodiesel and regular diesel fuel from Table 5.15 are compared, 1.57° of combustion timing advance is found. Using the same regression equation, a BSNOx emission increase of 12.6% can be calculated, which is very close to the 14% increase obtained by the engine tests presented in Figure 5.17.

When the start of injection timings of soybean biodiesel and No. 2 diesel fuel are compared, it is seen that soybean biodiesel was injected about 0.79° earlier than diesel fuel and it had a 0.78° shorter ignition delay period. The 1.57° advance in the start of combustion is equal to the total of the advance in the start of injection timing and the shorter ignition delay for soybean biodiesel. Therefore, the total increase in BSNOx emission of soybean biodiesel can be attributed equally to the 0.79° timing advance in injection timing and to the 0.78° advance in the combustion timing due to the shorter ignition delay period.

It was found in Section 5.3.3.1 that biodiesel's start of injection was advanced due to its lower heating value and due to its higher physical properties. It was observed that the start of injection timing was advanced about 1.34° for soybean biodiesel with pump #1 compared with No. 2 diesel fuel. It was also found that 0.68° of the 1.34° advance, which is about half, was due to the lower heating value effect. The lower heating value of the fuel was causing a power loss, and to compensate for this power loss, the amount of fuel was increased and the start of injection was advanced. The rest of the start of injection timing was 0.66° and this advance was due to the higher speed of sound and isentropic bulk modulus. Overall, it can be said that approximately 50% of the injection timing advance can be explained by the higher physical properties of biodiesel and the other 50% can be explained by the lower heating value effect on the start of injection timing for the pump #1 tests.

These numbers can be easily related back to the BSNOx emission. For the pump #1 test, the portion of the BSNOx emission produced due to the advance in the start of injection timing can be explained by attributing 50% of the increase to the lower heating value effect

and the other 50% to the higher speed of sound and isentropic bulk modulus. It was also found that viscosity had a significant effect on this portion.

In Section 5.3.3.4, engine tests to investigate the effect of fuel properties on pump #2 were presented. It was shown that the total advance in the start of injection timing for soybean biodiesel was only 0.6°. In Figure 5.33, it was shown that for the same volume of fuel injection there was no difference in the fuel injection timing between biodiesel and No. 2 diesel fuels, unlike the data presented in Figure 5.23 for pump #1 that showed 0.66° advancement. In this case, the effect of speed and the viscosity effects on the start of injection timing were investigated and it was found that viscosity had an effect on the start of injection timing of about 0.2° to 0.5° with pump #2 and pump #3. This viscosity effect was a function of each individual pump because of the factory tolerances. This may also explain part of the differences in BSNOx emissions of biodiesel observed by different researchers.

It should be recalled from the concept map given in Chapter 3 that when the cetane number shortens the ignition delay period, it also advances the start of combustion and it reduces the premixed combustion of the diesel engine. At this point, it should be noted that these two effects are working against each other, in terms of BSNOx emission. When the start of combustion timing is advanced, the BSNOx emission generally increases due to higher combustion temperatures. However, when the ignition delay period is reduced, that reduces the amount of fuel prepared during the ignition delay period, which reduces the premixed portion of the combustion, and this usually reduces the BSNOx emission.

In Section 5.3.4.1, the effect of biodiesel's higher cetane number was discussed. In Figure 5.44, the BSNOx emission of biodiesel from yellow grease with a cetane number of 62.6 and biodiesel from soybean oil with a cetane number of 50.4 were compared. The

soybean biodiesel and yellow grease biodiesel had the same volatility. The primary difference between the two samples was the 12 cetane number difference. Using the regression equations given in Figure 5.44, the soybean biodiesel produces a BSNOx level of 7.94 g/kW-h and yellow grease biodiesel produces 7.16 g/kW-h at the same start of combustion of 2° BTDC. It can be calculated that for the 12 cetane number increase, a 9.9% reduction is observed from the soybean BSNOx emission. When the global effects of biodiesel fuel were discussed in Section 5.3.2.1, it was noted that the yellow grease biodiesel produced about 1% lower BSNOx emission than the regular diesel fuel.

The lower volatility of biodiesel appears not to affect the BSNOx emission of biodiesel. It was shown that No. 2 diesel fuel with a cetane number of 53.5 produced less BSNOx emission than soybean biodiesel with a cetane number of 50.5. The ignition delay period of the diesel fuel was still about 10% longer than for the biodiesel fuel. A possible reason might be that biodiesel fuel degrades at high temperature so that when it enters the cylinder and mixes with air, it's volatility increases. Biodiesel is denser than No. 2 diesel fuel and improves the injection parameters, such as penetration and mixing [94]. Better fuel injection might improve the physical mixing of the fuel and air during the ignition delay period and overcomes the lower volatility effect.

In Tables 5.18-20, biodiesel's percentage of premixed combustion is about 10% less than for No. 2 diesel with cetane improver. It should be considered that the chemical structure of biodiesel is different than diesel fuel. Biodiesel includes about 11% oxygen. The combustion chemistry of biodiesel might be different and the oxygen in the fuel may promote NOx emission. These should be investigated in future work.

6. CONCLUSIONS AND RECOMMENDATIONS

Biodiesel has a higher cetane number and lower volatility than regular diesel fuel. It is normally expected that a fuel that has a higher cetane number and lower volatility will produce lower BSNOx emissions. This is because the higher cetane number of the fuel shortens the ignition delay period and reduces the premixed portion of the combustion. The lower volatility of the fuel limits the amount of prepared fuel before the combustion starts, which also reduces the premixed portion of the combustion. The traditional understanding of NOx formation in diesel engines indicates that these reductions in the premixed combustion should lower NOx emissions. Even though biodiesel has a higher cetane number and lower volatility, its NOx emission is higher than regular diesel fuel.

In order to understand the reasons for the higher NOx emission of biodiesel, a concept map was developed. Based on the concept map, the most important fuel properties were identified and test procedures to characterize their impact were proposed and conducted. The effects of the cetane number, volatility, lower heating value, speed of sound, isentropic bulk modulus, and viscosity of biodiesel on the start of injection and NOx emission were investigated.

During the course of the research, three different fuel injection pumps were used. Some test sequences were duplicated to see the pump differences and some tests were repeated with improved samples. Also, the speed effect on the start of injection timing was investigated. The effect of fuel viscosity on the start of injection timing was found during the course of the testing to be significant and the viscosity effect overlapped with the effect of the speed of sound and bulk modulus on the injection timing. The viscosity effect of the fuel

was judged to be a strong function of factory tolerances and changed for each individual pump.

Also in this study, the density, speed of sound, and isentropic bulk modulus of biodiesel and its constituents at higher temperatures and higher pressures were measured. The effect of chain length, saturation, hydrogenation, and oxidation on the density, speed of sound, and isentropic bulk modulus were investigated. Soybean biodiesel was blended with No. 2 and No. 1 diesel fuels at 75%, 50%, and 20% ratios and the blending effect on the fuel density, speed of sound, and isentropic bulk modulus were investigated. The purpose of this conclusion section is to summarize the experimental results and make recommendations for future work. The following section contains specific conclusions that can be drawn from the research presented earlier.

6.1 Conclusions

1. In the concept map presented in Figure 3.6, it was proposed that the increase in the NOx emission could be explained by a timing advance in the start of combustion and a change in the amount of premixed combustion. In this study, while it was not shown that no other mechanisms are involved, it was shown that the increase in the NOx emissions of soybean oil biodiesel are of the same magnitude as the NOx increase that would be expected from the advance in the combustion timing caused by fuel property differences between diesel fuel and biodiesel.
2. It was found that the combustion timing advance originates from an advance in the start of injection timing and from the shorter ignition delay of soybean biodiesel. In this research, it was found that approximately half of the total combustion timing advance of soybean oil biodiesel results from the higher cetane number of soybean biodiesel and the

other half of the total combustion timing advance results from the start of injection timing advance.

3. The start of injection timing advance was found to be a function of both the lower heating value (pump effect) and the physical properties of biodiesel fuel. It was also found that the viscosity has a strong effect on the start of injection due to internal leakage in the fuel pump and this is strongly related to the factory tolerances. It was also found that the fuel density has an effect on the fuel delivery and injection timing, due to the effect of density on the flow through orifices in the fuel injection pump. At the same viscosity, a greater volume of the less dense fuel, No. 2 diesel fuel, was delivered compared with biodiesel, the more dense fuel. For pump #1 tests, half of the total start of injection timing advance was due to the pump effect and the other half of the advance was due to changes in the viscosity, density, speed of sound, and isentropic bulk modulus. In the tests with pump #2 and pump #3, all of the start of injection timing advance was due to the pump effect as the other property effects appeared to cancel themselves out.
4. Fuel volatility has an effect on the premixed combustion as given in the concept map. The lower volatility of biodiesel was expected to reduce the premixed combustion and the NOx emission. However, it was found that volatility did not affect the NOx emission of biodiesel.
5. The NOx emission of yellow grease biodiesel is close to the NOx emission level of regular diesel fuel and this is believed to be due to its higher cetane number. The higher cetane number of the yellow grease diesel fuel reduced the premixed combustion portion of the combustion so that even though the start of combustion was advanced, the

premixed portion of the combustion was reduced by a sufficiently large amount that the NOx emission was equivalent to the diesel fuel level.

6.2 Recommendations

1. The effect of the lower volatility of biodiesel on combustion should be investigated further to confirm that it has no impact on premixed combustion and NOx production.
2. The difference in the combustion chemistry between the fuels should investigated to determine whether it plays a role in NOx production.
3. Since the oxygen level in the fuel can have an effect on the emissions, varying the oxygen content of the fuel and measuring the emissions can help significantly to understand the mechanisms that are involved.

APPENDIX A

PHYSICAL AND CHEMICAL PROPERTIES OF THE FUEL SAMPLES USED IN SPEED OF SOUND AND DENSITY MEASUREMENTS

Table A.1. Fuel analysis results.

Fuel	Acid Number	Iodine Number	Peroxides	Water And Sediment	Glycerides			Total Glycerin
Ester	mg KOH/g	mg I2/g	mg/kg	vol%	Mono-	Di-	Tri-	
1. Methyl Laurate	0.06	0.3	62	0	0.004	0	0.016	0.003
2. Methyl Palmitate	0.16	0.5	77	0	0.003	0	0.098	0.011
3. Methyl Stearate	9.13	0.5	74	0	0.058	0.004	0	0.016
4. Ethyl Stearate	0.01	1.0	58	0	0.055	0.012	0.073	0.025
5. Methyl Oleate	0.13	90	162	0	0.073	0.017	0.004	0.022
6. Ethyl Oleate	0.19	79	185	0	0.094	0.024	0.069	0.035
7. Methyl Linoleate	0.41	151	148	0	0.078	0.153	0.792	0.126
8. Ethyl Linoleate	0.81	140	655	0	0.326	0.03	0	0.089
9. Methyl Linolenate	0.23	165	544	0	0.085	0.133	0.452	0.089
10. Ethyl Linseed	6.1	157	21	0	0.098	0.025	0.112	0.041
11. Methyl Soy	0.15	121	340	0	0.684	0.216	0.063	0.223
12. Methyl Hydrogenated Soy	4.66	6	188	0	0.278	0.075	0.143	0.099
13. Ethyl Soy	3.02	122	123	0	0.083	0.036	0.013	0.031
14. Ethyl Hydrogenated soy	3.94	6	111	0	0.361	0.023	0	0.097
15. 2:1 Methyl Stearate: Methyl Linseed	1.62	116	295	0	0.084	0.023	3.105	0.024
16. 1:2 Methyl Stearate: Methyl Linseed	2.5	66	387	0	0.85	0.033	0.01	0.062
17. Oxidized Methyl Soy	0.6	131	1861	0	0.018	0.036	0.011	0.012
18. Oxidized Ethyl Soy	3.81	118	210	0				
19. High Acid Number Methyl Oleate	10.1	84	369	0	0.063	0.013	0.045	0.023
20. High Glyceride Ethyl Soy	6.3	117	125	0	2.489	1.035	2.357	1.045

Table A.2. Fatty acid composition of fuels tested (M=methyl ester, E=ethyl ester).

	Lauric	Myristic	Palmitic	Palmitoleic	Margaric	Stearic	Oleic	Linoleic	Linolenic
Ester	C12:0	C14:0	C16:0	C16:1	C17:0	C18:0	C18:1	C18:2	C18:3
1. Methyl Laurate	99.2 M	0	0	0	0	0	0.6 M	0.2 M	0
2. Methyl Palmitate	0.2 M	4.6 M	88.2 M	0	0.4 M	6.3 M	0	0	0
3. Methyl Stearate	0	1.3 M	42.1 M	0	1.0 M	52.6 M	0.9 M	2 M	0
4. Ethyl Stearate	0	2.2 E	43.6 E	0	2.4 E	49.8 E	0.2 E	0.1 E	0
5. Methyl Oleate	0	3.0 M	6.5 M	4.1 M	1.5 M	1.9 M	64.5 M	9.1 M	9 M
6. Ethyl Oleate	0	3.1E	6.7 E	4.2 E	4.6 E	2.5 E	58.1 E	9.1 E	9.1 E
7. Methyl Linoleate	0	0	1.4 M	0	0	0.7 M	5.2 M	86.5 M	6.2 M
8. Ethyl Linoleate	0	0	2.7 E	0	0	2.4 E	6.4 E	88.5 E	0
9. Methyl Linolenate	0	0	7.4 M	0	0	3.7 M	24.8 M	2.9 M	61.2 M
10. Ethyl Linseed	0	2.5 E	7.6 E	0	3.3 E	2.8 E	22.3 E	11.2 E	50.3 E
11. Methyl Soy	0	0	16.3 M	0	0	6 M	53.4 M	24.3	0
12. Methyl Hydrogenated	0	0	11.3 M	0	0	88.7 M	0	0	0
13. Ethyl Soy	0	0	5.2 M 8.8 E	0	0	2.9 M 6.1 E	18.6 M 34.1 E	10.6 M 13.7 E	0
14. Ethyl Hydrogenated soy	0	0	11.9 E	0	0	88.1 E	0	0	0
15. 2:1 Methyl Stearate: Methyl Linseed	0	0	38.6 M	0	0	44.1 M	4.8 M	2.4 M	10.1 M
16. 1:2 Methyl Stearate: Methyl Linseed	0	0	20.8 M	0	0	28 M	15.2 M	7.6 M	27.8 M
17. Oxidized Methyl Soy	0	0	15.2 M	0	0	5.3 M	57 M	22.5 M	0
18. Oxidized Ethyl Soy	0	0	4.9 M 10.1 E	0	0	2.5M 4.5 E	18.2 M 37.1 E	7.8 M 14.8 E	0
19. High Acid Number Methyl Oleate	0	4.2 E	43.6 M	0	0	3.4 M	73.1 M	7.4 M	7.4 M

In the Table letters E and M represent the amounts individual fatty acid esters when they were present during the measurement for the purpose of measurement.

Table A.3. Chemical properties of some ester samples.

Test Identification	Description	Methyl Soy Ester	Methyl Lard	Methyl Canola	Methyl Tallow
D93	Flash, Pensky Martens, °C	167	128	163	173
D97	Pour Point, °C	-4	13	-4	16
D130	Corrosion	1A	1A	1A	1A
D240	Heat of Combustion/Gross Calorific Value, BTU/lb	17153	17165	17241	17144
D445	Kinematic Viscosity, cSt @ 40 °C	4.546			4.908
D445	Kinematic Viscosity, cSt @ 100 °C		4.850	4.63	
D482	Ash from Petroleum Products, %	0.00	0.000	0.003	0.001
D524	Carbon Residue, Ramsbottom, 100% as 10%	0.008%	0.04	0.04	
D613	Cetane Number	59.0	xxxxxx	53.9	64.8
D664	Acid Number by Potentiometric Titration, mg KOH/g	0.32	0.76	0.13	0.32
D971	Interfacial Tension of Oil Against Water, mN/m	11.32	12.19	15.52	31.74
D1094	H2O RX & Rating I.R.=Interface Rating	2 I.R.	2 I.R.	2 I.R.	3 I.R.
	V.C.=Volume Change	1.0 mL V.C.	-1.0 mL V.C.	–2.0 mL V.C.	0.5 mL V.C.
D1298	Specific Gravity @ 23.3 °C, g/ml	0.8877	0.8762	0.8811	0.8708
D1322	Smoke Point	N/A-would not burn	N/A	N/A	N/A-wick burned
D1796	Sediment, %	0.00	0.60	0.00	0.05
D1959	Iodine, ppm	2.98	53	66	4.68
D2500	Cloud Point, °C	3	13	-3	19
D2622	Sulfur, wt%	0.000	0.0000	0.0000	0.000
D2624	Conductivity of Aviation Fuels, pS/m	181	122	147	809
D3241	Thermal Oxidation Stability	1 mm Hg; 1 Tube Rating	0 mm Hg; 1 Tube Rating	0 mm Hg; 1 Tube Rating	2 mm Hg; 4P0 Tube Rating
D3242	Neutralization Number, mg KOH/g	0.322	0.760	0.120	0.350
D4629	Total Nitrogen, ppm	3.0	3.0	<1.0	77.0

Table A.3. Continued

Test ID		Methyl Soy Ester	Methyl Lard	Methyl Canola	Methyl Tallow
D3241	Thermal Oxidation Stability	1 mm Hg; 1 Tupe Rating	0 mm Hg; 1 Tupe Rating	0 mm Hg; 1 Tupe Rating	2 mm Hg; 4P Tupe Rating
D3242	Neutralization Number, mg KOH/g	0.322	0.76	0.120	0.350
D4629	Total Nitrogen, ppm	3.0	3.0	<1.0	77.0
D5191	Vapor Pressure of Petroleum Products	Could not perform pour too high			Could not perform pour too high
D5291	CH				
D5291	Carbon, wt%	77.95	77.36	77.68	77.07
D5291	Hydrogen, wt%	11.98	12.5	12.25	12.05
D5452	Particulate Matter, Volume, Pad Rating	1.10 L; 78 min	789.00 mg/L;B6;0.17L ;18 min	11.00 mg/L; B5; 0.5L; 49 min	73.6 ml/L; B4; 1.0L; 301 min
IP309	Cold Filter Plugging Point, °F	-2	11	-4	
C. Plank	Impurities in Biodiesel Methyl Esters				
C. Plank	Free glycerin, wt%	0.001	0.000	0.001	0.000
C. Plank	Monoglycerides, wt%	0.870	0.563	0.738	0.320
C. Plank	Diglycerides, wt%	1.358	0.093	0.020	0.120
C. Plank	Triglycerides, wt%	3.542	0.005	0.010	0.014
C. Plank	Total glycerides, wt%	0.798	0.160	0.196	0.102
GCMS-OXY	Free Alcohols				41
	Methanol, ppm	79			<10
	Other Alcohol, ppm	<10			
	Propanal, ppm	28			54
	Acetaldehyde, ppm		85	95	
	Ethanol, ppm		8	14	
	Propanol, ppm		104	226	
	Formic Acid, ppm		28	16	
	Acetic Acid, ppm		59	57	
	Butanal, ppm		20	50	
	Pentanal, ppm		68	37	8
	2-Pentanal, ppm		10		
	Hexanal, ppm		198	110	7
	Butanol, ppm			81	

Table A.4. Distillation results of some samples.

Test Identification	Description	Methyl Soy Ester	Methyl Lard	Methyl Canola	Methyl Tallow
D86	Distillation Points, °C				
D86	IBP, °C	322.9	304.4	315.6	324.4
D86	10%, °C	339.6	322.2	323.9	278.9
D86	20%, °C	342.9	324.4	331.1	336.1
D86	50%, °C	345.7	328.9	335.6	341.1
D86	90%, °C	354.1	336.7	340.6	351.7
D86	EP, °C	356.3	354.4	355.0	361.1
D86	Recovery, mL	98.2	98.5	99	98.2
D86	Residue, mL	1.1	0.5	0.5	1.8
D86	Loss, mL	0.7	1.0	0.5	0.0
D1160	Vacuum Distillation				
D1160	IBP, °C	347.8	331.7	347.8	331.1
D1160	5%, °C	350.0	342.2	350.0	341.1
D1160	10%, °C	350.6	343.3	350.6	342.2
D1160	20%, °C	351.7	344.4	350.6	344.4
D1160	30%, °C	352.2	345.0	350.6	346.7
D1160	40%, °C	352.8	346.1	351.1	348.9
D1160	50%, °C	353.9	348.3	351.1	350.0
D1160	60%, °C	354.4	349.4	351.1	352.2
D1160	70%, °C	355.0	351.1	352.2	353.9
D1160	80%, °C	356.7	353.9	353.3	356.7
D1160	90%, °C	363.9	355.6	355.6	360.0
D1160	95%, °C	453.9	359.4	362.8	365.0
D1160	EP, °C	472.8	408.9	434.4	422.8
D1160	Recovery, %	97	99	99	98
D1160	Residue, %	3	1	1	2

Table A.5 The Physical and Chemical Properties of Commercial No.2 and No. 1 Diesel Fuels.

Test Property	Commercial No. 2 Diesel Fuel	Commercial No.1 Diesel Fuel
Carbon (% mass)	86.70[a]	86.83[a]
Hydrogen (% mass)	12.71[a]	12.72[a]
Oxygen (% mass)	-	-
C/H Ratio	6.82	6.826
Sulfur (% mass)	0.041[a]	0.045[a]
Cetane Number (ASTM D613)	42.6[a]	45.3[a]
Gross Heat of Combustion (kJ/kg)	45,339[a]	45,991[a]
Net Heat of Combustion (kJ/kg)	42,640[a]	43281[a]
Specific Gravity (@21 °C)	0.8537[c]	0.8162[c]
Kinematic Viscosity (cSt, @40 °C)	2.8271[c]	1.759[c]
Total Glycerin (%)	-	-
Free Glycerin (%)	-	-
Distillation (ASTM D86, °C)[a]		
Initial Boiling Point	177.8	175.6
5%	200.0	189.4
10%	211.7	195.6
20%	226.7	201.1
30%	238.9	207.8
40%	250.0	213.3
50%	261.1	218.9
60%	272.2	226.7
70%	283.9	234.4
80%	298.3	245.6
90%	316.7	261.7
95%	332.2	279.4
End Point	345.0	304.4
Recovery (%)	98.0	98.0
Residue (%)	1.9	1.9
Loss (%)	0.1	0.1

[a] Measured by Phoenix Chemical Laboratory Inc., Chicago IL.
[b] Measured by Williams Laboratory Services, Kansas City, KS.
[c] Measured in the Department of Mechanical Engineering, Iowa State University, Ames, IA.
[d] Calculated using Universal Oil Products Method 375-86, Des Plaines IL.
[e] Calculated from Fatty Acid Distribution.

APPENDIX B

CALIBRATION CURVES OF THE EMISSION ANALYZERS

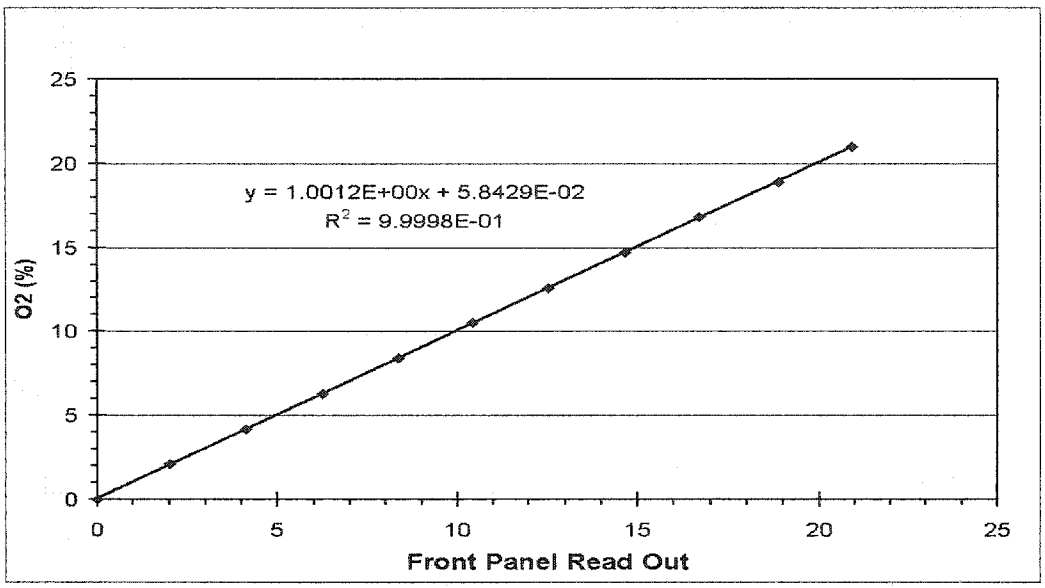

Figure B.1 Calibration curve for O_2 gas analyzer

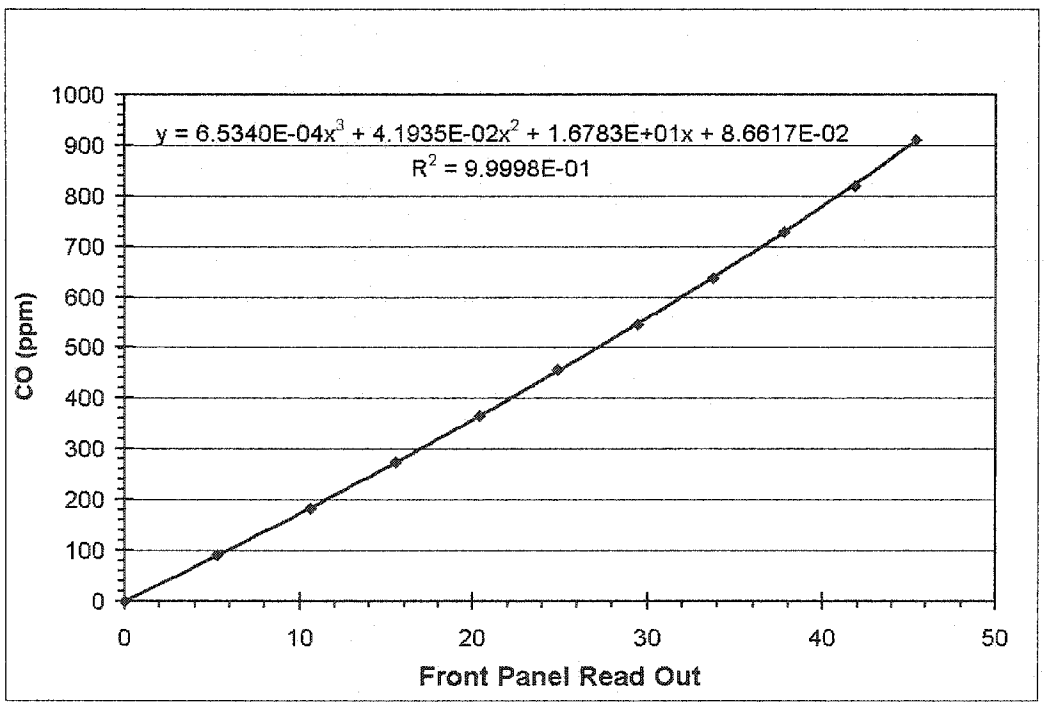

Figure B.2 Calibration curve for CO gas analyzer

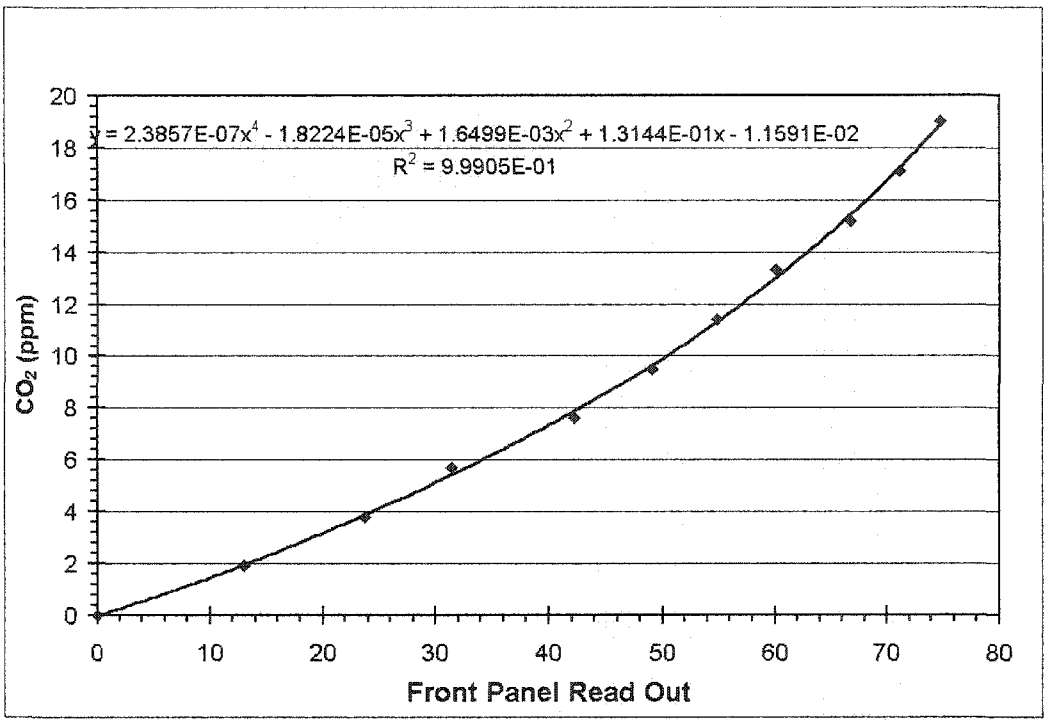

Figure B.3 Calibration curve for CO_2 gas analyzer

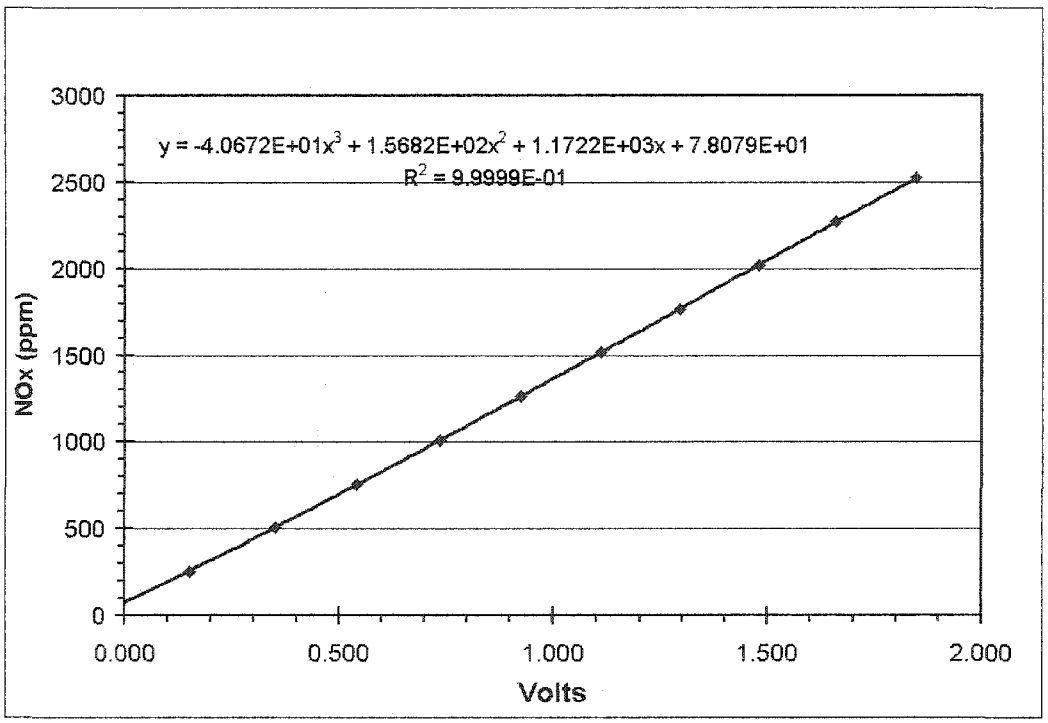

Figure B.4 Calibration curve for NO/NOx gas analyzer

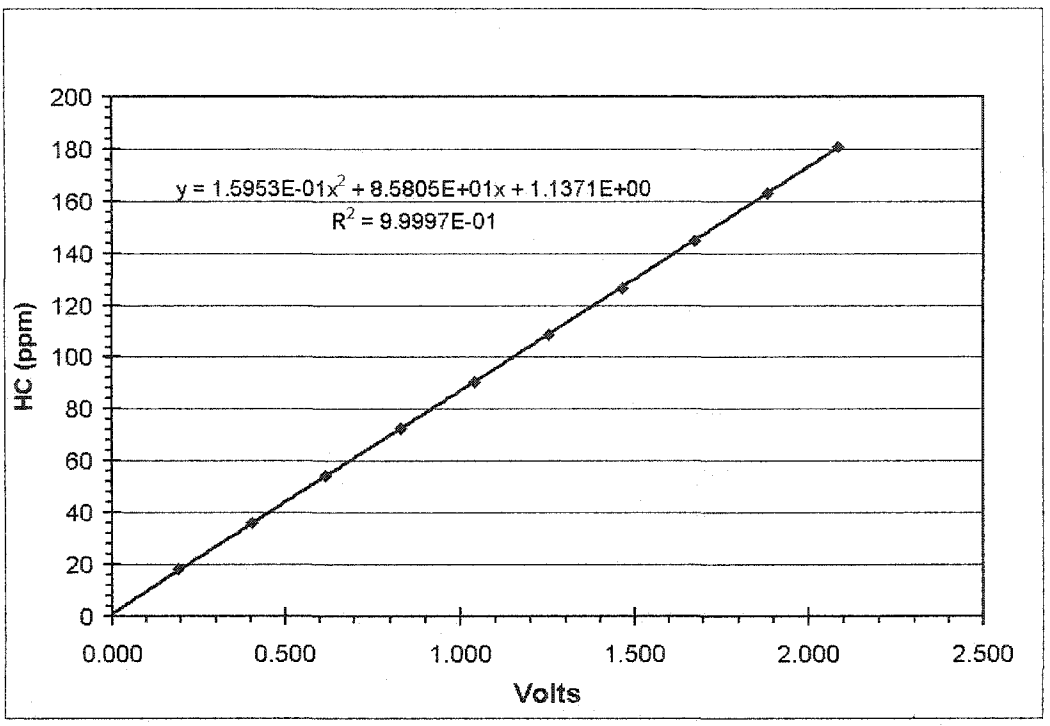

Figure B.5 Calibration curve for HC gas analyzer

APPENDIX C

CALIBRATIONS OF PRESSURE TRANSDUCERS

Kistler 6021 and 6230M1 pressure transducers were used in this study. The Kistler 6021 was used for cylinder pressure data collection. This transducer was calibrated with a dead-weight tester before it was installed in the fourth cylinder of the engine. The output signal of the transducer was amplified using a PCB Model 462A charge amplifier as a voltage. A linear regression equation fitted to the output of the amplifier and the equation was used for pressure determination. The regression equation is presented here in Figure C.1 along with the calibration data points. For Kistler the 6230M1 pressure transducer a factory calibration was used. The sensitivity of the transducer was 1.775 pC/bar and the charge amplifiers sensitivity was 100 pC/volt. The calculated pressure transducer's sensitivity was 56.98 bar/volt.

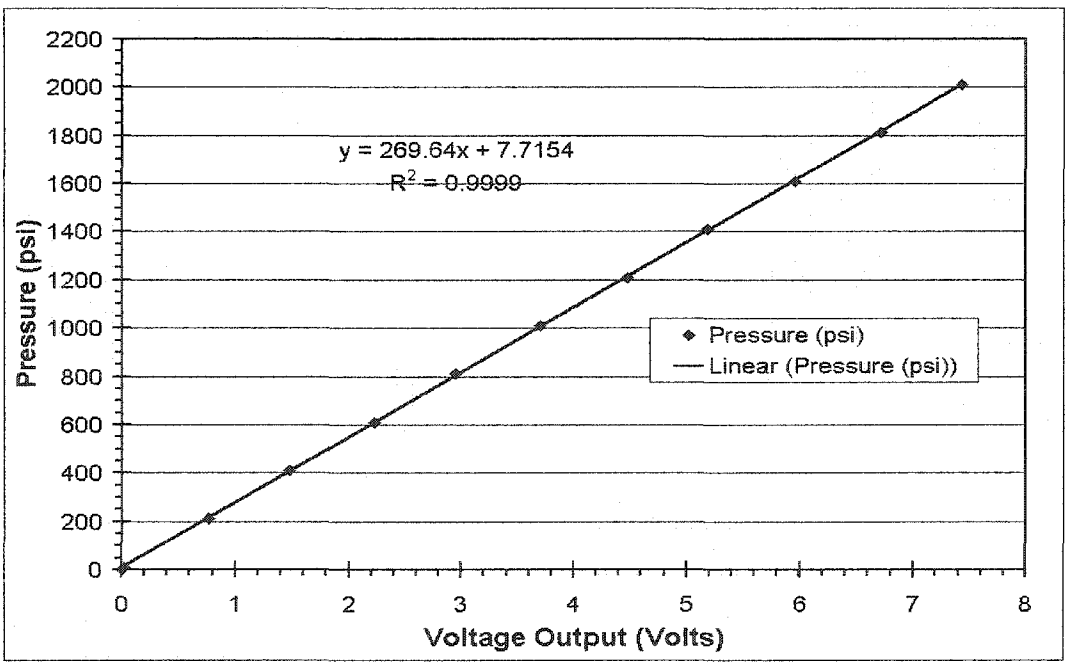

Figure C1 Calibration curve of Kistler model 6121 transducer for cylinder pressure data collection.

APPENDIX D

ANOVA TABLES STEP 1 WITH PUMP #2

REPORT D.1. STATISTICAL ANALYSIS FOR BSNOx EMISSION

Oneway Anova
Summary of Fit

Rsquare	0.88444
Adj Rsquare	0.84592
Root Mean Square Error	0.244987
Mean of Response	8.964824
Observations (or Sum Wgts)	9

Analysis of Variance

Source	DF	Sum of Squares	Mean Square	F Ratio	Prob > F
Fuel	2	2.7561144	1.37806	22.9605	0.0015
Error	6	0.3601117	0.06002		
C. Total	8	3.1162261			

Means for Oneway Anova

Level	Number	Mean	Std Error	Lower 95%	Upper 95%
No.2 Diesel Fuel	3	8.53742	0.14144	8.1913	8.884
Soybean Oil Biodiesel	3	9.74628	0.14144	9.4002	10.092
Yellow Grease Biodiesel	3	8.61077	0.14144	8.2647	8.957

Std Error uses a pooled estimate of error variance

Means Comparisons

Dif=Mean[i]-Mean[j]	Soybean Oil Biodiesel	Yellow Grease Biodiesel	No.2 Diesel Fuel
Soybean Oil Biodiesel	0.0000	1.1355	1.2089
Yellow Grease Biodiesel	-1.1355	0.0000	0.0734
No.2 Diesel Fuel	-1.2089	-0.0734	0.0000

Alpha=
0.05

Comparisons for all pairs using Tukey-Kramer HSD

q*	Alpha
3.06815	0.05

Abs(Dif)-LSD	Soybean Oil Biodiesel	Yellow Grease Biodiesel	No.2 Diesel Fuel
Soybean Oil Biodiesel	-0.61373	0.52179	0.59514
Yellow Grease Biodiesel	0.52179	-0.61373	-0.54037
No.2 Diesel Fuel	0.59514	-0.54037	-0.61373

Positive values show pairs of means that are significantly different.

Level		Mean
Soybean Oil Biodiesel	A	9.7462820
Yellow Grease Biodiesel	B	8.6107708
No.2 Diesel Fuel	B	8.5374196

Levels not connected by same letter are significantly different

REPORT D.2. STATISTICAL ANALYSIS FOR BSHC EMISSION

Oneway Anova
Summary of Fit

Rsquare	0.93686
Adj Rsquare	0.915813
Root Mean Square Error	0.011293
Mean of Response	0.096445
Observations (or Sum Wgts)	9

Analysis of Variance

Source	DF	Sum of Squares	Mean Square	F Ratio	Prob > F
Fuel	2	0.01135411	0.005677	44.5133	0.0003
Error	6	0.00076522	0.000128		
C. Total	8	0.01211932			

Means for Oneway Anova

Level	Number	Mean	Std Error	Lower 95%	Upper 95%
No.2 Diesel Fuel	3	0.146584	0.00652	0.13063	0.16254
Soybean Oil Biodiesel	3	0.074008	0.00652	0.05805	0.08996
Yellow Grease Biodiesel	3	0.068743	0.00652	0.05279	0.08470

Std Error uses a pooled estimate of error variance

Means Comparisons

Dif=Mean[i]-Mean[j]	No.2 Diesel Fuel	Soybean Oil Biodiesel	Yellow Grease Biodiesel
No.2 Diesel Fuel	0.00000	0.07258	0.07784
Soybean Oil Biodiesel	-0.07258	0.00000	0.00526
Yellow Grease Biodiesel	-0.07784	-0.00526	0.00000

Alpha=
0.05

Comparisons for all pairs using Tukey-Kramer HSD

q*	Alpha
3.06815	0.05

Abs(Dif)-LSD	No.2 Diesel Fuel	Soybean Oil Biodiesel	Yellow Grease Biodiesel
No.2 Diesel Fuel	-0.02829	0.04428	0.04955
Soybean Oil Biodiesel	0.04428	-0.02829	-0.02303
Yellow Grease Biodiesel	0.04955	-0.02303	-0.02829

Positive values show pairs of means that are significantly different.

Level		Mean
No.2 Diesel Fuel	A	0.14658390
Soybean Oil Biodiesel	B	0.07400818
Yellow Grease Biodiesel	B	0.06874335

Levels not connected by same letter are significantly different

REPORT D.3. STATISTICAL ANALYSIS FOR BSCO EMISSION

Oneway Anova
Summary of Fit

Rsquare	0.968649
Adj Rsquare	0.956109
Root Mean Square Error	0.039168
Mean of Response	1.022038
Observations (or Sum Wgts)	8

Analysis of Variance

Source	DF	Sum of Squares	Mean Square	F Ratio	Prob > F
Fuel	2	0.23699941	0.118500	77.2433	0.0002
Error	5	0.00767055	0.001534		
C. Total	7	0.24466996			

Means for Oneway Anova

Level	Number	Mean	Std Error	Lower 95%	Upper 95%
No.2 Diesel Fuel	2	1.31410	0.02770	1.2429	1.3853
Soybean Oil Biodiesel	3	0.88483	0.02261	0.8267	0.9430
Yellow Grease Biodiesel	3	0.96454	0.02261	0.9064	1.0227

Std Error uses a pooled estimate of error variance

Means Comparisons

Dif=Mean[i]-Mean[j]	No.2 Diesel Fuel	Yellow Grease Biodiesel	Soybean Oil Biodiesel
No.2 Diesel Fuel	0.00000	0.34956	0.42927
Yellow Grease Biodiesel	-0.34956	0.00000	0.07971
Soybean Oil Biodiesel	-0.42927	-0.07971	0.00000

Alpha=
0.05

Comparisons for all pairs using Tukey-Kramer HSD

q*	Alpha
3.25387	0.05

Abs(Dif)-LSD	No.2 Diesel Fuel	Yellow Grease Biodiesel	Soybean Oil Biodiesel
No.2 Diesel Fuel	-0.12745	0.23322	0.31293
Yellow Grease Biodiesel	0.23322	-0.10406	-0.02435
Soybean Oil Biodiesel	0.31293	-0.02435	-0.10406

Positive values show pairs of means that are significantly different.

Level		Mean
No.2 Diesel Fuel	A	1.3141006
Yellow Grease Biodiesel	B	0.9645381
Soybean Oil Biodiesel	B	0.8848282

Levels not connected by same letter are significantly different

REPORT D.4. STATISTICAL ANALYSIS FOR BOSCH SMOKE NUMBER

Oneway Anova
Summary of Fit

Rsquare	0.970523
Adj Rsquare	0.960697
Root Mean Square Error	0.112217
Mean of Response	1.937037
Observations (or Sum Wgts)	9

Analysis of Variance

Source	DF	Sum of Squares	Mean Square	F Ratio	Prob > F
Fuel	2	2.4876543	1.24383	98.7745	<.0001
Error	6	0.0755556	0.01259		
C. Total	8	2.5632099			

Means for Oneway Anova

Level	Number	Mean	Std Error	Lower 95%	Upper 95%
No.2 Diesel Fuel	3	2.67778	0.06479	2.5192	2.8363
Soybean Oil Biodiesel	3	1.51111	0.06479	1.3526	1.6696
Yellow Grease Biodiesel	3	1.62222	0.06479	1.4637	1.7808

Std Error uses a pooled estimate of error variance

Means Comparisons

Dif=Mean[i]-Mean[j]	No.2 Diesel Fuel	Yellow Grease Biodiesel	Soybean Oil Biodiesel
No.2 Diesel Fuel	0.0000	1.0556	1.1667
Yellow Grease Biodiesel	-1.0556	0.0000	0.1111
Soybean Oil Biodiesel	-1.1667	-0.1111	0.0000

Alpha=
0.05

Comparisons for all pairs using Tukey-Kramer HSD

q*	Alpha
3.06815	0.05

Abs(Dif)-LSD	No.2 Diesel Fuel	Yellow Grease Biodiesel	Soybean Oil Biodiesel
No.2 Diesel Fuel	-0.28112	0.77444	0.88555
Yellow Grease Biodiesel	0.77444	-0.28112	-0.17001
Soybean Oil Biodiesel	0.88555	-0.17001	-0.28112

Positive values show pairs of means that are significantly different.

Level		Mean
No.2 Diesel Fuel	A	2.6777778
Yellow Grease Biodiesel	B	1.6222222
Soybean Oil Biodiesel	B	1.5111111

Levels not connected by same letter are significantly different

REPORT D.5. STATISTICAL ANALYSIS FOR BRAKE SPECIFIC FUEL CONSUMPTION NUMBER

Oneway Anova
Summary of Fit

Rsquare	0.995406
Adj Rsquare	0.993875
Root Mean Square Error	1.032826
Mean of Response	228.6164
Observations (or Sum Wgts)	9

Analysis of Variance

Source	DF	Sum of Squares	Mean Square	F Ratio	Prob > F
Fuel	2	1386.9418	693.471	650.0903	<.0001
Error	6	6.4004	1.067		
C. Total	8	1393.3422			

Means for Oneway Anova

Level	Number	Mean	Std Error	Lower 95%	Upper 95%
No.2 Diesel Fuel	3	211.061	0.59630	209.60	212.52
Soybean Oil Biodiesel	3	237.304	0.59630	235.84	238.76
Yellow Grease Biodiesel	3	237.485	0.59630	236.03	238.94

Std Error uses a pooled estimate of error variance

Means Comparisons

Dif=Mean[i]-Mean[j]	Yellow Grease Biodiesel	Soybean Oil Biodiesel	No.2 Diesel Fuel
Yellow Grease Biodiesel	0.000	0.181	26.424
Soybean Oil Biodiesel	-0.181	0.000	26.243
No.2 Diesel Fuel	-26.424	-26.243	0.000

Alpha=
0.05

Comparisons for all pairs using Tukey-Kramer HSD

q*	Alpha
3.06815	0.05

Abs(Dif)-LSD	Yellow Grease Biodiesel	Soybean Oil Biodiesel	No.2 Diesel Fuel
Yellow Grease Biodiesel	-2.587	-2.406	23.836
Soybean Oil Biodiesel	-2.406	-2.587	23.656
No.2 Diesel Fuel	23.836	23.656	-2.587

Positive values show pairs of means that are significantly different.

Level		Mean
Yellow Grease Biodiesel	A	237.48469
Soybean Oil Biodiesel	A	237.30377
No.2 Diesel Fuel	B	211.06086

Levels not connected by same letter are significantly different

REFERENCES

1. Schmidt, K. and Van Gerpen, J.H. The Effect of Biodiesel Fuel Composition on Diesel Combustion and Emission, Society of Automotive Engineers Paper No. 961086, SAE, Warrendale, Penn., 1996.

2. Chang, Y.Z.D., Van Gerpen, J.H., Lee, I., Johnson, L.A., Hammond, E.G. and Marley, S.J. Fuel Properties and Emissions of Soybean Oil Esters as Diesel Fuel. Journal of American Oil Chemists Society 73(11): 1549-1555, 1996.

3. Graboski, S.M., Ross, J.D. and McCormick, R.L. Transient Emissions from No. 2 Diesel and Biodiesel Blends in a DDC Series 60 Engine. Society of Automotive Engineers Paper No. 961166, SAE, Warrendale, Penn., 1996.

4. Zhang, X.R., Haws, R., Wright, B., Reese, D., Moller, G., and Peterson, C. Biodegradation of Biodiesel Fuels. Second World Congress of the Society of Environmental Toxicology and Chemistry, Vancouver, British Columbia, Canada, November 5-9, 1995

5. Howell, S. U.S. Biodiesel Standards-An Update of Current Activities. Society of Automotive Engineers Paper No. 971687, SAE, Warrendale, Penn., 1997.

6. ASTM PS 121-99 Provisional Specification for Biodiesel Fuel (B100) Blend Stock For Distillate Fuels. American Society for Testing and Materials, Philadelphia, PA, 2002.

7. ASTM D6751-03 Standard Specification for Biodiesel Fuel (B100) Blend Stock for Distillate Fuels. American Society for Testing and Materials, Philadelphia, PA, 2000.

8. Korbitz, W. Biodiesel Production in Europe and North America, an Encouraging Prospect. Renewable Energy, 16:1078-1083, 1999.

9. Tat, M.E. and Van Gerpen, J.H. The Kinematic Viscosity of Biodiesel and Its Blends with Diesel Fuel. Journal of American Oil Chemists Society, 76(12):1511-1513, 1999.

10. Tat, M.E. and Van Gerpen, J.H. The Specific Gravity of Biodiesel and Its Blends with Diesel Fuel. Journal of American Oil Chemists Society, Vol. 77(2):115-119, 2000.

11. Tat, M. E., Van Gerpen, J.H., Soylu, S., Canakci, M., Monyem, A. and Wormley, S. The Speed of Sound and Isentropic Bulk Modulus of Biodiesel at 21 °C from Atmospheric Pressure to 35 MPa. Journal of American Oil Chemists Society, 77(3): 285-289, 2000.

12. Zhang, Y. Emissions and Combustion of Fatty Acid Esters of Soybean Oil in a diesel Engine. M.S. Thesis, Iowa State University, 1994.

13. Hill, J.W. Chemistry for Changing Times. Macmillan Publishing Company, New York, 1992.

14. Morrinson, R. T. and Boyd, R. N. Organic Chemsitry. Allyn and Bacon, Newton, MA, 1983.

15. O'Leary, M.H. Contemporary Organic Chemistry. McGraw-Hill Book Company, New York, NY, 1978.

16. Schmidt, K.J. The Effect of Fatty Acid Composition an Emissions from Biodiesel-Fueled Diesel Engines. M.S. Thesis, Iowa State University, 1995.

17. Goering, C.E., Schwab, A.W., Daugherty, M.J., Pryde, E.H. and Heakin, A.J. Fuel Properties of Eleven Vegetable Oils. Transactions of the ASAE 25(6):1472-1477, 1982.

18. Ryan, T.W., Callahan, T.J. and Dodge, L.G. Characterization of Vegetable Oils for Use as Fuels in Diesel Engines. Vegetable Oil Fuels-Proceedings of the International Conference on Plant and Vegetable Oils as Fuels, 70-81, Aug., 1982.

19. Tahir, A.R., Lapp, H.M. and Buchanan, L.C. Sunflower Oil as a Fuel for Compression Ignition Engines. Vegetable Oil Fuels-Proceedings of the International Conference on Plant and Vegetable Oils as Fuels, 82-91, Aug., 1982.

20. Fort, E.F. and Blumberg, P.N. Performance and Durability of a Turbocharged Diesel Fueled with Cottonseed Oil Blends. Vegetable Oil Fuels-Proceedings of the International Conference on Plant and Vegetable Oils as Fuels, 374-382, Aug., 1982.

21. Walter, J., Aakre, P. and Derry, J. The 1981 "Flower Power" Field Testing Program. Vegetable Oil Fuels- Preceeding of the International Conference on Plant and Vegetable Oils as Fuels, 384-393, Aug., 1982.

22. Baranescu, R.A. and Lusco, J.J. Performance, Durability and Low Temperature Evaluation of Sunflower Oil As a Diesel Fuel Extender. Vegetable Oil Fuels- Preceeding of the International Conference on Plant and Vegetable Oils as Fuels, 312-328, Aug., 1982.

23. Varde, K.S., Some Correlation of Diesel Engine Performance with Injection Characteristics Using Vegetable Oil As Fuel. Vegetable Oil Fuels-Proceedings of the International Conference on Plant and Vegetable Oils as Fuels, 303-311, Aug., 1982.

24. Radu, R. and Mircea, Z. The Use of Sunflower Oil in Diesel Engines. Society of Automotive Engineers Paper No. 972979, SAE, Warrendale, Penn., 1997.

25. Heywood, J.B. Internal Combustion Engine Fundamentals. McGraw-Hill, New York, 1988.

26. Allinger, N.L., Cava, N.P., De Jongh, D.C., Johnson, C.R., Lebel, N.A., and Stevens, C.L. Organic Chemistry. Worth Publishers, New York, NY, 1971.

27. Oxtoby D.W., Nachtrieb, N.H. and Freeman, W. A. Chemistry: Science of Change. Saunders College Publishing, Orlando, FL, 1990.

28. Wright, W.A. Prediction of Bulk Moduli and Pressure-Volume-Temperature Data for Petroleum Oils. ASLE Transactions, 10:349-356, 1967.

29. Varde, K.S. Dependence of Diesel Fuel Bulk Modulus on Temperature and Pressure. The Canadian Journal of Chemical Engineering, 60:710-712, October, 1982.

30. Wang, Z. and Nur, A. Ultrasonic Velocities in Pure Hydrocarbons and Mixtures. Journal of Acoustical Society of America, 89(6): 2725-2730, June 1991.

31. Monyem, A., Van Gerpen, J.H., and Canakci, M. The Effect of Timing and Oxidation on Emissions. Transactions of the American Society of Agricultural Engineers, 44(1): 35-42, 2001.

32. Gardiner, W.C. Gas-Phase Combustion Chemistry Springer-Verlag, New York, 2000.

33. Zeldovich, Ya. B. The Oxidation of Nitrogen in Combustion and Explosions, Acta Physicohimica, URRS, 21:577-628, 1946.

34. Fenimore, C.P. Formation of Nitric Oxide in Premixed Hydrocarbon Flames, Proceedings of 13th Symposium (International) on Combustion, The Combustion Institute, 373-380, 1971.

35. Malte, P. C. and Pratt, D. T The Role of Energy-Releasing Kinetics in NOx Formation: Fuel-Lean, Jet Stirred CO-Air Combustion. Combustion Science and Technology, 9:221-231, 1974.

36. Morley, C. Structure and Similarity of Nitric Oxide Productioin in Turbulent Diffusion Flames Proceedings of 18th Symposium (International) on Combustion, The Combustion Institute, :23-32, 1981.

37. Bozzelli, J. W. and Dean, A. M. O + NNH: A Possible New Route for NOx Formation in Flames International Journal of Chemical Kinetics, 27:1097-1109, 1995.

38. Hillard, J.C. and Wheeler, R. W. Nitrogen Dioxide in Engine Exhaust, Society of Automotive Engineers Paper No. 790691, SAE, Warrendale, Penn., 1979.

39. Merryman, E.L. and Levy, A. Nitrogen Oxide Formation in Flames: The Roles of NO_2 and Fuel Nitrogen. Proceedings of 15th Symposium on Combustion, The Combustion Institute, 1073-1083, 1975.

40. Monyem, A., Van Gerpen, J.H., and Canakci, M. The Effect of Timing and Oxidation on Emissions. Transactions of the American Society of Agricultural Engineers, 44(1):35-42, 2001.

41. Feldman, M. E. and Peterson, C.L. Fuel Injection Timing and Pressure Optimization on a DI Diesel Engine. Liquid Fuels From Renewable Resources. Proceedings of an Alternative Energy Conferences, 14-15 December, 1992, St. Joseph, MI ASAE.

42. Senatore, A., Cardone, M., Rocco, V., and Prati, M.V. A Comparative Analysis of Combustion Process in D.I. Diesel Engine Fueled with Biodiesel and Diesel Fuel. Society of Automotive Engineers Paper No. 2000-01-0691, SAE, Warrendale, Penn., 2000.

43. McCormick, R.L., Graboski, M.S., Alleman, T.L., and Herring, A.M. Impact of Biodiesel Source Material and Chemical Structure on Emissions of Criteria Pollutants from a Heavy-Duty Engine. Environmental Science and Technology 35(9):1742-1747, 2001.

44. McCormick, R.L., Alvarez, J.R., Graboski, M.S., Tyson K.S., and Vertin, K. Fuel Additive and Blending Approaches to Reducing NOx Emissions from Biodiesel Society of Automotive Engineers Paper No. 2000-01-1658, SAE, Warrendale, Penn., 2000.

45. Sharp, C.A., S.A. Howell, J. Jobe, The Effect of Biodiesel Fuels on Transient Emissions from Modern Diesel Engines, Part I Regulated Emissions and Performance Society of Automotive Engineers Paper No. 2000-01-1967, SAE, Warrendale, Penn., 2000.

46. Peterson, C.L., Taberski, J.S., and Thompson, J.C. The effect of biodiesel feedstock on Regulated Emissins in Chasis Dynamometer Tests of a Pickup Truck. Written for Presentation at the 1999 ASAE/CSAE-SGCR Annual Internatinal Meeting Paper No. 996135.

47. Peterson C.L. and Reece, D.L. Emissions Characteristics of Ethyl and Methyl Ester of Rapeseed Oil Compared with Low Sulfur Diesel Control Fuel in a Chassis Dynamometer Test of a Pickup Truck Transactions of the ASAE, 39(3):805-816, 1996.

48. Peterson C.L. and Reece, D.L. Emission Testing with Blends of Esters of Rapeseed Oil Fuel With and Without a Catalytic Converter Society of Automotive Engineers Paper No. 961114, SAE, Warrendale, Penn., 1996.

49. Rolling, R.E. and C.J. Vogt, The Adiabatic Bulk Modulus of Normal Paraffin Hydrocarbons from Hexane to Hexadecane, Transactions of the ASME – Journal of Basic Engineering, 82:635-644, 1960.

50. Gouw, T.H. and J.G. Vlugter, Physical Properties of Triglycerides III: Ultrasonic Sound Velocity, Fette-Seifen-Anstrichmittel, 69(3):159-164, 1967.

51. McClements J.D. and M.J.W Povey, Ultrasonic analysis of edible fats and oil, Ultrasonics 30(6):383-387, 1992.

52. Javanaud, C. and R.R Rahalkar, Velocity of Sound in Vegetable Oils, Fat Sci. Technol. 90:73-75, 1988.

53. Kuo, Hung-Liang Variation of Ultrasonic Velocity and Absorption with Temperature and Frequency in High Viscosity Vegetable Oils, Japanese Journal of Applied Physics,10(2):167-170, 1971.

54. McClements J.D. and M.J.W. Povey, Ultrasonic Velocity Measurements in Some Liquid Triglycerides and Vegetable Oils, J. Am. Oil Chem. Soc. 65(11):1787-1790, 1988.

55. Povey, M.J.W. and D.J. McClements, Ultrasonics in Food Engineering Part I: Introduction and Experimental Methods, Journal of Food Engineering, 216-245, 1988.

56. Mc Clements, D. J. Ultrasonic Characterizations of Emulsions and Suspensions. Advances in Colloid and Interface Science, 37:33-72, 1991.

57. Marczak, W. Water as a Standard in the Measurements of Speed of Sound in Liquids, the Journal of the Acoustical Society of America, 102(5):2776-2779, 1997.

58. Wong, George S.K., Speed of Sound in Seawater as a Function of Salinity, Temperature, and Pressure, the Journal of the Acoustical Society of America 97(3):1732-1736, 1995.

59. Bilaniuk, N. and S.K. Wong, Speed of Sound in Pure Water as a Function of Temperature, the Journal of the Acoustical Society of America, 93(3):1609-1612, 1993.

60. Chaves, M, V. Sosa, and R. Tsumura, Speed of Sound in Saturated Pure Water, the Journal of the Acoustical Society of America, 77(2):420-423, 1985.

61. Del Grosso, V. A. and C.W. Mader, Speed of Sound in Pure Water, the Journal of the Acoustical Society of America, 52(5):1442-1446, 1972.

62. Del Grosso, V. A. Sound Speed in Pure Water and Sea Water, The Journal of the Acoustical Society of America, 47(3):947-950, 1970.

63. Wilson, Wayne D. Speed of Sound in Distilled Water as a Function of Temperature and Pressure. The Journal of the Acoustical Society of America, 31(8):1067-1072, 1959.

64. Heywood, J.B. Internal Combustion Engine Fundamentals. McGraw-Hill, New York, 1988.

65. Owen, K. and Coley, T. Automotive Fuels Reference Book, Second Edition. Society of Automotive Engineers, Inc. Warrendale, PA, 1995.

66. Lavoie, G.A., Heywood, J.B. and Keck, J.C. Experimental and Theoretical Investigation of Nitric Oxide Formation in Internal Combustion Engines. Combustion Science Technology. 1:313-326, 1970.

67. Lyn, W.T. and Valdmanis, E. Effects of Physical Factors on Ignition Delay. Society of Automotive Engineers Paper No. 680101, SAE, Warrendale, Penn., 1968.

68. Wong, C.L. and Steere, D.E. The Effects of Diesel Fuel Properties and Engine Operating Conditions on Ignition Delay. Society of Automotive Engineers Paper No. 821231, SAE, Warrendale, Penn., 1982.

69. Freedman, B. and Bagby, M.O. Predicting Cetane Numbers of n-Alcohols and Methyl. Esters from their Physical Properties. Journal of American Oil Chemists Society, 67(9): 565-571, 1990.

70. Van Gerpen, J.H. Cetane Number Testing of Biodiesel. Liquid Fuels and Industrial Products from Renewable Resources. Proceedings of the Third Liquid Fuel Conference, 15-17 September, 1996, Nashville, Tennessee.

71. SAE Handbook. Society of Automotive Engineers, Inc. Warrendale, 1993, pp 25.04-25.05.

72. Standard Method for Determining Relative Humidity by Wet and Dry-Bulb Psychrometer. ASTM E337-72, American Society for Testing and Materials.

73. Keenan, J. H., Keyes, F. G., Hill, P. G. and Moore, J.G. Steam Tables: Thermodynamic Properties of Water Including Vapor, Liquid, and Solid Phase. John Willey & Sons, Inc, New York, 1978.

74. Kriger, R.B., and Borman, G.L. The Computation of Applied Heat Release for Internal Combustion Engines. ASME paper 66-WA/DGP-4, 1966.

75. Lyn, W.T. Study of Burning Rate and Nature of Combustion in Diesel Engines. In Proceedings of Ninth International Symposium on Combustion, The Combustion Institute, 1069-1082, 1962.

76. Kort, R.T., Mansouri, S.H., Heywood, J.B. and Ekchian, J.A. Divided-Chamber Diesel Engines Part II: Experimental Validation of a Predictive Cycly-Simulaiton and Heat Release Analysis. SAE paper 820274, SAE Trans, Vol. 91, 1982.

77. Olikara, C., and Borman, G.L. A Computer Program for Calculating Properties of Equilibrium Combustion Products with same Application to I.C. Engines. SAE paper 750468.

78. Van Gerpen, J.H. The Effect of Air Swirl and Fuel Injection System Parameters on Diesel Engine Simulation. Ph.D. thesis, University of Wisconsin-Madison, 1984.

79. Austen A.E.W., and Lyn, W.T. Relation Between Fuel Injection and Heat Release in a Direct-Injection Engine and the Nature of the Combustion Process. Proc. Instn. Mech. Engr. (No. 1), 25, November 8, 1960.

80. Galvincevski, B., Gulder, O.L., and Gardner, L. Cetane Number Estimation of Diesel Fuels from Carbon Type Structural Composition. Society of Automotive Engineers Paper No. 841341, SAE, Warrendale, Penn., 1984.

81. Andree, A., and Pachernegg, S.J. Ignition Conditions in Diesel Engines. Society of Automotive Engineers Paper No. 690253, SAE, Warrendale, Penn., 1969.

82. Monyem, A. The effect of biodiesel oxidation on engine performance and emissions. Ph.D. thesis, Iowa State University, 1998.

83. Chevron Products Co., Diesel Fuels-Technical Review, Chevron, USA.,1998.

84. Gouw, T. H. and Vlugter, J. C. Physical Properties of Fatty Acid Methyl Esters. IV. Ultrasonic Sound Velocity. The Journal of the American Oil Chemist's Society 41:524-526, 1964.

85. Gouw, T. H. and Vlugter, J. C. Physical Properties of Fatty Acid Methyl Esters. I. Density and Molar Volume. The Journal of the American Oil Chemist's Society 41:142-145, 1964.

86. Wayne, D. W. Speed of Sound in Distilled Water as a Function of Temperature and Pressure. The Journal of the Acoustical Society of America. 31:1067-1072, Aug. 1959.

87. McClements J.D. and M.J.W. Povey, Ultrasonic Velocity Measurements in Some Liquid Triglycerides and Vegetable Oils, The Journal of the American Oil Chemist's Society 65(11):1787-1790, 1988.

88. Tat, M.E. and Van Gerpen, J.H. Speed of Sound and Isentropic Bulk Modulus of Alkyl Monoesters at Elevated Temperatures and Pressures, The. Journal of American Oil Chemists Society, 80(12):1-8, 2003.

89. Knothe, G., Matheaus, A.C., and Ryan, T.W. Cetane Numbers of Branched and Straight-Chain Fatty Esters Determined in an Ignition Quality Tester. Fuels 82:971-975, 2003

90. Canakci, M. Production of biodiesel from feedstocks with high faty acids and its effect on diesel engine performance and emission. Ph.D. thesis, Iowa State University, 2001.

91. McDonald, J.F., Purcell, D.L., McClure, B.T., and Kittelson, D.B. Emission Characteristics of Soy Methyl Ester Fuels in an IDI Compression Ignition Engine. Society of Automotive Engineers Paper No. 950400, SAE, Warrendale, Penn., 1995.

92. Mittelbach, M, and Tritthart, Diesel Fuels Derived from Vegetable Oils, III. Emission Tests Using Methyl Esters of Used Frying Oil, The. Journal of American Oil Chemists Society, 65(7):1185-1189, 1988

93. Heisler, H. Advanced Engine Technology Hodder Headline Group, London, 1995

94. Choi, C.Y, Bower, G.R., and Reitz, R.D. Effects of Biodiesel Blended Fuels and Multiple Injections on D.I. Diesel Engine, Society of Automotive Engineers Paper No. 970218, SAE, Warrendale, Penn., 1997.

ACKNOWLEDGMENTS

There have been many people who helped me through my graduate work. I would like to especially thank Dr. Jon H. Van Gerpen for all his guidance, support, and understanding throughout this research. I would also to thank the other members of my committee, Dr. Howard N. Shapiro, Dr. Steven Hoff, Dr. Ron Nelson, and Dr. Brent Shanks.

I wish to thank James Dautremont, Chris Lassen, Petty Boone, Char Kravinsky, and Marti Steelman for all their assistance and technical support. A special thanks to Paul Wang and Trent Simpson for their sincere friendship and their support, and also to my other colleagues Kirk Menges and Jeff Rothermel.

I also deeply thank to the Turkish Ministry of Education for their financial support and the opportunities they supplied to me. I will be very grateful working for them.

Lastly, but not least, I wish to thank my wife Gülcan and to my mother Sevim Tat in Turkey for all their support, patience, and understanding and to my daughter Ayşe Bengisu Tat, and to my son Ahmet Caner Tat for all the happiness they provided to me. I also want to thank my sisters Ayşegül Kırmızı and Yasemin Tezel and also my brother-in-laws Hüseyin Kırmızı and İsamil Tezel in Turkey for their support and patience. I should also remember my niece Tugba Madden, and my nephews, Hasan Tanzer Kırmızı and Murat Tezel for their love. I also want to thank my elementary school teacher Perihan Demiral.

I want to remember the memories of my father Hasan Tat, my grandmother Lütfiye Akdemir, my uncle Ali Hikmet Akdemir, and my teacher Fikret Özcelik all their support for higher knowledge and education. One more time, Thank You All.